Strategies toward Highly Sensitive Polydiacetylene Supramolecules based Biosensors

by

Sung Baek Seo

A dissertation submitted in partial fulfillment
of the requirements for the degree of
Doctor of Philosophy
(Macromolecular Science and Engineering)
in The University of Michigan
2014

Doctoral Committee:

Associate Professor Jinsang Kim, Chair
Associate Professor Anne McNeil
Professor Shuichi Takayama
Assistant Professor Anish Tuteja

2014

ACKNOWLEDGEMENTS

I would like to thank for my advisor, Professor Jinsang Kim. He has been a great mentor and educator during my PhD studies. He has guided me to go in the right research direction, but has been patient with me as I proceeded on my own research development. I have appreciated his precious time and all his efforts to discuss experimental results, revise manuscripts, and review practice talks. In addition, I have respected his generous considerations about the graduate student's life. I strongly believe he will continue to be a role model in my research life. Also, I have been grateful to my committee members, Professor Shuichi Takayama, Professor Anne McNeil, and Professor Anish Tuteja. They suggested valuable ideas and gave opportunities for collaboration. I was honored to conduct my dissertation study under their guidance. Thanks to Professor Richard Laine and Nonna. He allowed me to start and finalize my research in Macro. Also, she helped me with all kinds of student matters and always supported me as a student.

I learned a lot and really enjoyed research in the Kim group. A past member, Dr. Jiseok, was a devoted research mentor for my PDA work~~s~~. He spent his time and efforts for teaching me organic synthesis, characterizations and sharing his thoughts on my research developments. I welcome his success and look forward to his future career. Dr. Bonggi, Dr. Eunjeong, Dr. Donghyuk, Dr. Minsang, Dr. Sunjong gave various advice on failure analysis. David helped me overcome my lab troubles and make English revisions on my manuscripts. I liked Dongwook's advice, encouragement and enjoyed our small talks. Alica, Noah, Kyeongwoon, Apoorv, Jaehun

made my lab life productive. I hope and expect Deokwon and Andrew will be successful in PDA related biomaterial/biosensor work. I appreciated candid discussions with Dohyun, who was a worthy collaborator for PDA work. Gibum was great buddy and we shared our ideas and research progress during my PhD program.

I am thankful to KPCAA Christians. They made my family welcome, and helped us to smoothly settle down in Ann Arbor and strongly supported me in my graduate student life. Thanks to my parents and parents in law. They always trusted and supported me, so that I was able to focus on my PhD studies. Lastly, I want to give many thanks to my wife, Hyunjoo Kim and my son, Daniel Jiho Seo. They were with me, motivated me to continue and overcome challenges on my PhD studies. I love them. Thanks to God for all these people and achievements He allowed me to accomplish.

TABLE OF CONTENTS

LIST OF FIGURES

Figure

ABSTRACT

Polydiacetylene (PDA) based biosensors have the merits of colorimetric and fluorometric dual signaling and self-assembly based easy fabrication. However, mediocre sensitivity is the limit of PDA-based sensors because large number of target analytes should be captured at the PDA liposome surface to generate enough steric repulsion and resulting sensory signal. In addition, the fluorescence quantum yield of PDA is rather low at only 1%. Rational design of receptors to provide specificity toward a target analyte is a challenging task as well. In this dissertation, systematic analysis of the signal generating mechanism of PDA liposomes and various strategies to enhance the sensitivity of the PDA sensory system are presented. A novel fluorescence turn-on sensory platform is also devised and demonstrated.

The signal generating mechanism of PDA liposomes was first systematically studied by investigating target size effect on the sensory signaling intensity of PDA liposome sensors. Influenza A virus M1 peptide and M1 antibody were selected as a probe-target pair but their role was switched in two different types of sensory system. When the larger M1 antibody was used as a target and M1 peptide was tethered at the liposome surface as a probe, a detectable sensory signal was generated. However, if their roles are switched no sensory signal was observed, revealing that the intensity of the PDA sensory signal is mainly related to the steric repulsion between probe-target complexes, not the strength of the probe-target binding force. In order to enhance the sensitivity, phospholipids were inserted into the PDA liposome to provide fluidic

mobility within the PDA liposome structure, enabling easy distortion of the PDA backbone. This approach enabled a detection limit comparable to a conventional influenza A virus detection kit.

PDA liposomes are known to easily accommodate various phospholipids. If phospholipids are utilized as the capturing moiety for target analytes, recognition events at the PDA liposome surface can distort the PDA intermolecular packing and produce sensory signals. While these PDA-phospholipid supramolecules were studied, a very unique phenomenon of Rhodamine6G (R6G) quenching with a phospholipid (1,2-dimyristoylsn-glycero-3-phosphate, DMPA) aqueous solution was discovered. Coulombic interaction between cationic R6G and the anionic DMPA phospholipid occurred in the aqueous phase and created spherical liposome structures. At the surface of the liposome, the R6G molecules are H-type aggregated on the head groups of DMPA and their emission is quenched. Based on this finding, a highly sensitive and selective new sensing platform was devised by co-assembling PDA and phospholipids that displays specific interactions with a target bioanalyte. Because this novel fluorescence turn-on system is readily applicable to the conventional 96-well plates and provides high performance, it can potentially be an alternative to ELISA, the standard fluorescence biosensor system.

Matrix polymer-assisted sensitive PDA sensory system and 1-dimensional PDA nanofibers are also studied to enhance colorimetric sensitivity of PDA systems. Hygroscopic alginate polymer films having embedded PDA liposomes and PDA nanowires are prepared, respectively, and were used to investigate a matrix-assisted sensory platform and the effect of dimensionality of PDA on sensory signaling properties. A colorimetric moisture sensor was developed based on the combination of PDA nanowires and hygroscopic polymer matrix for dental applications.

Design considerations for PDA supramolecule based biosensors are summarized in this dissertation with potential development of advanced PDA biosensors.

CHAPTER 1

Introduction

This chapter describes the development in the field of biosensors with focus on polydiacetylene (PDA)-based biosensors. Lately, the research and development in the field of biosensors has assumed greater significance and calls for more innovative efforts. Conjugated polymers (CP) based biosensors have come up as a great alternative to conventional biosensors and possess the unique property of sensory signal amplification which the conventional sensors lack. Among the CP used in biosensors, PDA has unique features such as self-assembly structures, topochemical polymerization, and stimuli-responsive colorimetric/fluorometric chromism. This chapter will discuss the aforementioned properties and features of PDA in detail. Finally, notable considerations for designing PDA biosensors will be discussed.

1.1. Biosensors development

The human nature for being healthy and safe in entire life has created a need for biosensors development. In these days, the growing threat of biological warfare agents, contagious disease, and foodborne pathogens triggered abrupt needs for rapid and sensitive detection before the target population becomes infected. For instance, the incident of the anthrax letters in October 2001, the emergence of influenza virus with swine origin in April 2009, and repeated occurrences of foodborne poisoning illustrate how necessary such detections are. To avoid

damage from toxic or/and infectious molecules, people want to have biosensors to screen out and monitor the harmful compounds. Accordingly, research articles related biosensors developments are growing and market size for biosensors continues to increase (Figure 1.1). The biosensors market is categorized as biodefense, process industries, research laboratories, environmental monitoring, home diagnostics, and point-of-care testing. Among them, point-of-care which is medical testing at or near patient care continues to be the largest market for biosensors. The goal of these testing is to collect the specimen and obtain the results in a very short period of time at or near the location of the patient so that the treatment plan can be adjusted as necessary. The representative examples are blood glucose testing, urine strips testing and pregnancy testing.

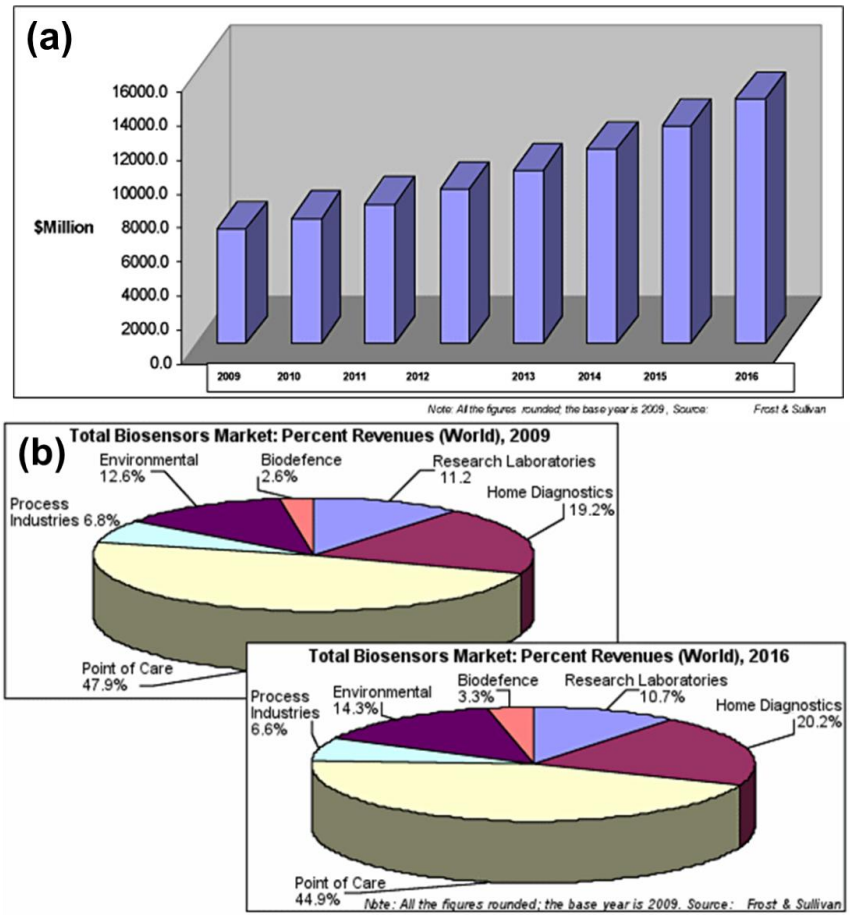

Figure 1.1 (a) The biosensors market presenting the world revenue forecast for 2009-2016, (b) Categorized biosensor market showing the percent of revenues for 2009 and 2016. Reproduced from Ref[1] with permission.

Biosensors are analytical tools that identify and quantify desired target analytes from the unknown samples. Targets of interest (glucose, hormone, toxic chemicals, organophosphate, and infectious pathogens) are critical or harmful molecules to human body, so that the compounds should be detected. The most successful example of biosensors is the blood glucose meter. It is invented by Clark in 1962 and conveniently used to this day by diabetic patients in order to monitor blood glucose at home. By end-user applications, the glucose monitoring kits hold the biggest market (32 %) in total biosensors market. Rapid analysis is possible from just single drop of blood. The instrument uses enzyme glucose oxidase to oxidize blood glucose and uses two electrons to reduce the flavin adenine nucleotide (FAD, the active site of the enzyme glucose oxidase) to $FADH_2$ (Figure 1.2). Then, the resulting current is able to count glucose numbers.

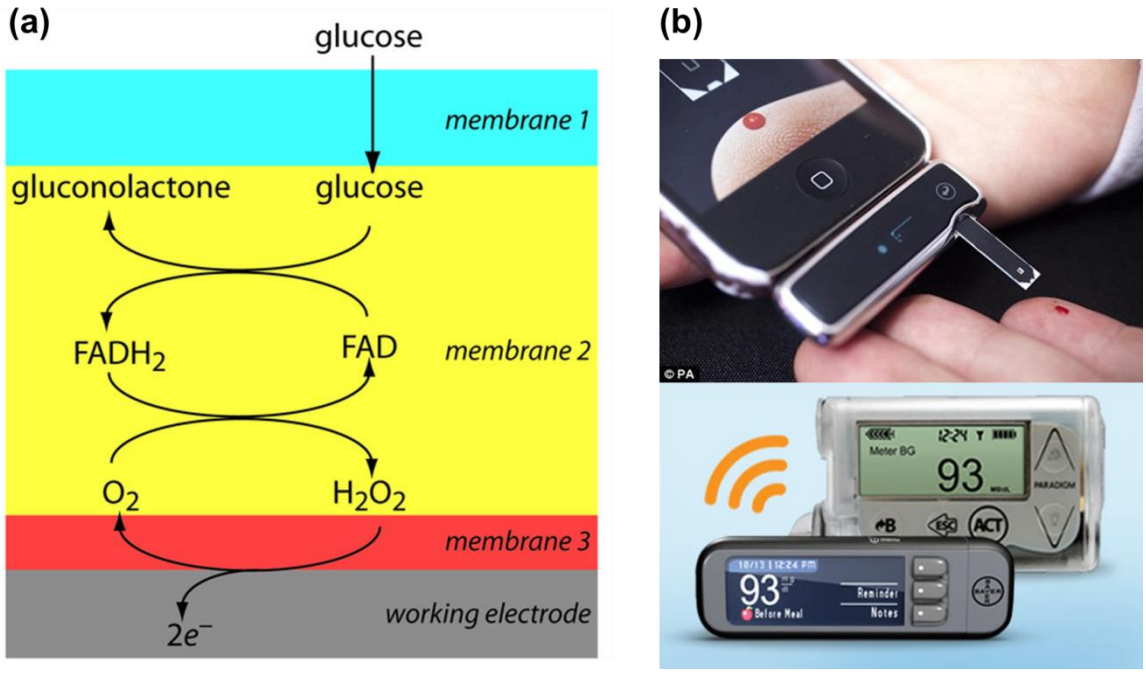

Figure 1.2 (a) Schematic diagram of glucose mediated reactions by which an amperometric glucose biosensor. Reproduced from Ref[2] with permission, (b) Commercialized blood glucose monitoring products. iBGStar blood glucose meter for iPhone (upper) Bayer glucose monitoring system communicable wirelessly with Medtronic insulin devices (lower).

1.2. Conjugated polymers for biosensors

Conjugated polymers (CPs) are compounds consisted of alternating saturated and unsaturated bonds and backbone atoms that are sp^1 or sp^2-hybridized.[3] The resulting p-orbital overlap provides conductivity and fluorescence in CPs. Changes in intramolecular conformation and intermolecular packing in CPs can change effective conjugation length, resulting in changes in absorption, fluorescence, and conductive properties of CPs.[4] Likewise, the signaling mechanism originated from intra- or intermolecular rearrangement can be applied to biosensor design. By incorporating CPs with a specific receptor moiety that can bind to molecules of interest, the specific recognition event provides selectivity to CP based biosensors. In addition, CP based sensors are more advantageous than small-molecular fluorophore based biosensors because they can amplify the signal from a recognition event.[5] An environmental change at onesite along the conjugated polymer chain can influence electronic properties of an entire chain in macromolecular chromophores, producing large signal amplification. While a binding event on a small molecular fluorophore only causes a single chromophore to change its fluorescence. This signal amplification provided by CPs is important for biosensing applications because the molecules of interest are often present in extremely dilute concentrations.

Since many biological targets in biosensors require an aqueous environment to maintain their form and function, it is desired to develop water-soluble CPs. However, since CPs have carbon based hydrophobic and rigid-rod like backbones by nature, they are easily aggregated in aqueous environments. To meet this requirement, water-soluble and highly emissive conjugated polyelectrolytes (CPEs) have become emerging topics for biosensor applications. CPEs are conjugated polymers having a charged (anionic or cationic) side chains. Sulfoante (SO_3^-), carboxylate (CO_2^-), and phosphate (PO_4^{3-}) ions are negatively charged groups and a quaternary

ammonium (NR_3^+) is a positively charged group. These functional groups are most commonly used functional group to give water-solubility in the CPE design.[6] These pendant groups, often combined with non-ionic yet water-soluble poly(ethylene oxide) side chains, help CPEs dissolve in water and prevent the aggregation of multiple chains. The first CPEs were reported by Shi and Wudl in 1990 and others have been developed in recent years for biosensor applications.[7] Figure 1.3 shows the chemical structures of CPEs used in the literature. A recent review published by Pinto and Schanze gives an in-depth overview of the synthetic methods to make conjugated polyelectrolyte, including those having poly(p-phenylene), poly(phenylene vinylene) and poly(phenyleneethynylene) backbone structures. However, synthesis of completely water-soluble and highly emissive CPEs is demanding and challenging work.

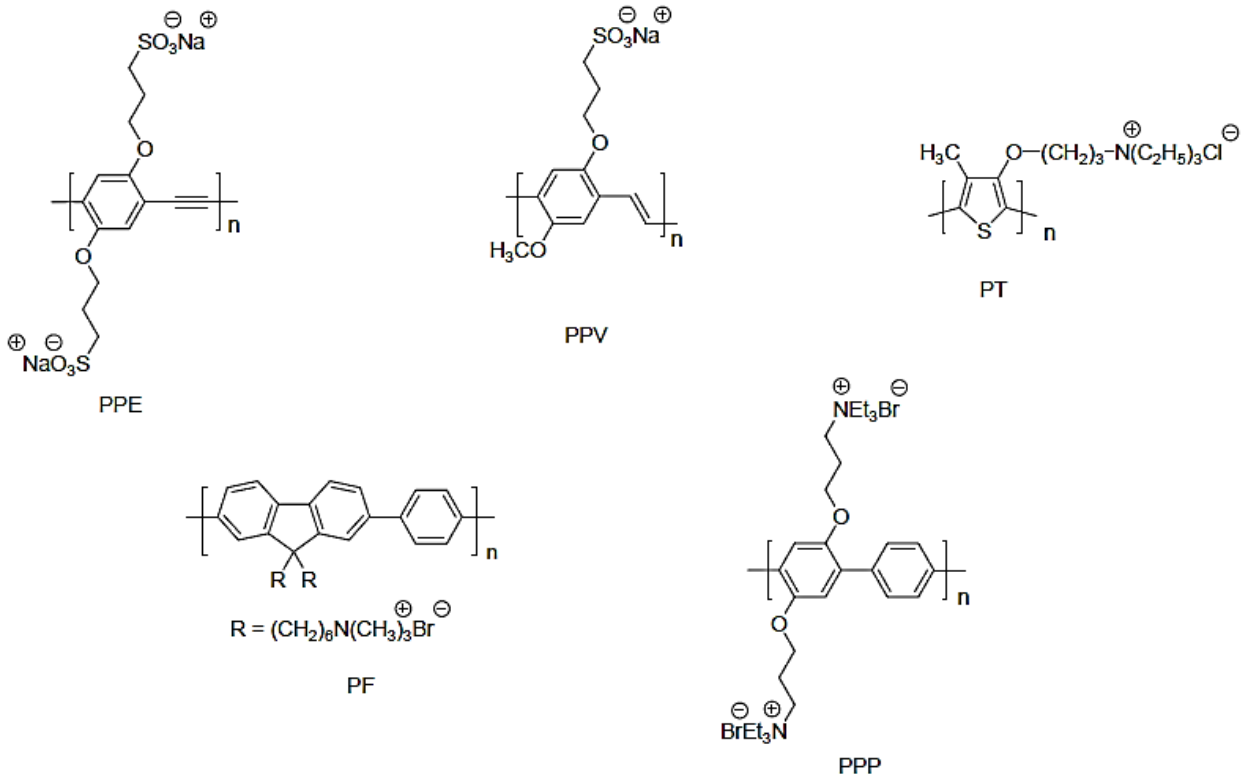

Figure 1.3 Examples of water-soluble CPs used in biosensor applications. Reproduced from Ref[6a] with permission.

1.3. Polydiacetylene for biosensors

Polydiacetylene (PDA), one of conjugated polymers, is compound having alternating double and triple bonds (ene-yne) along its main chain. PDA has optical properties that have formed the basis for detection of biological entities.[8] The advantages of PDA materials for sensing applications come from environmentally sensitive (pH,[9] temperature,[10] mechanical pressure[11] and ligand-receptor interactions[12]) optical characteristics and easy formation in self-assembled system.

PDA based biosensors are unique in terms of the sensitive colorimetric/fluorescence dual detection capability and the convenient preparation method through self-assembly and subsequent photopolymerization (see section 1.4.3.1). To date, representative target analytes using PDA biosensors in literatures include influenza virus,[13] *E.coli*,[14] microorganisms,[15] proteins[16] and biologically relevant molecules.[17]

1.4. Properties of PDA supramolecule

1.4.1. Self-assembled structures

Diacetylene (DA) monomers are amphiphilic molecules composed of two parts: 1) a polar head group and 2) a hydrophobic tail containing the diacetylene group. This amphiphilic nature renders a convenient self-assembly feature in an aqueous environment to DA. Each tail can be broken down into three moieties: the diacetylene group, a spacer between the head group and the diacetylene, and the terminal alkyl chain. Each element of the diacetylene amphiphile plays a crucial role in determining if an amphiphile will form a self-assembly and, if it does, what properties that the assembled structures will have. For instance, headgroup chirality strongly influences colloidal structure; amphiphilic monomers with achiral headgroups usually form

spherical liposomes, whereas chiral amphiphiles often form non-spherical structures such as helices and tubules. Because of the amphiphilic moiety, DAs are likely to form intermolecular (between diacetylene monomers) packing in aqueous medium via hydrophobic-hydrophobic interactions of adjacent tails of DAs. Moreover, hydrophilic head groups such as carboxylic acid or amide groups in DAs also have chances of intermolecular hydrogen bonding, and/or aromatic head groups of DAs can promote π-π stacking interactions, stabilizing the self-assembled structure of DAs.

Herein, self-assembled PDA forms can be divided into four different categories: *Langmuir* films,[18] self-assembled monolayers (SAMs),[19] spherical colloids,[20] and non-spherical colloids. Particular assembly formation provides specific advantages for different biosensing applications. For example, colloidal solutions are suitable for assay applications where liquid handling techniques are used, such as automated high throughput screening in drug delivery. In contrast, solid supported PDA materials are more suitable for incorporation in devices where ruggedness and ease-of-use are paramount design considerations. For these reasons, *Langmuir* films or SAMs have been utilized for solid supported biosensory device systems. Following sections will describe basic formative principle of each PDA structure, suitable applications, and advantage/disadvantages of their systems, respectively.

1.4.1.1. *Langmuir*, *Langmuir-Blodgett* (*LB*), and *Langmuir-Schaefer* (*LS*) films

Langmuir films are formed by spreading amphiphilic diacetyelnes at an air/water interface and compressing them into close-packed arrays (Figure 1.4). These films can be studied at the air/water interface or transferred to a variety of solid substrates to make *LB*, *LS* or similar films. *Langmuir* films are a useful formation for both spectroscopic and microscopic studies; such studies have discovered on the structural characteristic of PDA materials.

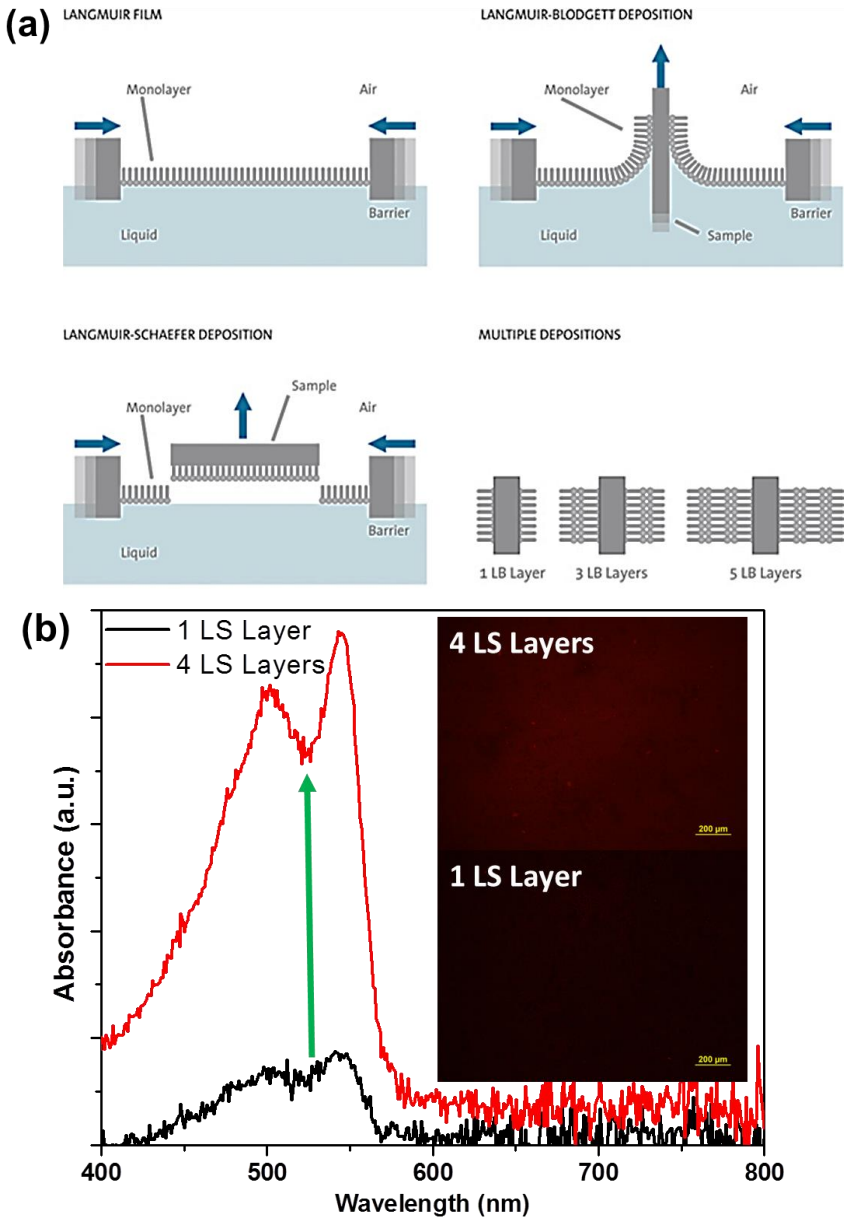

Figure 1.4 (a) Schematic illustration of *Langmuir* film, *Langmuir-Blodgett* deposition, *Langmuir-Schaefer* deposition and multilayers obtained after repeated deposition. Reproduced from Ref[21] with permission, (b) monolayer and multilayers deposition using PCDA diacetylene by *Langmuir-Schaefer* method via *Langmuir-Blodgett* through.

Monolayer *Langmuir* films have been used for UV-Vis detection of bio-analytes though the relatively low amounts of PDA present in a monolayer hardly support spectroscopy based detection. Geiger *et al.*[18b] and Jelinek and co-workers[22] found that at least three diacetylene

layers are required for chromatic detection. Multi-layers *LB* and *LS* films have been used for a variety of detection platforms, but they are delicate and complicate to prepare, require skilled workers and/or sophisticated automation, and it is difficult to create large area films of consistent quality.

1.4.1.2. Self-assembled monolayer (SAM)

Most diacetylene SAMs have been fabricated from thiol monomers on gold surfaces, and the formation and polymerization of diacetylene monolayers on pyrolytic graphite has also been reported (Figure 1.5).[23] Even though SAMs have created interesting model systems for studying the ordering of diacetylenes on surfaces and the formation of PDA in coatings, they have not as yet been proven to have particular sensing applications. The small amount of PDA in the monolayers makes detection of optical signals challenging; however, they might have applications in an evanescent wave fluorescence or plasmon surface resonance detection platform.

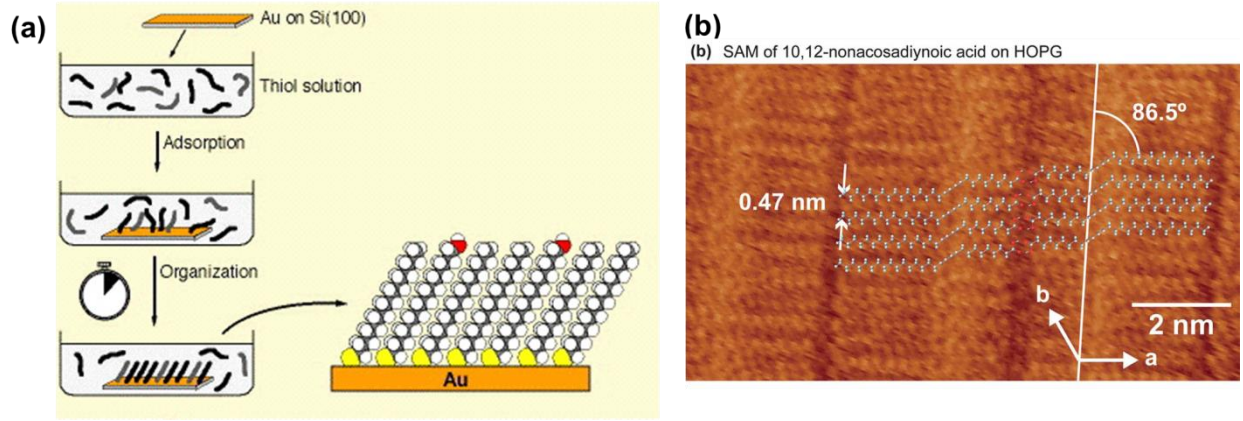

Figure 1.5 (a) Preparation of SAMs. The substrate, Au on Si, is immersed into an ethanol solution of the desired thiol(s). Initial adsorption is fast (seconds); then an organization phase follows which should be allowed to continue for >15 h for best results. A schematic of a fully assembled SAM is shown to the right. Reproduced from Ref[24] with permission, (b) STM images of a self-assembled monolayer (SAM) of 10,12-nonacosadiynoic acid on graphite. Reproduced from Ref[25] with permission of The Royal Society of Chemistry.

1.4.1.3. Spherical colloids: liposomes/vesicles

Liposome is defined a spherical vesicle composed of lipid bilayers. The words, liposomes and vesicles, have been used somewhat interchangeably to refer to spherical particles with bilayers. For simplicity, the term liposomes will be used in this dissertation. Diacetylene amphiphiles can be dispersed in water, usually by probe sonication,[26] to form self-assembled liposome particles, and photopolymerized *in situ*. Alternatively, injection of a small amount of a DMF or DMSO solution containing amphiphilic diacetylene monomers into water leads to the spontaneous formation of diacetylene supramolecules (Figure 1.6). Brief sonication followed by storing in a refrigerator for at least a few hours gives the formation of stabilized diacetylene liposomes. In detail, hydrophobic moieties are likely to far away from the aqueous phase, while hydrophilic modalities are willing to contact with the aqueous phase.

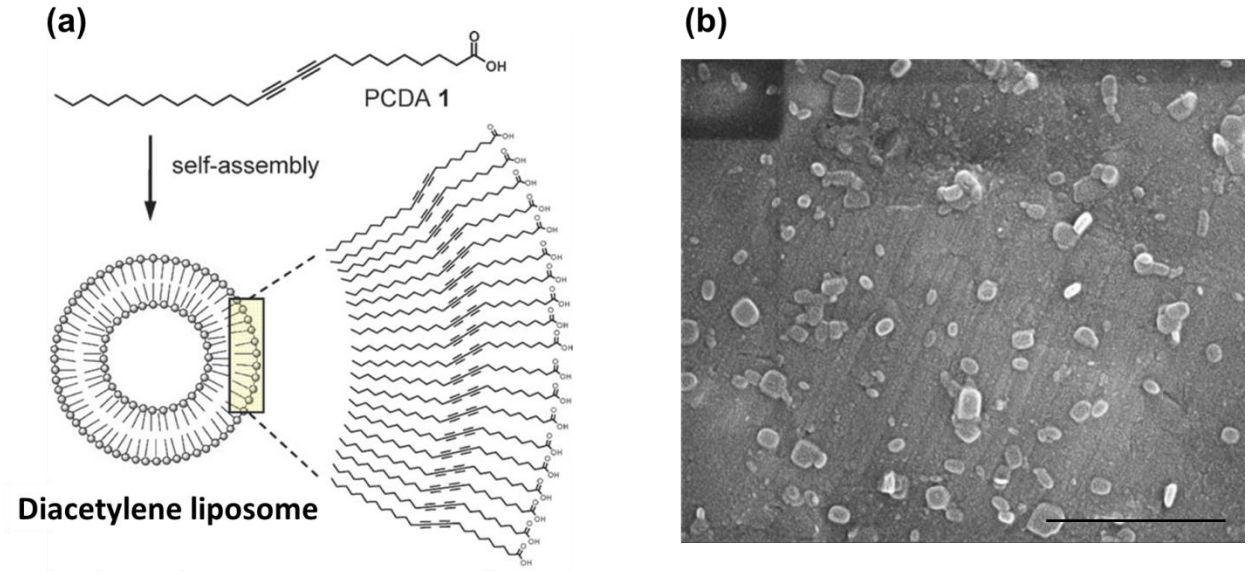

Figure 1.6 (a) Diacetylene liposome from self-assembled diacetylene derived from 10, 12-pentacosadiynoic acid (PCDA). Reproduced from Ref[8d] with permission of The Royal Society of Chemistry, (b) SEM image of PCDA liposomes. Scale bar is 1 μm.

The formation of polymerized liposomes has advantages and disadvantages of such systems

as models for biological membrane. The liposomes are easy to prepare and more readily scaled to larger volume production. They are also more easily used as reagents in assays than films or coatings as they can be readily dispensed in controlled amounts. The ease of preparation and biomimetic nature of the PDA colloidal materials have made them a popular platform for developing bioassays. Most of my PDA works in this dissertation are based on liposome platform as well.

A disadvantage of this self-assembly structure is that post-preparation modification of the colloids, such as conjugating reactive or binding groups to their surfaces, requires size exclusion column chromatography or dialysis steps to separate unreacted material from the liposomes. Ignoring to remove unreacted antibodies or other ligands give chances of competitive binding by the free ligands to targets and reduction of the response of the PDA materials. These disadvantages can be addressed by attaching PDA liposomes to a surface. I successfully utilized this approach to PDA microarray sensor for influenza A virus detection. Ringsdorf and co-workers noted early on that PDA liposome membranes lacked the fluidity characteristic of biological membranes, though with increased stability to detergents.[27] It is possible to incorporate significant percentages of non-polymerizable lipids in diacetylene liposomes to give them a more biomimetic character and still photopolymerize the diacetylene components to form PDA.

1.4.1.4. Non-spherical colloids: nanowire, nanofiber, ribbons, sheets

Diacetylenes have also been discovered that are able to self-assemble into a variety of non-spherical structures such as tubules,[20b] helices,[20c] ribbons,[28] and sheets[29] (Figure 1.7). A recent review discusses formation of PDA nanowires from strongly H-bonding symmetric bolaamphiphiles, and from asymmetric bolaamphiphiles with one head group capable of π–π

stacking and the other H-bonding.[30]

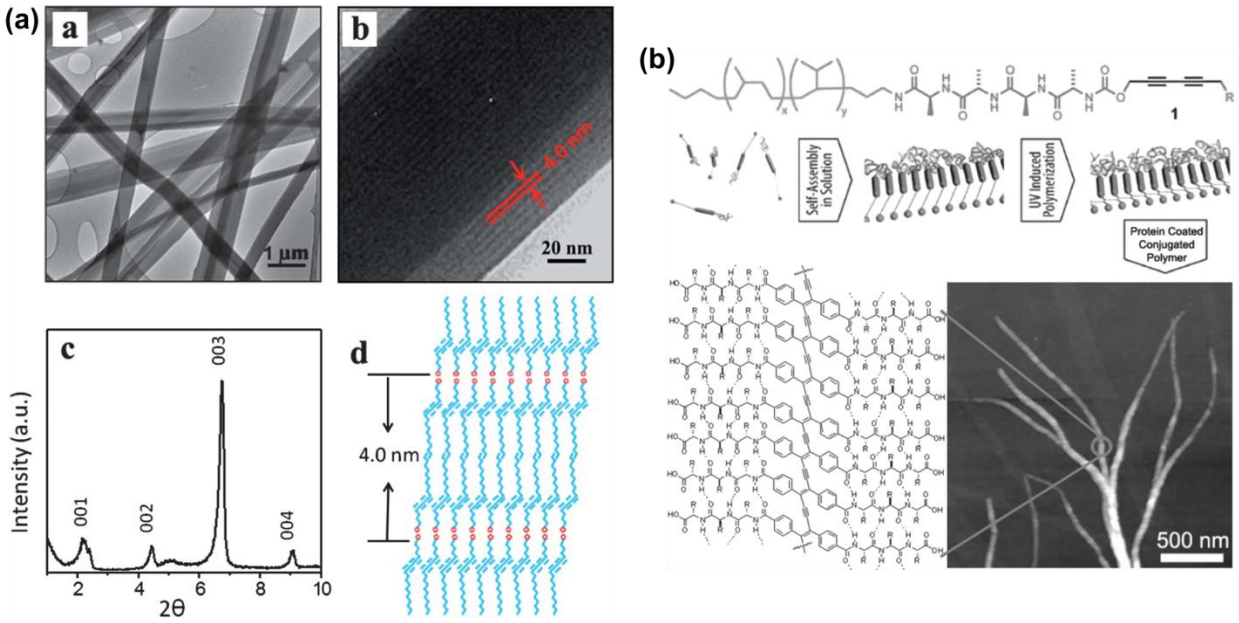

Figure 1.7 (a) a) Structure of single 5,7-octadecadiynoic acid (ODDNa) nanowires. b) A representative low resolution TEM image of the single ODDNa nanowires. c) High-resolution TEM of single ODDNa nanowires, showing a layer structure with d-spacing of 4.0 nm between the nearest two layers. c) XRD patterns of single ODDNa nanowires. d) A schematic molecular packing of lamellar nanostructure. Here only the p–p interactions between conjugated chains are displayed. The hydrophilic head groups are represented using circles. Reproduced from Ref[31] with permission of The Royal Society of Chemistry, (b) AFM images of PDA nanostructures derived from peptide. Reproduced from Ref[32] with permission of John Wiley and Sons.

Tubules, ribbons and fiber structures form an interesting contrast to liposomes. For example, Plant et al. showed that was more tightly packed in tubules than liposomes[33] and Stupp group designed nanofiber assembly with DA-peptide sequence molecules.[34] These non-spherical structures generally have significantly larger dimensions than liposomes, many examples have lengths greater than 10 mm. The structures are often not stable in solution, forming gels and aggregates. While the PDA in these structures has shown similar chromatic behavior to PDA liposomes in response to heating and pH changes,[35] they have not, to date, been known explicitly used in biosensing applications. However, I will introduce PDA nanofiber embedded hydrogel

system which shows chromism by hydrogel swelling (see Chapter 4).

1.4.2. Topochemical polymerization

PDA is formed from the 1,4-photopolymerization of diacetylenes, which makes a conjugated backbone with side alkyl chains (Figure 1.8). The polymerization only proceeds when the diacetylenes are arranged in a lattice with appropriate geometry. This topochemical constraint means that polymerization can only occur in solids or other highly ordered structures. Also, polymerization of self-assembled monomers leads to physical stabilization of the structure, increasing thermal stability and mechanical strength.

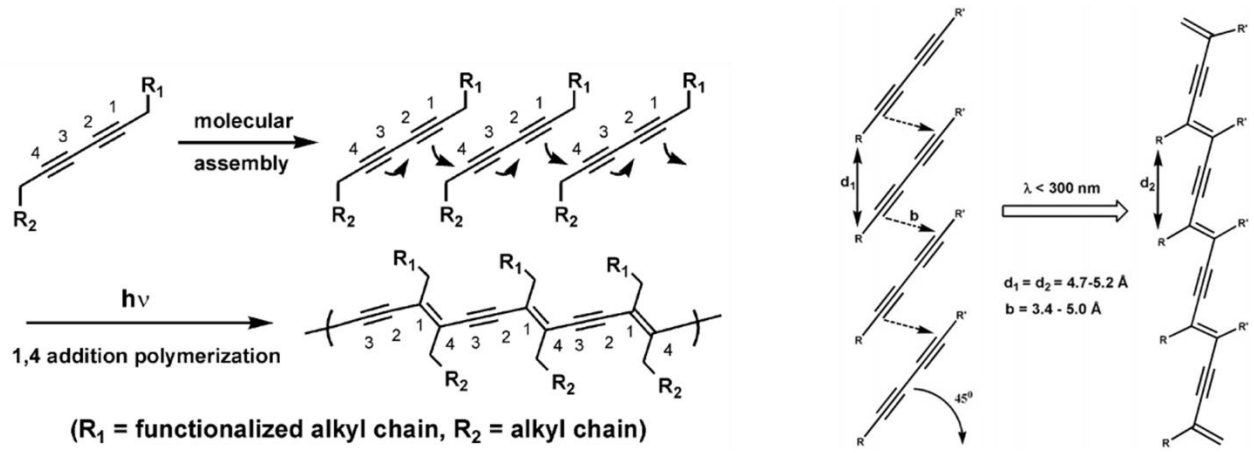

Figure 1.8 Schematic representation of topochemical photopolymerization of assembled diacetylenes. Reproduced with permission from Ref[36] Copyright 2005 American Chemical Society. Reproduced with permission from Ref[34] Copyright 2008 American Chemical Society.

It is known that precise conditions in the arrangement of monomers are required in such topochemical reactions of diacetylene, that is, there must be 4.9 Å of translational distance between the DA units and an inclination angle of 45° between the DA axes.[37] Recently, numerous studies on the topochemical reactions of DA have been conducted not only in the crystalline states, but also in the mesophases such as in micelles,[38] *Langmuir-Blodgett* films,[39]

and self-assembled monolayers.[40] Moreover, Shinkai group demonstrated that the photopolymerizable unit with flexible linkers is expected to be strongly stabilized by intermolecular hydrogen bondings between two amide linkages that are surrounded by the gel-forming segments.[41] The amide groups are widely used to fix DA in a suitable orientation because the distance between them (about 4.8 Å) is comparable to that of the DA units (about 4.9 Å).

1.4.3. Colorimetric/fluorometric transition

1.4.3.1. Colorimetric transition

PDA shows either a blue or a red color, depending on the polymerization conditions; however, the origin of the color difference has not yet been well understood. In 1984, Wegner et al. summarized the relationship between the wavelength of the absorbance and the effective conjugation length (ECL) in PDAs.[42] They found that ECL is strongly affected by the planarity of the main chain of PDA in a linear relationship. According to their analyses, PDAs having an ECL of around 20-mer should show a red color, and those having an ECL of 30-mer should show a blue color.[41]

Here I describe the detail how PDA presents colorimetric transition. Before polymerization, self-assembly solution of diacetylene monomers is transparent and does not have absorption in the visible region. Through photopolymerization, conjugation is formed by overlap of the p-orbitals of the adjacent double and triple bonds, and makes planar overlap (Figure 1.9). The degree of p-orbital overlap determines the conjugation length, which means how much backbone planarity is maintained.[43] The longer the conjugation length, the smaller the energy gap between the valence and conduction bands. After the polymerization, PDA has its absorption maximum at

650 nm and is blue color (Figure 1.9 inset). While the blue phase PDAs is exposed by external stimuli, i.e., pH, temperature, mechanical stress, receptor-ligand interactions, the conjugated backbone becomes twisted and non-planar p-orbital overlap. Eventually it reduces the conjugation length and enlarges the energy band gap. As the consequence, the twisted PDAs absorb maximum at 550 nm and become red.

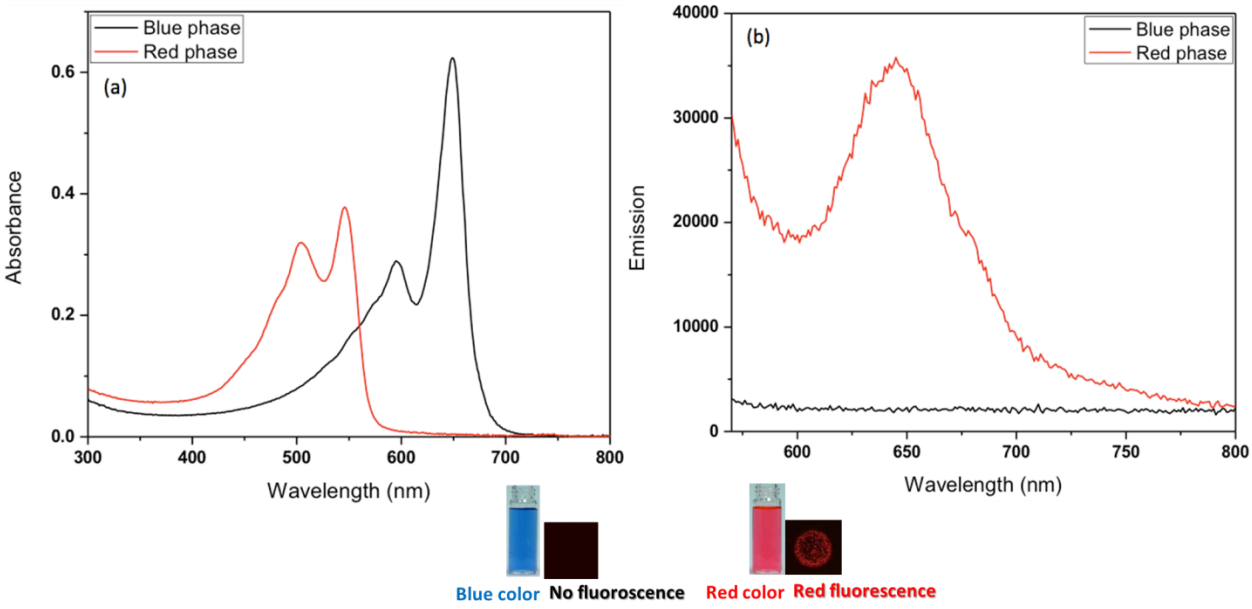

Figure 1.9 (a) Absorption and (b) Emission spectra of poly(10,12-PCDA) liposomes solution.

1.4.3.2. Emission

The red phase PDA is emissive in fluorescence while the blue phase is not. It can be explained by energy shifts based on symmetry from excited state to ground state. The lowest excited state in blue phase has the same symmetry as the ground state, so called, A_g symmetry. While, in the red phase, the lowest excited state has B_u symmetry, generating radiative decay.[10a, 44] Thus, the red fluorescence can be detected at 650 nm while no fluorescence is observed in the blue phase (Figure 1.9 inset).

1.4.3.3. Mechanisms of color and emission change

The mechanisms of color and fluorescence change continue to be investigated. The one major theory described the mechanism is as follow; polymerization changes the hybridization of the terminal alkyne carbons from sp to sp^2 and therefore changes the preferred bond angle from 180° to 120°, but the packing of the side chains does not allow the polymer backbone to reorient and relieve strain, resulting in accumulation of stress in the material as polymerization proceeds (Figure 1.10).[45] The different ways to induce color change can be thought of as overcoming the barrier to reorganization of the polymer backbone created by the packing of the side chains. For example, thermal energy at high temperatures increases motion of the side chains and allow changes in the packing of the chains, UV exposure extends polymer lengths and increases the overall stress of the system effectively reducing the energy required for backbone reorientation, and pH changes alter the H-bonding in head groups allowing the methylenes between the head group and the backbone to reorganize. In addition to these enthalpic considerations, transition of the polymer backbone from extended rod like segments associated with the blue form to zigzags or coils proposed for the red form would have entropic gains (Figure 1.11).[46]

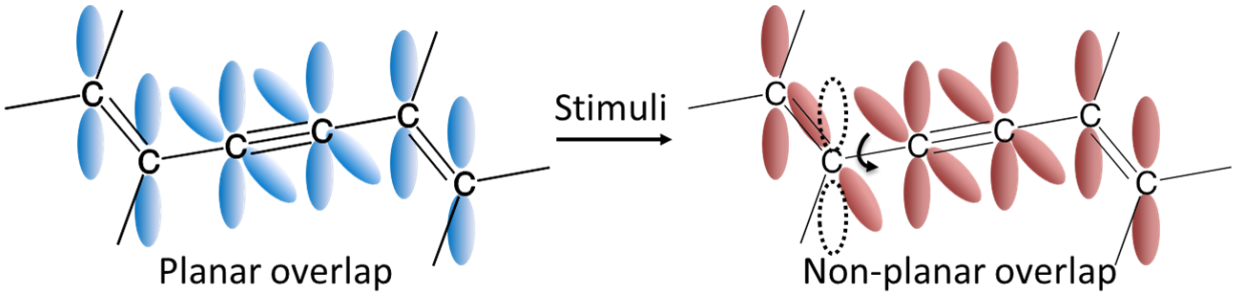

Figure 1.10 Schematic diagram of π-orbital overlap in the conjugated PDA backbone. By stimuli, the planar overlap is twisted by rotation about one of the C-C bonds in the backbone. The red phase consists of a non-planar backbone with rotated alkyl side chains.

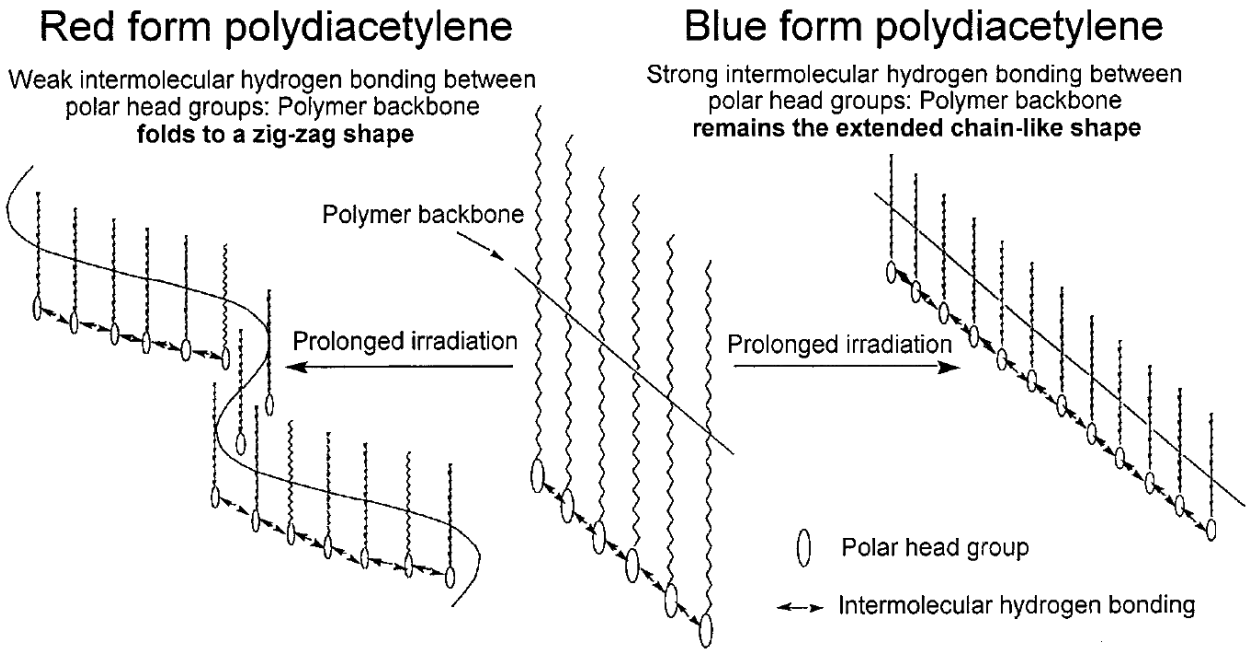

Figure 1.11 "Self-folding" model of the polymer backbone to explain the chromatic properties of polydiacetylene films upon prolonged UV irradiation. Reproduced with permission from Ref[46]. Copyright 1999 American Chemical Society.

1.5. Design considerations for PDA supramolecules biosensors

1.5.1. Sensing mechanism

The commonly accepted scenario in sensing mechanism regardless of target molecules is that probe-target binding events should be enough to distort the organized intermolecular packing of the PDA assembled structure. Obviously, PDA conjugated backbone is created within the intermolecular packing structure, and becomes origin of sensory chromism. The sensing mechanisms of recently developed PDA sensors in our lab, in the view of how target of interest generates PDA sensory signals, can be classified as following (Figure 1.12): 1) Potassium or mercury ion detection: negatively charged probe-target binding complexes ionically repulse each other at adjacent distance. Accordingly, that steric repulsion force disturbs PDA intermolecular packing and conjugated backbone distorted,[12a, b] 2) melamine detection: intra- and inter-

liposomal strong hydrogen bonding interactions between probes and targets perturb the organized PDA packing structure,[12c] and 3) nerve agent detection: not only intra liposomal steric hindrance between probe-target binding complexes, but hydrophobized PDA liposome surface by target binding promotes disturbance to the PDA liposome structure and generates color change.[47]

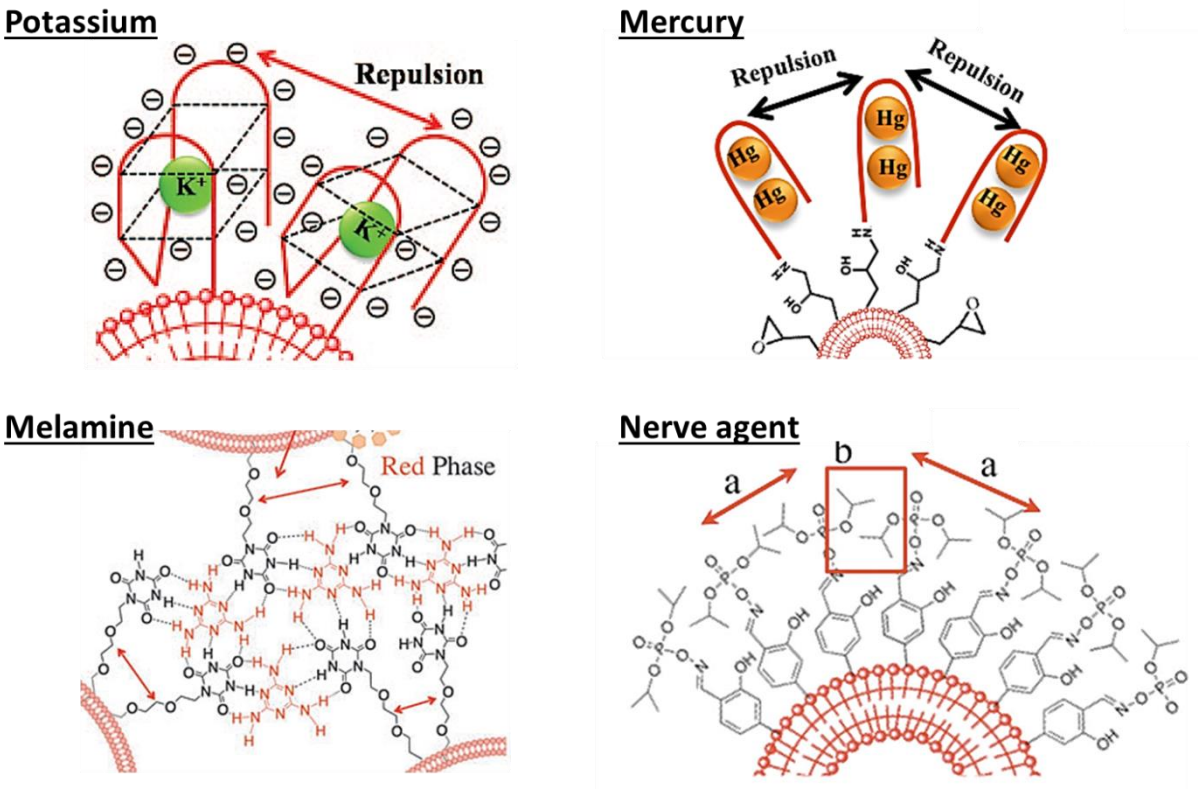

Figure 1.12 Schematic illustration of sensing mechanisms in PDA liposome based sensors for small-molecule targets detection. Reproduced with permission from Ref[12b] Copyright 2008 American Chemical Society. Reproduced from Ref[12a,47] with permission of John Wiley and Sons. Reproduced from Ref[12c] with permission of The Royal Society of Chemistry.

Regarding the sensor developments for biological targets detection, we need consider that the main driving force for PDA sensory signal generation is steric hindrance between adjacent probing receptor-biological target complexes. Mostly, the binding pair will possess protein-protein interaction which influence on H-bonding between diacetylene monomers and alkyl chain packing in PDA sensors. It is similar to those described for thermochromic and pH based

color changes, presumably permitting relief of backbones strain as described in section 1.4.3.3.,[13] but the assumption is not fully demonstrated. It can be expected, however, that the binding of microorganisms at the surface of PDA liposome will affect the structure and optical properties of the polymer through different mechanisms, i.e., the insertion of a target protein into the diacetylene bilayer or the cleavage of diacetylenes by a target enzyme.

1.5.2. Sensitivity

PDA presents colorimetric and fluorometric transition simultaneously when targets of interest bind onto PDA liposome surface. Color change is generally from blue to red, while fluorometric transition from no fluorescence to red fluorescence. The background emission from the blue-phase PDAs is almost negligible due to the extremely low quantum yield ($<1 \times 10^{-4}$).[48] Generally, turn-on type fluoroscence based sensing has higher sensory contrast compared to the colorimetric sensing regarding before and after targeting. However, the fluorescence quantum yield of the PDAs in the red form is only approximately 2×10^{-2} that is much lower than other fluoropohores. Moreover, repulsion based sensing mechanism requires enough number and force of probe-target binding. For these reasons, we should identify molecular design and/or system design parameters that can enhance PDA sensitivity.

1.5.2.1. Target analyte size effect

Seo *et al.* demonstrated that analyte size influences PDA chromism. Small acids did not trigger any noticeable colorimetric transition, while relatively larger nerve agent generated chromism.[49] It was found that a strong correlation exists between the extent of PDA chromatic transition and the molecular size of acid analytes (Figure 1.13a). As an example for PDA sensors, we have studied PDA liposomes having RNA aptamer a the surface to achieve neomycin detection (a similar or larger size target than nerve agent). However, we hardly observed any

turn-on PDA fluorescence after incubating with neomycin. This can be attributed to minimal conformational change or too small repulsion force resulting from the relatively large RNA aptamer probe-small target complexes as illustrated in Figure 1.13b.

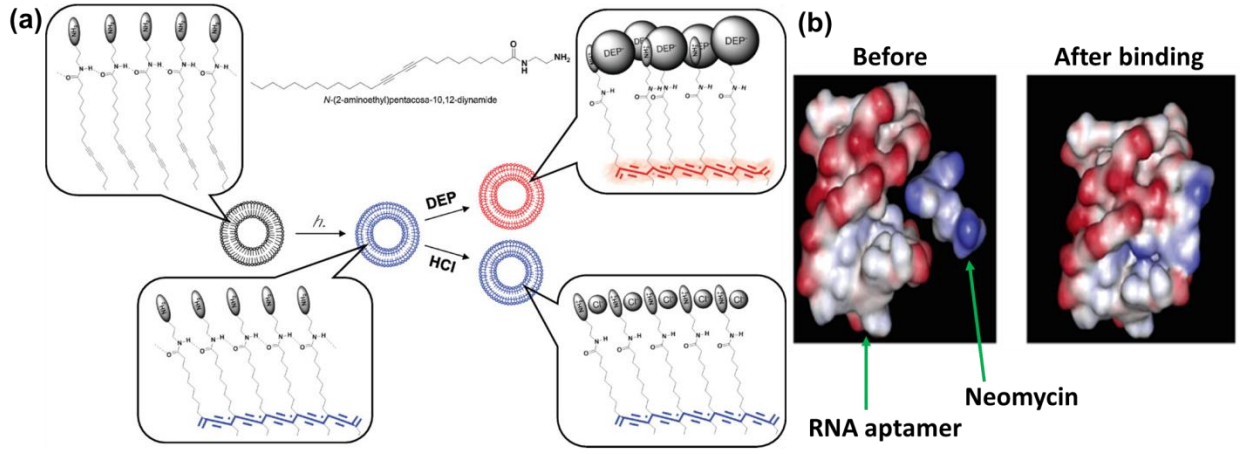

Figure 1.13 (a) Schematic illustration of PDA's selective chromatic transition dependent on the molecular size of acid analytes. Reproduced from Ref[49] with permission of John Wiley and Sons. (b) Recognition event of the RNA aptamer and neomycin showing negligible structural change of the RNA aptamer upon binding with Neomycin. Reproduced with permission from Ref[50] Copyright 2003 American Chemical Society.

Compared with small target molecules (potassium ions, mercury ions, melamine, nerve agents, neomycin) that are less than 1,000 Da (a few nanometer expected at the largest), biological targets are relatively larger and various in size, i.e., antibody (≈ 10 nm), virus (≈ 100 nm), and bacteria (0.5-5 μm in diameter). Therefore, to devise sensitive PDA biosensors, we should design proper probe-target binding pair considering the target size effect. A smaller size probe for a larger target will provide a more sensitive signal generating property to PDA sensors.

1.5.2.2. Character of probe-target binding

In order to devise a selective and sensitive PDA base sensors from a known recognizing pair, we should understand well the features of the recognition event. For example, a specific probe DNA sequence forms bulky quadruplex via intramolecular hydrogen bonding by wrapping

around a target potassium ion. Even though the target is a very small ionic analyte, the bulky quadruplex complexes formation can produce large enough steric repulsion and induce PDA sensory signal. In this regard, we should have specific information about probe-target binding pairs for biosensors development. Most of the selective biosensor design utilizes protein-protein pairing due to their so-called specific lock-key interaction.[51] Also, the biological protein-protein binding requires certain kinetic for complete binding.

1.5.2.3. Efficient transduction of recognition force to PDA backbone

For a long time, researchers have studied alkyl spacer length effect on PDA sensitivity. As expected, the shorter the alkyl chain, the more efficiently the binding event induced force is delivered to the PDA backbone. It was systemically demonstrated that flexible alkyl spacers affect this chromism by decreasing the extent of PDA chromatic transition as the length of the alkyl spacers increases.[49] While the colorimetric response from PDA liposome having a 4-unit ethylene glycol linker was greater than the response from a 3-unit linker, which in turn was greater than the response from material with a 1-unit linker.[14b] It is known that the ethenoxy group in spacer [-$(CH_2CH_2O)_n$-] is hydrophilic, which makes a spacer extending into the water solution and forms a hard rod. According to the leverage principle, longer spacer has a longer arm of force, which exerts a larger force on the PDA liposome when they combine with *E. coli.* target detection. The reduction in the H-bonding between PDA intermolecular packing reduced the energy barrier to changes in the polymer conformation and increased the corresponding color change.

1.5.2.4. Hydrophobic/hydrophilic balance of DAs

For melamine target sensing with PDA molecules, proper hydrophobic/hydrophilic balance for well-ordered liposome formation is essential to generate sensitive sensory signal. To match

the balance, ethylene glycol unit was attached to diacetylenes, and it showed higher sensitivity. As shown in Figure 1.14, there is spatial mismatch between the hydrophilic and hydrophobic parts of PCDA-CA and PCDA.

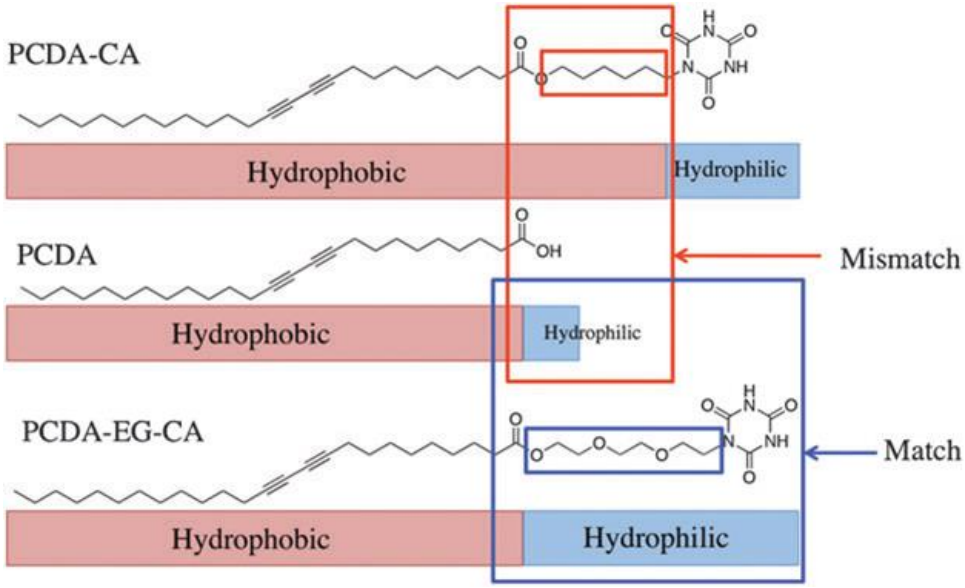

Figure 1.14 Schematic illustration of amphiphilic matching of PCDA, PCDA-CA and PCDA-EG-CA molecules. Reproduced from Ref[12c] with permission of The Royal Society of Chemistry.

The weak blue color after the polymerization was explained by the amphiphilic mismatch and imbalance. Accordingly, PCDA-EG-CA having hydrophilic and flexible linker was designed to achieve improved ordering of the self-assembled liposome.[12c] PCDA-EG-CA has the ethylene glycol linker to match the length of its hydrophobic part with that of PCDA and also has a more balanced amphiphilic structure. As expected, PCDA-EG-CA/PCDA liposomes produced intense blue color upon polymerization and showed better detection limit.

1.5.2.5. Strength of intermolecular packing

Kim *et al.* demonstrated the relationship between functional groups in head moiety of DAs and intermolecular packing.[36] For example, hydrogen bonding between amide groups or between carboxylic acid showed strong intermolecular packing. Moreover, π-π stacking of aromatic rings

in head groups added more strength to the intermolecular binding, resulting in reversible chromism. Therefore, we should consider reducing H-bonding or/and aromatic stacking between PDA head groups to provide high sensitivity (Figure 1.15). Otherwise the strong intermolecular binding among the PDA head groups will make it difficult to perturb the ene-yne backbone by external stimuli. Another way to reduce intermolecular packing is to insert phospholipid into PDA liposome. In general, the insertion of lipids into PDA liposome has a merit to modify the physical properties of PDA liposome such as size,[52] surface charge, and packing of lipids,[53] which, in turn, affect the sensitivity and stability of PDA liposome biosensor.[16b, 54] It has been also reported that a PDA liposome of small size appears to improve sensitivity by compartmentalization of receptor sites. Namely, a smaller liposome can generate an equivalent signal to a larger liposome in spite of less binding of target molecule on the liposome surface.[54a, 55] An appropriate level of surface charge of liposome can also introduce electrostatic repulsion providing resistivity against aggregation and fusion of liposomes.[53b] Likewise, weak packing of lipids (or high membrane fluidity) in PDA liposome enhances sensitivity by making easy distortion of π-conjugated chain of PDA. However, ironically, the weak packing can interrupt polymerization into a stable conjugated chain and deteriorates the degree of fusion.[56] Therefore, we need to make mobile but colloidal stable liposome assembly.

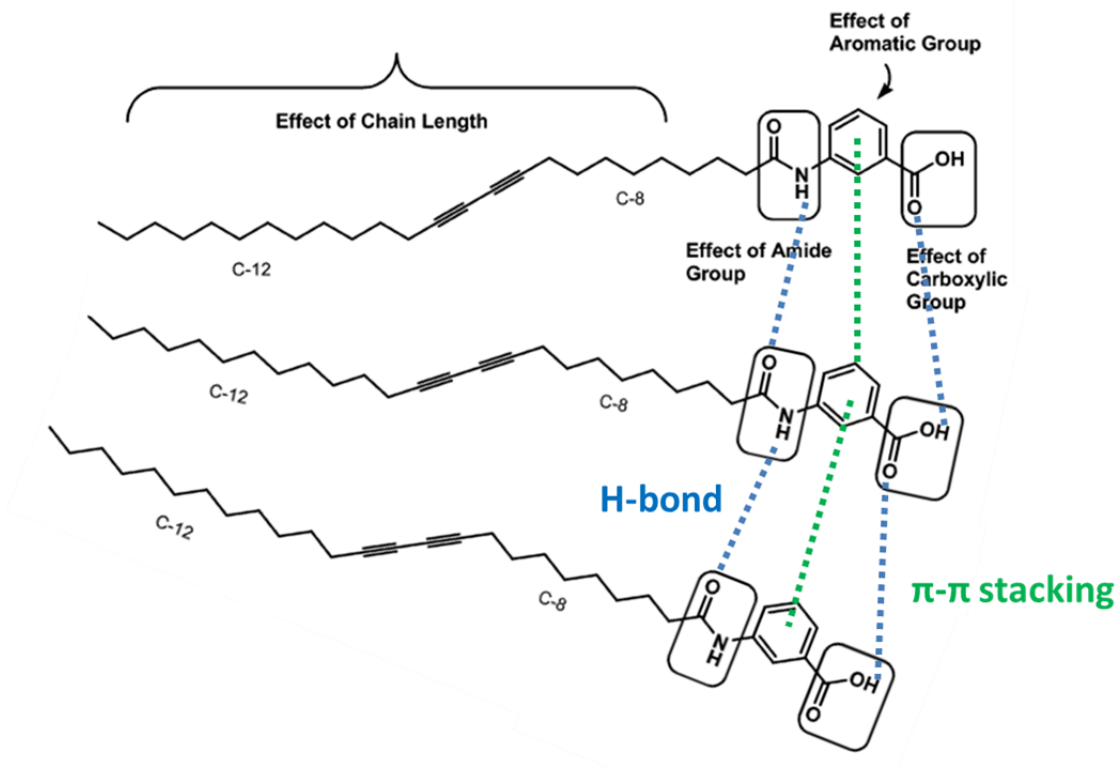

Figure 1.15 Schematic intermolecular packing structures showing secondary interactions (H-bonding, π-π stacking). Reproduced with permission from Ref[36] Copyright 2005 American Chemical Society.

1.5.3. Selectivity

Over the last decades, research has been focused on mimicking cell membrane with PDA monomers, such as sialic acid modified lipid or membrane active compound secreted by pathogens.[57] But these studies had inherently lack of selectivity to target pathogens. Most of the biosensor development is based on identification of a target molecule and availability of a suitable biological recognition element. To date, selectivity of the developed small-molecule detection is evaluated by testing chemicals with similar structures with the target analytes as a negative control. For the detection of biological analytes such as virus and bacteria, probe molecules are usually protein based antibodies and the selectivity of such PDA sensors is assessed by incubating non-specific/different type of antigen or viruses as a negative control.

1.5.4. Stability of PDA supramolecules

Depending on diacetylene derivative monomers, self-assembled PDAs in aqueous medium preserve their shape and sensitivity toward target anayltes from few days to months. If PDA colloids are photopolymerized in PBS buffer medium, blue color turns to pale violet at room temperature after one day. (Figure 1.16a) It is because of sodium chloride in PBS buffer trigers false alarm. It has been confirmed that the PDA liposomes are stable in PBS buffer with less amounts of sodium chloride (50 % of NaCl in 1xPBS). Therefore, diluted 0.1 x PBS buffer condition or solid-state detection are more suitable conditions for clinical biosensor applications.

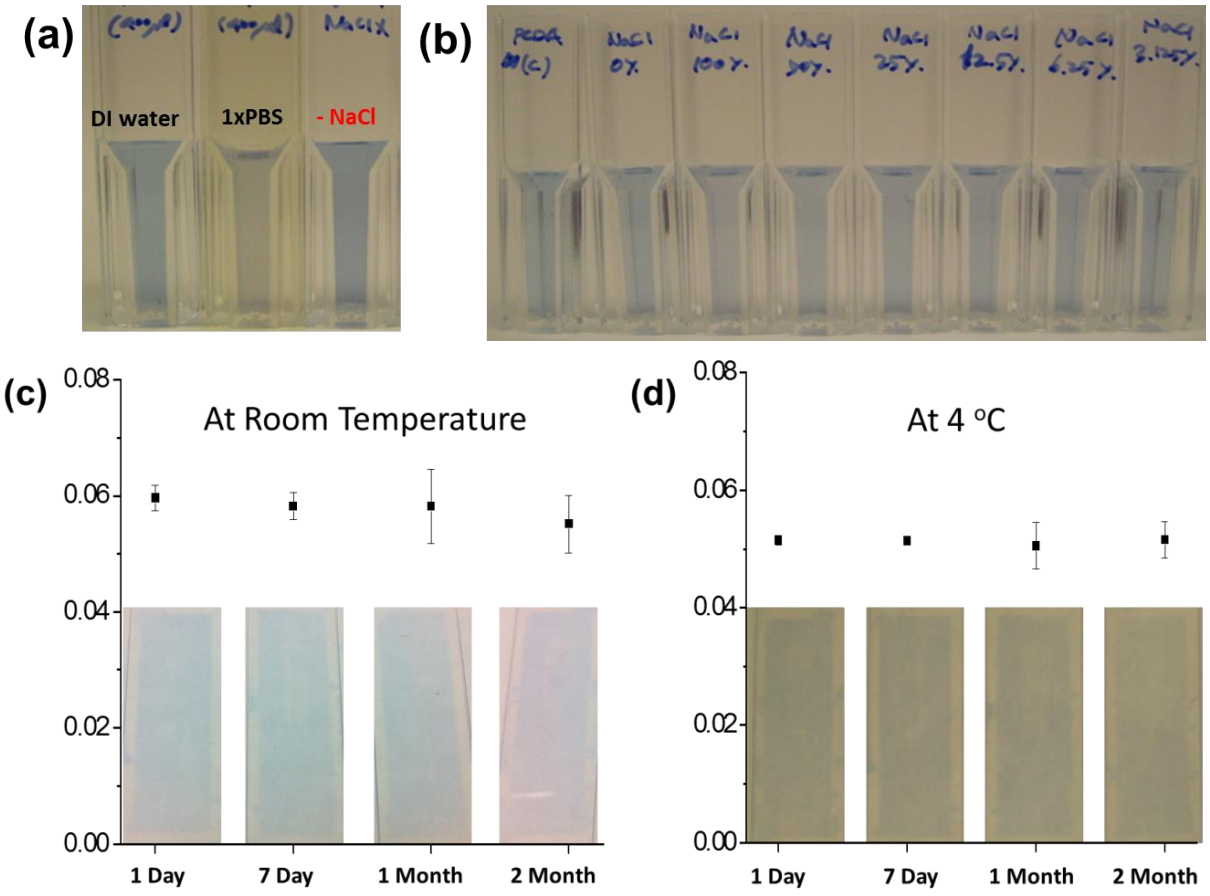

Figure 1.16 Colloidal stability test of PDA liposome at room temperature (after 1 day) by adding (a) deionized water, 1xPBS, and 1xPBS without NaCl, (b) 1xPBS at various NaCl concentrations. Time-lapse stability of solid-state PDA liposome microarray at (c) room temperature, (d) 4 ^{o}C.

1.6. References

1. Thusu, Rajender. Strong growth predicted for biosensors market. Sensors magazine. Oct. 1. 2010. Retrieved from http://www.sensorsmag.com/specialty-markets/medical/strong-growth-predicted-biosensors-market-7640.
2. Harvey, David. Under a Creative Commons license. Retrieved from http://chemwiki.ucdavis.edu/Analytical_Chemistry/Analytical_Chemistry_2.0/11_Electrochemical_Methods/11D_Voltammetric_Methods.
3. Shirakawa, H.; Louis, E. J.; MacDiarmid, A. G.; Chiang, C. K.; Heeger, A. J., Synthesis of electrically conducting organic polymers: halogen derivatives of polyacetylene, (CH). *Journal of the Chemical Society, Chemical Communications* **1977,** (16), 578-580.
4. (a) KimJ; SwagerM, erratum: Control of conformational and interpolymer effects in conjugated polymers. *Nature* **2001,** *413* (6855), 548-548; (b) Kim, J.; Levitsky, I. A.; McQuade, D. T.; Swager, T. M., Structural Control in Thin Layers of Poly(p-phenyleneethynylene)s: Photophysical Studies of Langmuir and Langmuir−Blodgett Films. *Journal of the American Chemical Society* **2002,** *124* (26), 7710-7718; (c) Wang, Y.; Zappas, A. J.; Wilson, J. N.; Kim, I.-B.; Solntsev, K. M.; Tolbert, L. M.; Bunz, U. H. F., Optical Spectroscopy of Grafted Poly(p-phenyleneethynylene)s in Water and Water−DMF Mixtures. *Macromolecules* **2008,** *41* (4), 1112-1117; (d) Lebouch, N.; Garreau, S.; Louarn, G.; Belletête, M.; Durocher, G.; Leclerc, M., Structural Study of the Thermochromic Transition in Poly(2,5-dialkyl-p-phenyleneethynylene)s. *Macromolecules* **2005,** *38* (23), 9631-9637; (e) Zhao, X.; Pinto, M. R.; Hardison, L. M.; Mwaura, J.; Müller, J.; Jiang, H.;

Witker, D.; Kleiman, V. D.; Reynolds, J. R.; Schanze, K. S., Variable Band Gap Poly(arylene ethynylene) Conjugated Polyelectrolytes. *Macromolecules* **2006,** *39* (19), 6355-6366; (f) Bunz, U. H. F.; Imhof, J. M.; Bly, R. K.; Bangcuyo, C. G.; Rozanski, L.; Vanden Bout, D. A., Photophysics of Poly[p-(2,5-didodecylphenylene)ethynylene] in Thin Films. *Macromolecules* **2005,** *38* (14), 5892-5896.

5. (a) McQuade, D. T.; Pullen, A. E.; Swager, T. M., Conjugated Polymer-Based Chemical Sensors. *Chemical Reviews* **2000,** *100* (7), 2537-2574; (b) Zhou, Q.; Swager, T. M., Fluorescent Chemosensors Based on Energy Migration in Conjugated Polymers: The Molecular Wire Approach to Increased Sensitivity. *Journal of the American Chemical Society* **1995,** *117* (50), 12593-12602; (c) Swager, T. M., The Molecular Wire Approach to Sensory Signal Amplification. *Accounts of Chemical Research* **1998,** *31* (5), 201-207.
6. (a) Lee, Kangwon. Functionalized conjugated polymers for signal amplifying biosensors and sensor arrays (Doctoral dissertation). ; (b) Lee, K.; Lee, J.; Jeong, E. J.; Kronk, A.; Elenitoba-Johnson, K. S. J.; Lim, M. S.; Kim, J., Conjugated Polyelectrolyte-Antibody Hybrid Materials for Highly Fluorescent Live Cell-Imaging. *Advanced Materials* **2012,** *24* (18), 2479-2484.
7. Wang, F.; Bazan, G. C., Aggregation-Mediated Optical Properties of pH-Responsive Anionic Conjugated Polyelectrolytes. *Journal of the American Chemical Society* **2006,** *128* (49), 15786-15792.
8. (a) Reppy, M. A.; Pindzola, B. A., Biosensing with polydiacetylene materials: structures, optical properties and applications. *Chemical Communications* **2007,** (42), 4317-4338; (b) Jelinek, R.; Kolusheva, S., Biomolecular Sensing with Colorimetric Vesicles. In *Creative Chemical Sensor Systems*, Schrader, T., Ed. Springer Berlin Heidelberg: 2007; Vol. 277, pp

155-180; (c) Ahn, D. J.; Kim, J. M., Fluorogenic polydiacetylene supramolecules: immobilization, micropatterning, and application to label-free chemosensors. *Acc Chem Res* **2008,** *41* (7), 805-16; (d) Yoon, B.; Lee, S.; Kim, J.-M., Recent conceptual and technological advances in polydiacetylene-based supramolecular chemosensors. *Chemical Society Reviews* **2009,** *38* (7), 1958-1968; (e) Lee, K.; Povlich, L. K.; Kim, J., Recent advances in fluorescent and colorimetric conjugated polymer-based biosensors. *Analyst* **2010,** *135* (9), 2179-2189.

9. (a) Cheng, Q.; Stevens, R. C., Charge-Induced Chromatic Transition of Amino Acid-Derivatized Polydiacetylene Liposomes. *Langmuir* **1998,** *14* (8), 1974-1976; (b) Jonas, U.; Shah, K.; Norvez, S.; Charych, D. H., Reversible Color Switching and Unusual Solution Polymerization of Hydrazide-Modified Diacetylene Lipids. *Journal of the American Chemical Society* **1999,** *121* (19), 4580-4588.
10. (a) Carpick, R. W.; Sasaki, D. Y.; Burns, A. R., First Observation of Mechanochromism at the Nanometer Scale. *Langmuir* **2000,** *16* (3), 1270-1278; (b) Chance, R. R.; Patel, G. N.; Witt, J. D., Thermal effects on the optical properties of single crystals and solution-cast films of urethane substituted polydiacetylenes. *The Journal of Chemical Physics* **1979,** *71* (1), 206-211.
11. Tashiro, K.; Nishimura, H.; Kobayashi, M., First Success in Direct Analysis of Microscopic Deformation Mechanism of Polydiacetylene Single Crystal by the X-ray Imaging-Plate System. *Macromolecules* **1996,** *29* (25), 8188-8196.
12. (a) Lee, J.; Jun, H.; Kim, J., Polydiacetylene–Liposome Microarrays for Selective and Sensitive Mercury(II) Detection. *Advanced Materials* **2009,** *21* (36), 3674-3677; (b) Lee, J.; Kim, H.-J.; Kim, J., Polydiacetylene Liposome Arrays for Selective Potassium Detection.

Journal of the American Chemical Society **2008,** *130* (15), 5010-5011; (c) Lee, J.; Jeong Jeong, E.; Kim, J., Selective and sensitive detection of melamine by intra/inter liposomal interaction of polydiacetylene liposomes. *Chemical Communications* **2011,** *47* (1), 358-360.

13. Charych, D.; Nagy, J.; Spevak, W.; Bednarski, M., Direct colorimetric detection of a receptor-ligand interaction by a polymerized bilayer assembly. *Science* **1993,** *261* (5121), 585-588.
14. (a) Zhang, Y.; Fan, Y.; Sun, C.; Shen, D.; Li, Y.; Li, J., Functionalized polydiacetylene-glycolipid vesicles interacted with Escherichia coli under the TiO2 colloid. *Colloids and Surfaces B: Biointerfaces* **2005,** *40* (3-4), 137-142; (b) Ma, Z.; Li, J.; Jiang, L.; Cao, J.; Boullanger, P., Influence of the Spacer Length of Glycolipid Receptors in Polydiacetylene Vesicles on the Colorimetric Detection of Escherichia coli. *Langmuir* **2000,** *16* (20), 7801-7804.
15. Pindzola, B. A.; Nguyen, A. T.; Reppy, M. A., Antibody-functionalized polydiacetylene coatings on nanoporous membranes for microorganism detection. *Chemical Communications* **2006,** (8), 906-908.
16. (a) Su, Y.-l.; Li, J.-r.; Jiang, L., Chromatic immunoassay based on polydiacetylene vesicles. *Colloids and Surfaces B: Biointerfaces* **2004,** *38* (1–2), 29-33; (b) Lee, S. W.; Kang, C. D.; Yang, D. H.; Lee, J. S.; Kim, J. M.; Ahn, D. J.; Sim, S. J., The Development of a Generic Bioanalytical Matrix Using Polydiacetylenes. *Advanced Functional Materials* **2007,** *17* (13), 2038-2044; (c) Kolusheva, S.; Kafri, R.; Katz, M.; Jelinek, R., Rapid Colorimetric Detection of Antibody−Epitope Recognition at a Biomimetic Membrane Interface. *Journal of the American Chemical Society* **2000,** *123* (3), 417-422.
17. (a) Rozner, S.; Kolusheva, S.; Cohen, Z.; Dowhan, W.; Eichler, J.; Jelinek, R., Detection and

analysis of membrane interactions by a biomimetic colorimetric lipid/polydiacetylene assay. *Analytical Biochemistry* **2003,** *319* (1), 96-104; (b) Rangin, M.; Basu, A., Lipopolysaccharide Identification with Functionalized Polydiacetylene Liposome Sensors. *Journal of the American Chemical Society* **2004,** *126* (16), 5038-5039; (c) Chen, X.; Lee, J.; Jou, M. J.; Kim, J.-M.; Yoon, J., Colorimetric and fluorometric detection of cationic surfactants based on conjugated polydiacetylene supramolecules. *Chemical Communications* **2009,** (23), 3434-3436.

18. (a) Deckert, A. A.; Horne, J. C.; Valentine, B.; Kiernan, L.; Fallon, L., Effects of Molecular Area on the Polymerization and Thermochromism of Langmuir-Blodgett Films of Cd2+ Salts of 5,7-Diacetylenes Studied Using UV-Visible Spectroscopy. *Langmuir* **1995,** *11* (2), 643-649; (b) Geiger, E.; Hug, P.; Keller, B. A., Chromatic Transitions in Polydiacetylene Langmuir-Blodgett Films due to Molecular Recognition at the Film Surface Studied by Spectroscopic Methods and Surface Analysis. *Macromolecular Chemistry and Physics* **2002,** *203* (17), 2422-2431; (c) Wang, S.; Ramirez, J.; Chen, Y.; Wang, P. G.; Leblanc, R. M., Surface Chemistry, Topography, and Spectroscopy of a Mixed Monolayer of 10,12-Pentacosadiynoic Acid and Its Mannoside Derivative at the Air−Water Interface. *Langmuir* **1999,** *15* (17), 5623-5629; (d) Gaboriaud, F.; Golan, R.; Volinsky, R.; Berman, A.; Jelinek, R., Organization and Structural Properties of Langmuir Films Composed of Conjugated Polydiacetylene and Phospholipids. *Langmuir* **2001,** *17* (12), 3651-3657.

19. (a) Kim, T.; Crooks, R. M.; Tsen, M.; Sun, L., Polymeric Self-Assembled Monolayers. 2. Synthesis and Characterization of Self-Assembled Polydiacetylene Mono- and Multilayers. *Journal of the American Chemical Society* **1995,** *117* (14), 3963-3967; (b) Mowery, M. D.; Menzel, H.; Cai, M.; Evans, C. E., Fabrication of Monolayers Containing Internal Molecular

Scaffolding: Effect of Substrate Preparation. *Langmuir* **1998,** *14* (19), 5594-5602.

20. (a) Evrard, D.; Touitou, E.; Kolusheva, S.; Fishov, Y.; Jelinek, R., A New Colorimetric Assay for Studying and Rapid Screening of Membrane Penetration Enhancers¥. *Pharm Res* **2001,** *18* (7), 943-949; (b) Schnur, J. M.; Price, R.; Schoen, P.; Yager, P.; Calvert, J. M.; Georger, J.; Singh, A., Lipid-based tubule microstructures. *Thin Solid Films* **1987,** *152* (1–2), 181-206; (c) Frankel, D. A.; O'Brien, D. F., Supramolecular Assemblies of Diacetylenic Aldonamides. *Journal of the American Chemical Society* **1994,** *116* (22), 10057-10069; (d) Yamanaka, S. A.; Charych, D. H.; Loy, D. A.; Sasaki, D. Y., Solid Phase Immobilization of Optically Responsive Liposomes in Sol-Gel Materials for Chemical and Biological Sensing. *Langmuir* **1997,** *13* (19), 5049-5053; (e) Gill, I.; Ballesteros, A., Immunoglobulin–Polydiacetylene Sol–Gel Nanocomposites as Solid-State Chromatic Biosensors. *Angewandte Chemie* **2003,** *115* (28), 3386-3389.
21. KSV NIMA web. Retrieved from http://www.ksvnima.com/technologies/langmuir-blodgett-langmuir-schaefer-technique.
22. Gaboriaud, F.; Volinsky, R.; Berman, A.; Jelinek, R., Temperature dependence of the organization and molecular interactions within phospholipid/diacetylene Langmuir films. *Journal of Colloid and Interface Science* **2005,** *287* (1), 191-197.
23. Sullivan, S. P.; Schnieders, A.; Mbugua, S. K.; Beebe, T. P., Controlled Polymerization of Substituted Diacetylene Self-Organized Monolayers Confined in Molecule Corrals. *Langmuir* **2004,** *21* (4), 1322-1327.
24. Martinsson, Erik. Retrieved fromhttps://www.ifm.liu.se/applphys/molphys/research/self/.
25. Okawa, Y.; Akai-Kasaya, M.; Kuwahara, Y.; Mandal, S. K.; Aono, M., Controlled chain polymerisation and chemical soldering for single-molecule electronics. *Nanoscale* **2012,** *4*,

3013-3028.

26. Okada, S.; Peng, S.; Spevak, W.; Charych, D., Color and Chromism of Polydiacetylene Vesicles. *Accounts of Chemical Research* **1998,** *31* (5), 229-239.

27. Hupfer, B.; Ringsdorf, H.; Schupp, H., Liposomes from polymerizable phospholipids. *Chemistry and Physics of Lipids* **1983,** *33* (4), 355-374.

28. Park, K. H.; Lee, J.-S.; Park, H.; Oh, E.-H.; Kim, J.-M., Vancomycin-induced morphological transformation of self-assembled amphiphilic diacetylene supramolecules. *Chemical Communications* **2007,** (4), 410-412.

29. Park, H.; Lee, J. S.; Choi, H.; Ahn, D. J.; Kim, J. M., Rational Design of Supramolecular Conjugated Polymers Displaying Unusual Colorimetric Stability upon Thermal Stress. *Advanced Functional Materials* **2007,** *17* (17), 3447-3455.

30. Zhou, W.; Li, Y.; Zhu, D., Progress in Polydiacetylene Nanowires by Self-Assembly and SelfPolymerization. *Chemistry – An Asian Journal* **2007,** *2* (2), 222-229.

31. Bai, F.; Sun, Z.; Lu, P.; Fan, H., Smart polydiacetylene nanowire paper with tunable colorimetric response. *Journal of Materials Chemistry* **2012,** *22* (30), 14839-14842.

32. Diegelmann, S. R.; Hartman, N.; Markovic, N.; Tovar, J. D., Synthesis and Alignment of Discrete Polydiacetylene-Peptide Nanostructures. *Journal of the American Chemical Society* **2012,** *134* (4), 2028-2031.

33. Plant, A. L.; Benson, D. M.; Trusty, G. L., Probing the structure of diacetylenic phospholipid tubules with fluorescent lipophiles. *Biophysical Journal* **1990,** *57* (5), 925-933.

34. Hsu, L.; Cvetanovich, G. L.; Stupp, S. I., Peptide Amphiphile Nanofibers with Conjugated Polydiacetylene Backbones in Their Core. *Journal of the American Chemical Society* **2008,** *130* (12), 3892-3899.

35. (a) Cheng, Q.; Yamamoto, M.; Stevens, R. C., Amino Acid Terminated Polydiacetylene Lipid Microstructures: Morphology and Chromatic Transition. *Langmuir* **2000,** *16* (12), 5333-5342; (b) Song, J.; Cisar, J. S.; Bertozzi, C. R., Functional Self-Assembling Bolaamphiphilic Polydiacetylenes as Colorimetric Sensor Scaffolds. *Journal of the American Chemical Society* **2004,** *126* (27), 8459-8465.

36. Kim, J.-M.; Lee, J.-S.; Choi, H.; Sohn, D.; Ahn, D. J., Rational Design and in-Situ FTIR Analyses of Colorimetrically Reversibe Polydiacetylene Supramolecules. *Macromolecules* **2005,** *38* (22), 9366-9376.

37. (a) Baughman, R. H.; Yee, K. C., Solid-state polymerization of linear and cyclic acetylenes. *Journal of Polymer Science: Macromolecular Reviews* **1978,** *13* (1), 219-239; (b) Enkelmann, V., Structural aspects of the topochemical polymerization of diacetylenes. In *Polydiacetylenes*, Cantow, H.-J., Ed. Springer Berlin Heidelberg: 1984; Vol. 63, pp 91-136.

38. Lu, Y.; Yang, Y.; Sellinger, A.; Lu, M.; Huang, J.; Fan, H.; Haddad, R.; Lopez, G.; Burns, A. R.; Sasaki, D. Y.; Shelnutt, J.; Brinker, C. J., Self-assembly of mesoscopically ordered chromatic polydiacetylene/silica nanocomposites. *Nature* **2001,** *410* (6831), 913-917.

39. Berman, A.; Ahn, D. J.; Lio, A.; Salmeron, M.; Reichert, A.; Charych, D., Total Alignment of Calcite at Acidic Polydiacetylene Films: Cooperativity at the Organic-Inorganic Interface. *Science* **1995,** *269* (5223), 515-518.

40. Batchelder, D. N.; Evans, S. D.; Freeman, T. L.; Haeussling, L.; Ringsdorf, H.; Wolf, H., Self-Assembled Monolayers containing Polydiacetylenes. *Journal of the American Chemical Society* **1994,** *116* (3), 1050-1053.

41. Fujita, N.; Sakamoto, Y.; Shirakawa, M.; Ojima, M.; Fujii, A.; Ozaki, M.; Shinkai, S., Polydiacetylene Nanofibers Created in Low-Molecular-Weight Gels by Post Modification:

Control of Blue and Red Phases by the Odd−Even Effect in Alkyl Chains. *Journal of the American Chemical Society* **2007,** *129* (14), 4134-4135.

42. Wenz, G.; Mueller, M. A.; Schmidt, M.; Wegner, G., Structure of poly(diacetylenes) in solution. *Macromolecules* **1984,** *17* (4), 837-850.
43. Shand, M. L.; Chance, R. R.; LePostollec, M.; Schott, M., Raman photoselection and conjugation-length dispersion in conjugated polymer solutions. *Physical Review B* **1982,** *25* (7), 4431-4436.
44. Soos, Z. G.; Galvão, D. S.; Etemad, S., Fluorescence and excited-state structure of conjugated polymers. *Advanced Materials* **1994,** *6* (4), 280-287.
45. Dobrosavljević, V.; Stratt, R. M., Role of conformational disorder in the electronic structure of conjugated polymers: Substituted polydiacetylenes. *Physical Review B* **1987,** *35* (6), 2781-2794.
46. Huo, Q.; Russell, K. C.; Leblanc, R. M., Chromatic Studies of a Polymerizable Diacetylene Hydrogen Bonding Self-Assembly: A "Self-Folding" Process To Explain the Chromatic Changes of Polydiacetylenes. *Langmuir* **1999,** *15* (11), 3972-3980.
47. Lee, J.; Seo, S.; Kim, J., Colorimetric Detection of Warfare Gases by Polydiacetylenes Toward Equipment-Free Detection. *Advanced Functional Materials* **2012,** *22* (8), 1632-1638.
48. (a) Jundt, C.; Klein, G.; Le Moigne, J., Yields of triplet exciton pairs in polydiacetylene films. *Chemical Physics Letters* **1993,** *203* (1), 37-40; (b) Olmsted, J.; Strand, M., Fluorescence of polymerized diacetylene bilayer films. *The Journal of Physical Chemistry* **1983,** *87* (24), 4790-4792.
49. Seo, D.; Kim, J., Effect of the Molecular Size of Analytes on Polydiacetylene Chromism.

Advanced Functional Materials **2010,** *20* (9), 1397-1403.

50. Arya, D.; Micovic, L.; Charles, I.; Coffee, R. L.; Willis, B.; Xue, L., Neomycin Binding to Watson-Hoogsteen (W-H) DNA Triplex Groove: A Model. *Journal of the American Chemical Society* **2003,** *125* (13), 3733-3744.
51. Margulies, D.; Hamilton, A. D., Combinatorial protein recognition as an alternative approach to antibody-mimetics. *Current Opinion in Chemical Biology* **2010,** *14* (6), 705-712.
52. Kolusheva, S.; Wachtel, E.; Jelinek, R., Biomimetic lipid/polymer colorimetric membranes: molecular and cooperative properties. *Journal of Lipid Research* **2003,** *44* (1), 65-71.
53. Kim, K.-W.; Choi, H.; Lee, G. S.; Ahn, D. J.; Oh, M.-K., Effect of phospholipid insertion on arrayed polydiacetylene biosensors. *Colloids and Surfaces B: Biointerfaces* **2008,** *66* (2), 213-217.
54. (a) Guo, C. X.; Boullanger, P.; Liu, T.; Jiang, L., Size Effect of Polydiacetylene Vesicles Functionalized with Glycolipids on Their Colorimetric Detection Ability. *The Journal of Physical Chemistry B* **2005,** *109* (40), 18765-18771; (b) Yaroslavov, A. A.; Sybachin, A. V.; Kesselman, E.; Schmidt, J.; Talmon, Y.; Rizvi, S. A. A.; Menger, F. M., Liposome Fusion Rates Depend upon the Conformation of Polycation Catalysts. *Journal of the American Chemical Society* **2011,** *133* (9), 2881-2883.
55. Schneider, H.-J.; Tianjun, L.; Lomadze, N., Sensitivity increase in molecular recognition by decrease of the sensing particle size and by increase of the receptor binding site - a case with chemomechanical polymers. *Chemical Communications* **2004,** (21), 2436-2437.
56. Wilschut, J.; Duzgunes, N.; Hoekstra, D.; Papahadjopoulos, D., Modulation of membrane fusion by membrane fluidity: temperature dependence of divalent cation induced fusion of phosphatidylserine vesicles. *Biochemistry* **1985,** *24* (1), 8-14.

57. (a) Deng, J.; Sheng, Z.; Zhou, K.; Duan, M.; Yu, C.-y.; Jiang, L., Construction of Effective Receptor for Recognition of Avian Influenza H5N1 Protein HA1 by Assembly of Monohead Glycolipids on Polydiacetylene Vesicle Surface. *Bioconjugate Chemistry* **2009,** *20* (3), 533-537; (b) Silbert, L.; Ben Shlush, I.; Israel, E.; Porgador, A.; Kolusheva, S.; Jelinek, R., Rapid Chromatic Detection of Bacteria by Use of a New Biomimetic Polymer Sensor. *Applied and Environmental Microbiology* **2006,** *72* (11), 7339-7344.

CHAPTER 2

Polydiacetylene Liposome Microarray Sensor Development for Influenza A Virus Detection

Published in Macromolecular Rapid Communications, vol. 34, pp 743-748, 2013

2.1. Introduction

The emergence of the influenza A virus pandemic in 2009 aroused an increasing need for its rapid and sensitive detection.[1] There are two ways to identify the influenza A virus infection. The first one is a direct detection method, such as recognizing peptides or proteins originated from the influenza A virus, or sensing the virus itself. For an alternative indirect detection strategy, produced antibodies from influenza A virus infections are identified by using enzyme linked immunosorbent assays (ELISA) or real time polymerase chain reaction (RT-PCR). However, because these methods are expensive and require long sample preparation and operation, a cheaper and more rapid diagnostic test system is strongly desired.

Polydiacetylene (PDA) has been attractive for sensory applications due to its unique optical property; PDA undergoes colorimetric transitions by various external stimuli, such as temperature,[2] pH,[3] mechanical stress,[4] and receptor–ligand interactions.[5] The thermochromism and pH-based colorimetric transitions have been attributed to conformational changes in the head group hydrogen bonding and alkyl side chain packing of PDA molecules by an external

stimulus.[6] We have developed PDA-based sensors using the intermolecular force that receptor–ligand interactions produce, as an external stimulus, i.e., a DNA sequence or a phospholipid as a selective probe for the detection of a target molecule such as K^+, Hg^{2+}, and aminoglycosidic antibiotic.[7] The steric repulsion between the bulky probe–target complexes induced the perturbation of the conjugated ene-yne backbone of PDA, resulting in a colorimetric transition from blue to red and red fluorescence development as well. However, even though systematic investigation has been made to build better understanding about the effect of the analyte size on the signaling property of PDA, the mechanisms for the color change in the presence of biological probe-target interactions at the surface of PDA are not fully understood.[8] For example, how microorganism induces the color change of PDA has been debated through various hypotheses, such as conformational change of PDA backbone via the insertion of proteins into the bi-layer of PDA liposomes or cleavage of PDA lipids by an enzyme.[6a] Therefore, to design sensitive and practically applicable biosensors, developing better understanding about the critical factors causing the colorimetric transition under biological probe–target interactions is very important.

In this contribution, we demonstrated a rapid and sensitive PDA-based microarray sensor for influenza A virus detection. We chose the pair of influenza A virus M1 peptide-M1 antibody as a probe–target model. Due to easy tethering of biomolecules such as peptide or antibody at the surface of PDA liposomes, we designed and analyzed direct and indirect detection strategies by switching the role of M1 peptide and M1 antibody as a probe molecule or a target molecule. By using the same pair but only switching their role in the detection system, we could keep the same paring affinity and therefore expound the target size effect on the turn-on signaling of PDA-based sensory systems. For the development of a real detection system, we incorporated 1,2-dimyristoyl-sn-glycero-3-phosphocholine (DMPA) phospholipid into the PDA liposome in order

to give better mobility to the PDA backbone in the liposome, which as a consequence improved the sensitivity of the PDA microarray for influenza A H1N2 virus detection.

2.2. Experimental section

2.2.1. Materials and methods

All solvents were purchased from Sigma–Aldrich. 10,12-pentacosadiynoic acid (PCDA) was purchased from GFS Chemicals. N-hydroxysuccinimide (NHS) and 1-ethyl-3-(3-dimethylaminopropyl) carbodiimide hydrochloride were obtained from Acros Organics. 2-(2-aminoethoxy)ethanol, epibromohydrin, sodium hydride, 4-(2-hydroxyethyl)piperazine-1-ethanesulfonic acid (HEPES), phosphate buffered saline (PBS), and Tween® 20 were purchased from Sigma–Aldrich. 1,2-dimyristoylsn-glycero-3-phosphate (DMPA) were purchased from Avanti Polar Lipids. The frame-seal slide chambers for the liposome immobilization was obtained from Bio-Rad.

Influenza A virus M1 peptide (Matrix Protein 1 peptide, purity > 90%, SIIPSGPLK, Mw 911.1) was purchased from AnaSpec. Mouse monoclonal to influenza A virus M1 antibody and NP antibody were obtained from Abcam. Influenza A H1N2 virus (swine/Korea/H1N2) was supplied by Animal Plant and Fisheries Quarantine and Inspection Agency (QIA).

The synthesis of PCDA derivatives was described in our previous work.[7a] The PDA monomers were characterized with 1H NMR spectra (500 MHz) using Varian Inova 500 instrument. UV–Vis absorption spectra were obtained by Varian Cary 50 UV–Vis spectrophotometer. Fluorescence images were taken by Olympus BX51 with DP71 fluorescent microscope. Evaluation of the fluorescent dot intensity was carried out by using Image J software.

2.2.2. Preparation of PDA liposome solution

PDA liposome solution was prepared by the injection method. PCDA-Epoxy and PCDA (4:1 molar ratio) were dissolved in 0.2 mL of tetrahydrofuran. The homogeneous solution was injected into a 20 mL of 5×10^{-3} M HEPES buffer at pH 8 and subsequently dispersed in a bath sonicator for 10 s to produce the final concentration of the liposome of 0.5×10^{-3} M . After filtration through a 0.8 μm cellulose acetate syringe filter, the resulting PDA liposome solution was stored at 5 ℃ at least 2 h for the next immobilization step.

2.2.3. Fabrication of PDA liposome microarray

An amine-modified glass slide was prepared similarly through the literature procedure.[7b] Glass slides were cleaned with chloroform, acetone, and 2-propanol for 3 min each. The pre-cleaned glass slides were then sonicated in sulfuric acid containing NOCHROMIX. After thorough rinse with deionized water and dry, the glass slides were stirred in a 2 wt% 3-aminopropyltriethoxysilane toluene solution using an orbital shaker for 1 h and afterward baked at 115 ℃ for 30 min. The glass slides were sonicated in toluene, toluene: methanol (1:1), and methanol for 3 min each to remove any unbound silane monomer.

We devised PDA liposome microarrays using two strategies. First, as illustrated in Scheme 1 of Figure 2.2, PDA liposome was immobilized onto the prepared amine glass by means of 20 min incubation and by successive thorough rinse with 5×10^{-3} M HEPES buffer at pH 8.0 followed by additional rinse with deionized water. Onto the immobilized PDA layer, a probe solution (M1 peptide or M1 antibody) was microarrayed using a manual microarrayer (VP 478A, V&P Scientific) and incubated at 5 ℃ for overnight. After washing with 0.2% (v/v) PBST (0.2% Tween 20 in 1 x PBS) and deionized water, the probe-tethered PDA slides were treated with ethanolamine to block the unreacted area. The prepared PDA microarrays were

photopolymerized by 254 nm UV light for 30 s right before the detection tests. Second, as depicted in Scheme 2 of Figure 2, PDA liposome was microarrayed onto the amine glass using the manual microarrayer for a 20 min incubation period. It was then rinsed with 5×10^{-3} M HEPES buffer at pH 8.0, and washed with deionized water. Then, a probe solution (M1 peptide or M1antibody) was covered onto the prepared PDA layer and the slides were stirred using an orbital shaker at room temperature for 1 h and left at 5 ℃ for overnight. After washing with 0.2% (v/v) PBST and deionized water, respectively, the probe-tethered PDA slides were treated with ethanolamine to block the unreacted area. The prepared PDA microarrays were photopolymerized by 254 nm UV light for 30 s right before the detection tests.

2.2.4. Detection tests

To investigate the selectivity and sensitivity, the PDA liposome microarrays were incubated with a target solution (M1 peptide, M1 antibody, NP antibody, or influenza A H1N2 virus) at room temperature for 1 h.

2.3. Results and discussion

We investigated how the known specific interaction between the M1 peptide and the M1 antibody[9] can be rationally combined with our PDA liposome-based sensory system to detect influenza A virus. We prepared PDA liposome microarrays for influenza A virus detection as schematically illustrated in Figure 2.1.

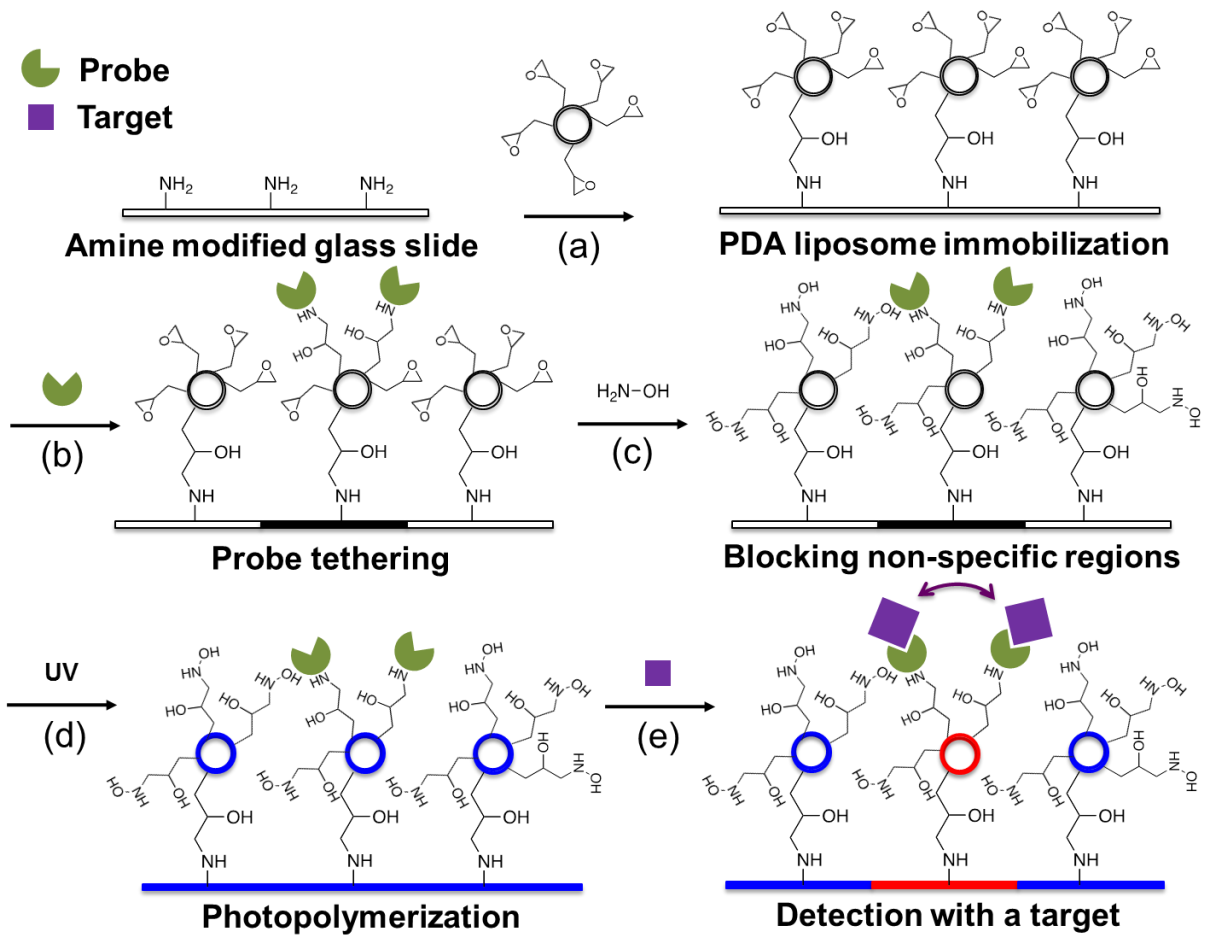

Figure 2.1 Schematic illustration of the PDA liposome microarray fabrication. (a) Immobilization of PDA liposomes onto an amine-modified glass slide, (b) probe molecule tethering, (c) blocking the probe-free area with ethanolamine to prevent non-specific binding, (d) photopolymerization, and (e) detection with a target. Arrow presents repulsion between adjacent probe–target complexes.

The bare glass (60 mm × 19 mm) was silanized with aminopropyltriethoxysilane to modify the surface to have primary amine groups. The epoxy functionality was used for the probe tethering as well as the liposome immobilization. Through optimization study, the 4:1 molar ratio of PCDA–Epoxy to PCDA was established to provide the most stable and sensitive detection. The liposome was covalently bound on the amine glass by amine-epoxide reaction. The M1 antibody was used as a probe molecule for M1 peptide detection while the M1 peptide

was utilized as a probe for M1 antibody detection. After tethering the probe molecules (M1 antibody or M1 peptide) as circular dots having diameter of 400 μ m, with ethanolamine we blocked the area where probe molecules are not present in order to avoid any signal generation by nonspecific binding.

First, as illustrated in the Scheme 1 of Figure 2.2, we fully covered the amine modified substrate with the PDA liposome. Then, the probe molecules were microarrayed onto the PDA liposome layer. This afterward-tethering strategy of probe molecules provides convenient spotting of various probe molecules on the microarray surface, rendering high-throughput detection possible.[7b]

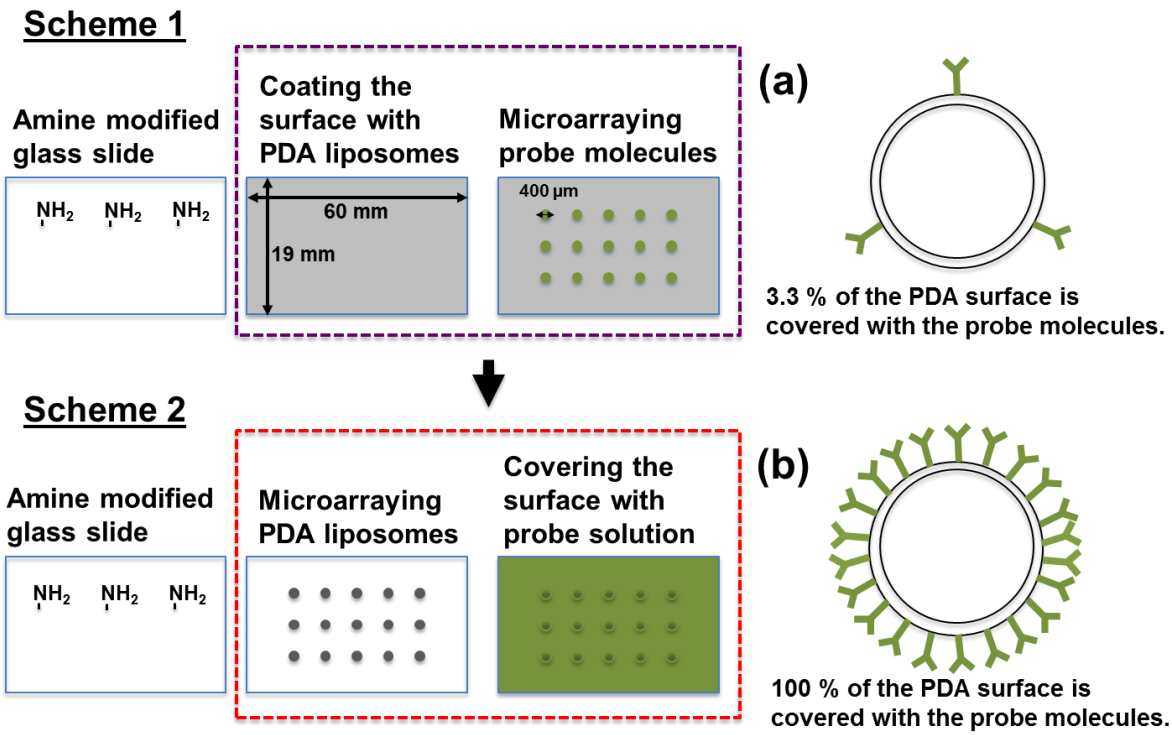

Figure 2.2 Schematic illustration of PDA liposome microarray fabrication protocols for controlling the number of probes tethered to the PDA liposome surface. (a) PDA liposome containing 3.3% probe molecules, (b) PDA liposome fully tethered with probe molecules.

After 30 s of 254 nm UV irradiation, we observed blue color development confirming successful photopolymerization of the PDA liposomes on the microarray. We anticipated that the probe–target binding events at the PDA liposome surface produced red emission due to the induced stress by the formation of bulky probe–target complex. However, we could not observe noticeable signals regardless of whether the M1 peptide was used as a probe or a target.

Our calculation implied that the number of probe molecules actually tethered at the PDA liposome surface was too few to form good enough complex formation for efficient steric perturbation of the PDA conjugated backbone. To quantity the probe molecules at the PDA surface, we first calculated the number of epoxy groups at the PDA surface available for the reaction with probe molecules (M1 antibody and M1 peptide). Since we used 0.5×10^{-3} M PDA liposome solution consisting of PCDA-Epoxy and PCDA at 4:1 molar ratio, the 0.5×10^{-3} M PDA liposome solution is equivalent to 400×10^{-6} M of epoxy groups. We covered 300 μ L of the PDA liposome solution onto the amine glass slide for immobilization, which means that 0.12 μ mole of epoxy groups is available in the volume. Through the immobilization step, 45% of the initial PDA liposome bound on the glass slide, which was calculated by comparing the UV-Vis absorption intensity at 648 nm of the initial PDA liposome solution before the immobilization and the unbound PDA liposome solution after the immobilization. Then, the number of actually immobilized epoxy groups per glass slide should be 0.054 μ mole (0.12 μ mole x 0.45). Because the size of the glass slide was 60 mm x 19 mm and the diameter of the microarray dots where the probe molecules were microarrayed was 400 μm, the number of the immobilized epoxy groups per microarray dot was calculated to be 6 pmole. The concentration of the purchased M1 antibody was 6.67×10^{-6} M. Considering the spotting volume of 30 nL per spot by a manual microarrayer, 200 fmole M1 antibody is available to react with the immobilized epoxy groups

within each microarray spot. Therefore, the calculation showed that at best only 3.3% epoxy groups on the tethered PDA liposome surface would react with M1 antibody (Figure 2.2a, 200 fmole antibody onto 6 pmole epoxy groups). Even though a more concentrated M1 peptide solution was commercially available, we used M1 peptide solution at the same concentration of 6.67×10^{-6} M for M1 antibody detection, in order to match the same probe molecule density on the PDA liposome surface. We did not observe any sensory signal generation in this case either.

To enhance the number of tethered probe molecules at the PDA surface, we used the strategy illustrated in the Scheme 2 of Figure 2.2. Instead of tethering PDA liposomes to fully cover the amine glass, PDA liposomes were spotted to form 36 microarray dots having an average diameter of 400 μ m by means of a manual microarrayer. Then, the PDA microarray was covered with 300 μL of 1.2×10^{-6} M M1 peptide solution and enclosed under a sealing slide chamber. The amount of M1 peptide in the volume was calculated to be 1.67 times excess to the number of the epoxy groups per microarray dot. While the PDA microarray under the sealing slide chamber was stirred on an orbital shaker for 1 h, the epoxy group should have enough chances to react with the excess amount of the probe molecules. Hence, this strategy significantly increases the mole ratio of the available M1 peptide to the epoxy moiety at the PDA liposome surface, largely enhancing the number of expressed M1 peptides at the PDA liposome surface (Figure 2.2b). As the consequence of the increased number of probing molecules, larger number of probe–target complex is expected to form, and indeed we observed strong red emission from the microarrays upon incubating with M1 antibody (Figure 2.3a). We confirmed that the fluorescence signal was generated from the specific interaction between M1 peptide and M1 antibody because we could not observe any noticeable signal when NP antibody was incubated as a non-specific target (Figure 2.3c). We plotted the fluorescence emission intensity

of the microarray against the M1 antibody concentration as shown in Figure 2.3d. As one can see from the correlation curve, a quantitative analysis of M1 antibody is possible.

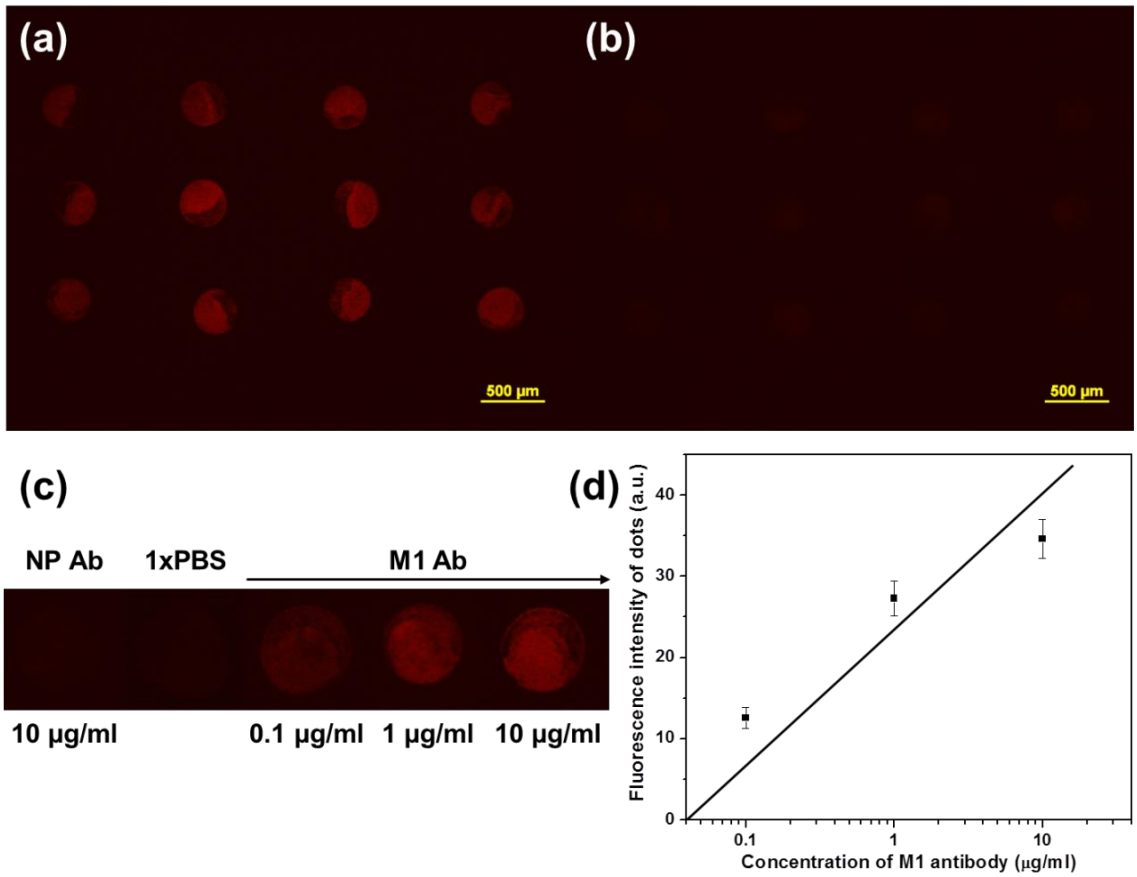

Figure 2.3 Fluorescent microscope images of PDA liposome microarray (a) having M1 peptide probes for the detection of M1 antibody (10 μ g/mL), (b) having M1 antibody probes for the detection of M1 peptide, and (c) enlarged fluorescent microscope image of PDA microarray dots having M1 peptide probes after 1 h incubation with NP antibody, 1xPBS, and various concentrations of M1 antibody from 0.1 to 10 μ g mL^{-1} at room temperature (excitation at 550 nm and a emission filter with 600 nm cutoff were used) (d) correlation curve between fluorescence intensity of dots and concentration of M1 antibody. Dot intensity is calculated as numerical values from the dot images by using ImageJ software. Each point and error bar represent a mean value and a standard deviation, respectively.

When M1 antibody was used as a probe for the detection of M1 peptide by means of the same second strategy, on the contrary, we could not observe noticeable sensory signal generation (Figure 2.3b). From this unexpected result, we postulated the target size effect on turn-on

signaling of the PDA liposome microarray. The M1 peptide is a nonapeptide having an estimated length of a few nm (M_w: ≈ 1000) at most, and the M1 antibody is thought to have a hydrodynamic diameter of 7-10 nm (M_w: ≈ 150,000).[10] As depicted in Figure 2.5, the small target, M1 peptide, cannot produce large enough steric repulsion to warrant a sensory signal even after being captured by the M1 antibody probe having a much larger size. However, the large target, M1 antibody, can produce the red fluorescence signal because once being captured by the densely packed M1 peptide probes, the captured M1 antibodies will generate large enough steric repulsion at the PDA liposome surface. In this study, we could make a very important finding that the intensity of the PDA sensory signal is mainly related to the steric repulsion between probe–target complexes not the strength of the binding force between a probe and its target.

We applied the lesson from the direct influenza A virus experiments to the porcine reproductive respiratory syndrome virus (PRRSV) antibody detection by using a peptide specific to PRRSV antibody as a small probe. The PRRSV peptide was tethered at the PDA surface to detect PRRSV antibody to develop an indirect detection system. Fluorescence sensory signal was observed from the PDA liposome microarrays, while non-specific classical swine fever virus (CSFV) antibody did not generated any sensory signal (Figure 2.4).

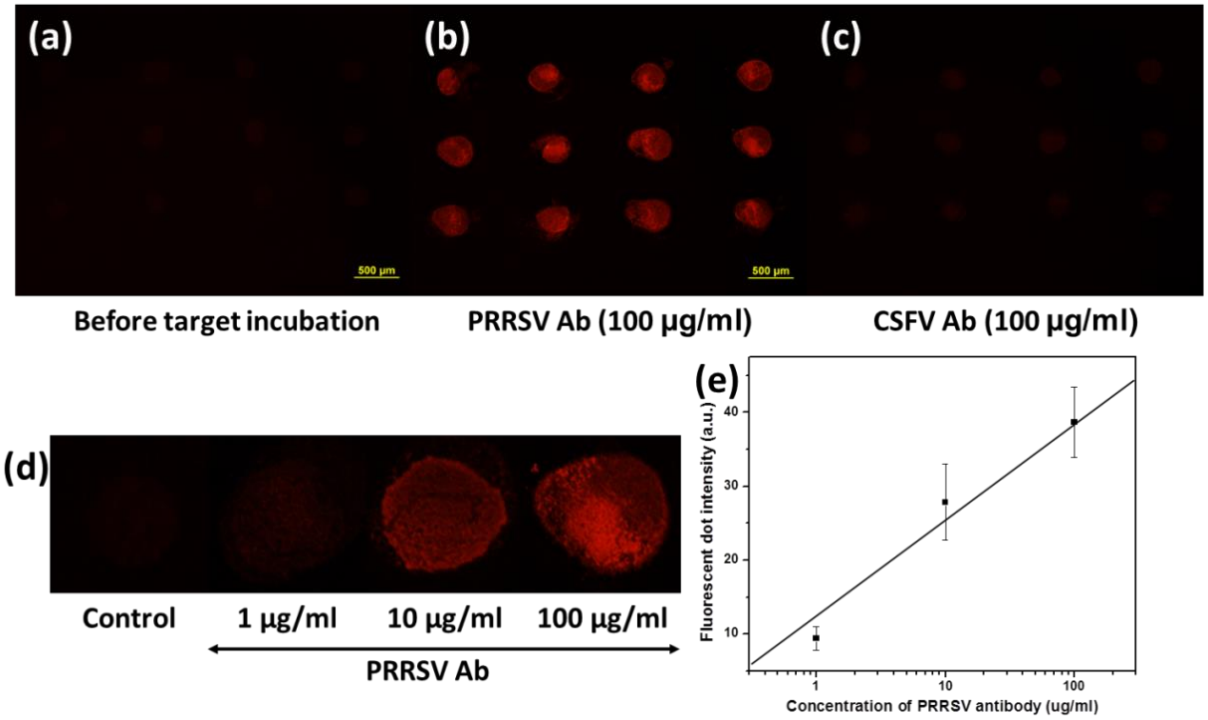

Figure 2.4 Fluorescent microscopy images of PDA microarray for the detection of (a) Before target sample introduction and after incubation with (b) PRRSV antibody, (c) CSFV antibody. (d) Enlarged fluorescent microscopy image of PDA liposome dots after 24 hr incubation with CSFV antibody, 1xPBS and various concentrations of PRRSV antibody from 1 to 100 μg/ml at 37^{o}C. (b) Correlation between fluorescence intensity of dots and concentration of PRRSV antibody.

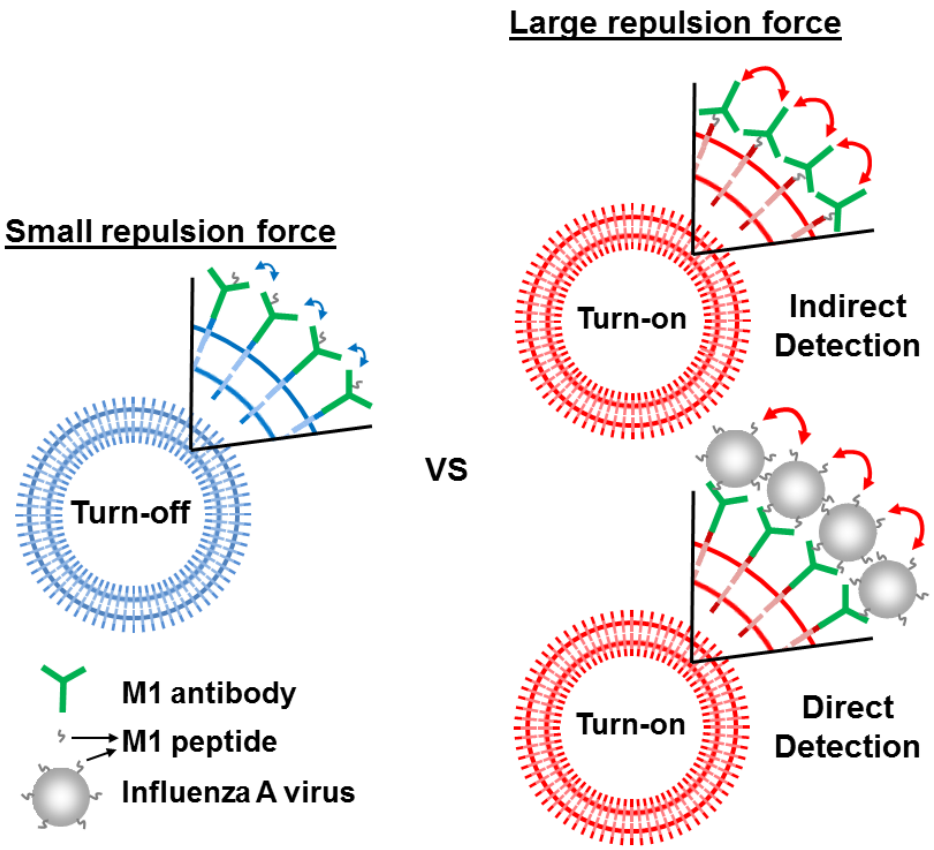

Figure 2.5 Schematic illustration of the target size effect on turn-on signaling of the PDA liposome microarray.

Based on this finding, we anticipated that influenza A virus can be directly detected by PDA liposome having M1 antibody probes because the whole virus is larger than M1 antibody. As shown in Figure 2.6a, indeed red dots appeared on the PDA liposome microarray after incubation with H1N2 viruses, which confirms the target size effect on the turn-on signaling of PDA. We could achieve the detection limit of 2^2 HAU from PDA liposome consisting of PCDA-Epoxy and PCDA (4:1 molar ratio) while conventional influenza A virus kits have the general detection limit of 0.1–0.5 HAU.[11] To further improve the sensitivity of the PDA liposome microarray, we incorporated a phospholipid, DMPA, into the PDA liposome to provide more mobility and ensuing easier perturbation of PDA backbone by probe–target complex formation and repulsion.

It is well known that incorporating non-polymerizable phospholipids into PDA liposome weakens the intermolecular packing of PDA monomers by lowering the hydrogen bonding strength among their side chains.[12] As shown in Figure 2.6b, when we used PDA liposome of PCDA-Epoxy and DMPA (4:1 molar ratio) the brighter red emission appeared at 2^3 HAU of H1N2 viruses. We ultimately reached the detection limit of 2^{-2} HAU from the PDA liposome microarray, which is comparable to the detection limit conventional influenza A virus kits can provide. The quantitative correlations between the emission intensity of the PDA microarrays and the concentration of influenza A virus H1N2 are shown in Figure 2.6d.

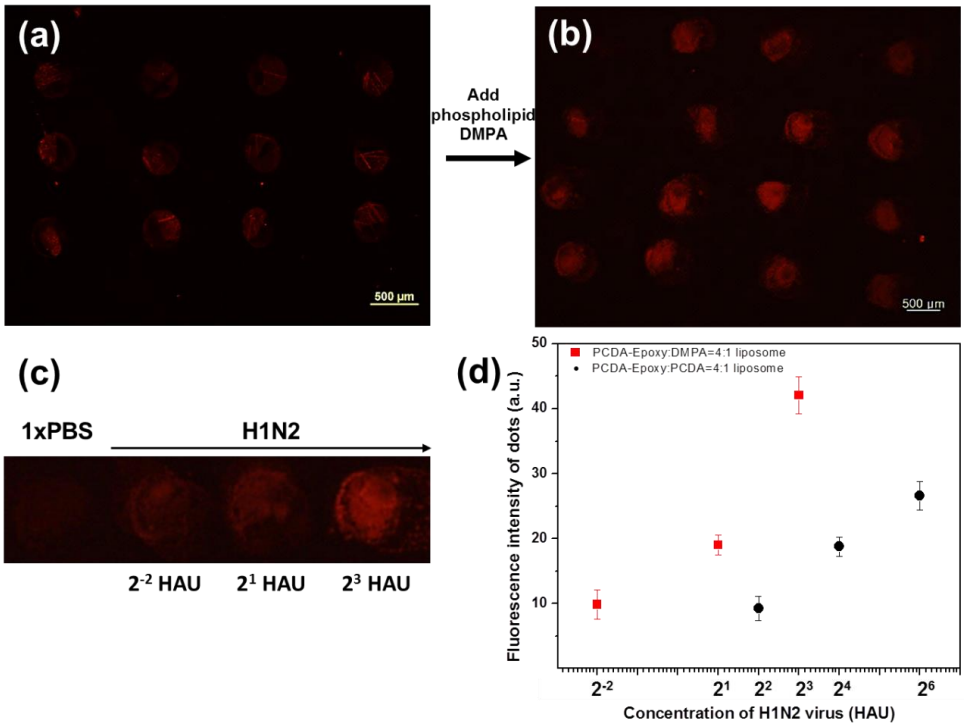

Figure 2.6 (a) Fluorescent microscope images of PCDA-Epoxy:PCDA (4:1) liposome microarray having M1 antibody probes for the detection of H1N2 virus (2^4 HAU), (b) Fluorescent microscope images of PCDA-Epoxy:DMPA (4:1) liposome microarray having M1 antibody probes for the detection of H1N2 virus (2^3 HAU), and (c) enlarged fluorescent microscope image of the PCDA-Epoxy:DMPA (4:1) liposome microarray dots after 1 h incubation with 1xPBS and various concentrations of H1N2 virus from 2^{-2} to 2^3 HAU at room temperature (excitation at 550 nm and a emission filter with 600 nm cutoff were used), (d) Correlation between fluorescence intensity of dots and concentration of H1N2 virus. Dot intensity is calculated as numerical values from the dot images by ImageJ software. Each point and error bar represents a mean value and a standard deviation, respectively.

2.4. Conclusions

We systematically studied the effects of the target size on the turn-on signaling of PDA sensory systems for the detection of biological molecules based on the intermolecular interactions between a probe molecule and its target. The interaction between the M1 peptide and the M1 antibody of influenza A virus was rationally coined into a PDA sensor design for direct and indirect detection of influenza A virus. By using the same pair but only switching their role as a probe or a target in the detection system, we could keep the same paring affinity and therefore unquestionably examine the target size effect. While the larger M1 antibodies produced red fluorescence emission upon binding with densely packed M1 peptides at the PDA liposome surface, the smaller M1 peptides could not generate any noticeable signal when they bound to tightly packed M1 antibodies. When the probe density at the PDA surface was low, we could not observe any sensory signal generation from the PDA microarray regardless of the role of M1 antibody and M1 peptide. These results clearly revealed that the PDA sensory signal is mainly from the steric repulsion between probe-target complexes not the strength of the probe-target binding force. Based on the finding, we developed PDA microarray for direct detection of influenza A virus. The PDA liposome microarrays having densely packed M1 antibody probes and co-assembled phospholipids sensitively detected influenza A virus with the detection limit of 2^{-2} HAU. The demonstrated target size effect can be readily applicable to various PDA-based biosensor designs and developments.

2.5. Author contributions

Sungbaek Seo synthesized the polymers using the monomer (PCDA-Epoxy) Jiseok Lee synthesized. Sungbaek Seo fabricated microarray sensor and tested the sensor for antibody and influenza A virus detection. Eun-Jin Choi and Eun-Ju Kim identified M1 peptide-M1 antibody binding pair and confirmed the binding affinity.

2.6. References

1. Neumann, G.; Noda, T.; Kawaoka, Y., Emergence and pandemic potential of swine-origin H1N1 influenza virus. *Nature* **2009,** *459* (7249), 931-939.
2. (a) Carpick, R. W.; Sasaki, D. Y.; Burns, A. R., First Observation of Mechanochromism at the Nanometer Scale. *Langmuir* **2000,** *16* (3), 1270-1278; (b) Ryu, S.; Yoo, I.; Song, S.; Yoon, B.; Kim, J.-M., A Thermoresponsive Fluorogenic Conjugated Polymer for a Temperature Sensor in Microfluidic Devices. *Journal of the American Chemical Society* **2009,** *131* (11), 3800-3801.
3. (a) Cheng, Q.; Stevens, R. C., Charge-Induced Chromatic Transition of Amino Acid-Derivatized Polydiacetylene Liposomes. *Langmuir* **1998,** *14* (8), 1974-1976; (b) Jonas, U.; Shah, K.; Norvez, S.; Charych, D. H., Reversible Color Switching and Unusual Solution Polymerization of Hydrazide-Modified Diacetylene Lipids. *Journal of the American Chemical Society* **1999,** *121* (19), 4580-4588.
4. (a) Tomioka, Y.; Tanaka, N.; Imazeki, S., Effects of side-group interactions on pressure-induced chromism of polydiacetylene monolayer at a gas-water interface. *Thin Solid Films* **1989,** *179* (1–2), 27-31; (b) Tashiro, K.; Nishimura, H.; Kobayashi, M., First Success in Direct Analysis of Microscopic Deformation Mechanism of Polydiacetylene Single Crystal by the X-ray Imaging-Plate System. *Macromolecules* **1996,** *29* (25), 8188-8196.

5. (a) Charych, D.; Nagy, J.; Spevak, W.; Bednarski, M., Direct colorimetric detection of a receptor-ligand interaction by a polymerized bilayer assembly. *Science* **1993,** *261* (5121), 585-588; (b) Kolusheva, S.; Kafri, R.; Katz, M.; Jelinek, R., Rapid Colorimetric Detection of Antibody−Epitope Recognition at a Biomimetic Membrane Interface. *Journal of the American Chemical Society* **2000,** *123* (3), 417-422; (c) Jung, Y. K.; Kim, T. W.; Kim, J.; Kim, J.-M.; Park, H. G., Universal Colorimetric Detection of Nucleic Acids Based on Polydiacetylene (PDA) Liposomes. *Advanced Functional Materials* **2008,** *18* (5), 701-708; (d) Park, C. H.; Kim, J. P.; Lee, S. W.; Jeon, N. L.; Yoo, P. J.; Sim, S. J., A Direct, Multiplex Biosensor Platform for Pathogen Detection Based on Cross-linked Polydiacetylene (PDA) Supramolecules. *Advanced Functional Materials* **2009,** *19* (23), 3703-3710; (e) Lee, J.; Jeong Jeong, E.; Kim, J., Selective and sensitive detection of melamine by intra/inter liposomal interaction of polydiacetylene liposomes. *Chemical Communications* **2011,** *47* (1), 358-360; (f) Chen, X.; Kang, S.; Kim, M. J.; Kim, J.; Kim, Y. S.; Kim, H.; Chi, B.; Kim, S.-J.; Lee, J. Y.; Yoon, J., Thin-Film Formation of Imidazolium-Based Conjugated Polydiacetylenes and Their Application for Sensing Anionic Surfactants. *Angewandte Chemie International Edition* **2010,** *49* (8), 1422-1425; (g) Lee, J.; Seo, S.; Kim, J., Colorimetric Detection of Warfare Gases by Polydiacetylenes Toward Equipment-Free Detection. *Advanced Functional Materials* **2012,** *22* (8), 1632-1638.

6. (a) Reppy, M. A.; Pindzola, B. A., Biosensing with polydiacetylene materials: structures, optical properties and applications. *Chemical Communications* **2007,** (42), 4317-4338; (b) Ahn, D. J.; Kim, J. M., Fluorogenic polydiacetylene supramolecules: immobilization, micropatterning, and application to label-free chemosensors. *Acc Chem Res* **2008,** *41* (7), 805-16; (c) Yoon, B.; Lee, S.; Kim, J.-M., Recent conceptual and technological advances in

polydiacetylene-based supramolecular chemosensors. *Chemical Society Reviews* **2009,** *38* (7), 1958-1968; (d) Lee, K.; Povlich, L. K.; Kim, J., Recent advances in fluorescent and colorimetric conjugated polymer-based biosensors. *Analyst* **2010,** *135* (9), 2179-2189.

7. (a) Lee, J.; Kim, H.-J.; Kim, J., Polydiacetylene Liposome Arrays for Selective Potassium Detection. *Journal of the American Chemical Society* **2008,** *130* (15), 5010-5011; (b) Lee, J.; Jun, H.; Kim, J., Polydiacetylene–Liposome Microarrays for Selective and Sensitive Mercury(II) Detection. *Advanced Materials* **2009,** *21* (36), 3674-3677; (c) Kang, D. H.; Jung, H.-S.; Ahn, N.; Lee, J.; Seo, S.; Suh, K.-Y.; Kim, J.; Kim, K., Biomimetic detection of aminoglycosidic antibiotics using polydiacetylene-phospholipids supramolecules. *Chemical Communications* **2012,** *48* (43), 5313-5315.
8. Seo, D.; Kim, J., Effect of the Molecular Size of Analytes on Polydiacetylene Chromism. *Advanced Functional Materials* **2010,** *20* (9), 1397-1403.
9. Poungpair, O.; Pootong, A.; Maneewatch, S.; Srimanote, P.; Tongtawe, P.; Songserm, T.; Tapchaisri, P.; Chaicumpa, W., A Human Single Chain Transbody Specific to Matrix Protein (M1) Interferes with the Replication of Influenza A Virus. *Bioconjugate Chemistry* **2010,** *21* (7), 1134-1141.
10. (a) Ban, N.; Escobar, C.; Garcia, R.; Hasel, K.; Day, J.; Aaron, G.; McPherson, A., Crystal Structure of an Idiotype-Anti-Idiotype Fab Complex. *Proceedings of the National Academy of Sciences of the United States of America* **1994,** *91* (5), 1604-1608; (b) Driskell, J. D.; Jones, C. A.; Tompkins, S. M.; Tripp, R. A., One-step assay for detecting influenza virus using dynamic light scattering and gold nanoparticles. *Analyst* **2011,** *136* (15), 3083-3090.
11. (a) Lien, K.-Y.; Hung, L.-Y.; Huang, T.-B.; Tsai, Y.-C.; Lei, H.-Y.; Lee, G.-B., Rapid detection of influenza A virus infection utilizing an immunomagnetic bead-based

microfluidic system. *Biosensors and Bioelectronics* **2011,** *26* (9), 3900-3907; (b) Ong, W. T.; Omar, A. R.; Ideris, A.; Hassan, S. S., Development of a multiplex real-time PCR assay using SYBR Green 1 chemistry for simultaneous detection and subtyping of H9N2 influenza virus type A. *Journal of Virological Methods* **2007,** *144* (1–2), 57-64.

12. (a) Kim, K.-W.; Choi, H.; Lee, G. S.; Ahn, D. J.; Oh, M.-K., Effect of phospholipid insertion on arrayed polydiacetylene biosensors. *Colloids and Surfaces B: Biointerfaces* **2008,** *66* (2), 213-217; (b) Kang, D. H.; Jung, H.-S.; Lee, J.; Seo, S.; Kim, J.; Kim, K.; Suh, K.-Y., Design of Polydiacetylene-Phospholipid Supramolecules for Enhanced Stability and Sensitivity. *Langmuir* **2012,** *28* (19), 7551-7556.

CHAPTER 3

Approaches for Enhanced PDA Sensitivity: Polydiacetylene-Phospholipid Supramolecules

3.1. Introduction

As we mentioned in Chapter 2, incorporating non-polymerizable phospholipids into PDA liposome weakens the intermolecular packing of PDA monomers by lowering the hydrogen bonding strength among their side chains. Consequently, this weakened intermolecular packing of PDA liposome makes PDA backbone readily distorted by probe-target binding events linked on diacetylene monomers, finally generating PDA sensory signal. This approach is demonstrated in biosensor applications, i.e., bovine viral diarrhea virus (BVDV) antibody[1] and influenza A virus detection.[2]

Besides, phospholipid can be utilized as capturing moiety for target analyte inside PDA liposome. For example, phosphatidylinositol-4,5-bisphosphate (PIP_2) phospholipid is known to bind aminoglycosidic antibiotics especially neomycin. Accordingly, the PIP2 is designed to co-assembly with diacetylene to make PDA-phospholipids liposomes as sensory system and successfully showed a detection limit of 100 nM (61 ppb) for neomycin.[3] However, the detection limit did not satisfy regulation limits in some countries including South Korea. In this regard, an invention of highly sensitive sensing platform for bioanalyte detection is always desired.

Liposome is a spherical nanostructure consisted of a lipid bilayer. Analogous structure of liposome with a cell membrane inspires us to design multifunctional liposome scaffolds. For example, a cell membrane carries necessary nutrients, processes essential reactions inside the membrane without interrupts from its surroundings, and regulates signal transduction pathways on the membrane surface.[4] Moreover, flexible architecture and softness of a cell membrane structure allows biocompatibility in physiological environments. For these reasons, liposome based scaffolds have been mostly developed as carriers for drug delivery and analytical purpose.

One of promising applications using liposomes is a sensing platform. Our group developed various polydiacetylene (PDA) liposome based sensors.[5] By binding analytes on receptor lipids in the liposome surface, the PDA conjugated backbone was distorted, generating colorimetric and fluorogenic chromism. However, the sensitivity is limited by low quantum yield, and repulsion based detection mechanism.[6]

Another approach to prepare liposome sensors used is encapsulating fluorophores within hydrophobic bilayer or into innermost aqueous area. Ma *et al.* developed a liposome based cupric ion sensor containing Nile red dye within a bilayer space.[7] When cupric ions bound onto liposome surface, receptor lipids selectively formulated lipid-cupric ion chelate complex. Then, absorption of the complex overlapped with Nile red fluorescence emission, resulting forster resonance energy transfer based Nile red quenching. However, the encapsulating methods lower the loading efficiency of signaling fluorophores, hardly to control numbers of fluorophores, and released fluorophores within a certain time due to disassembly of liposome structure.[8]

3.2. Experimental section

3.2.1. Materials

10,12-pentacosadiynoic acid (PCDA) was obtained from GFS Chemicals. Rhodamine 6G (R6G) was purchased from Acros Organics. 1,2-dimyristoylsn-glycero-3-phosphate (DMPA) and phosphatidylinositol-4,5-bisphosphate (PIP_2) were obtained from Avanti Polar Lipids. Hexadecyltrimethylammonium bromide (CTAB), sodium dodecyl sulfate (SDS), Tween® 20, potassium phosphate monobasic (KH_2PO_4), neomycin, gentamycin, tobramycin, streptomycin, oxytetracycline, and all solvents were purchased from Sigma–Aldrich.

3.2.2. Titration study of R6G solution with DMPA

During a fluorescence titration, 1 ml of R6G aqueous solution (1×10^{-5} M) was placed in a quartz cuvette (10 × 10 × 40 mm) and initial emission spectra was measured with excitation at 420 nm using PTI QuantaMasterTM spectrofluorometer. 20 µl aliquots of DMPA solution in deionized water (1×10^{-4} M, 0.2 molar equivalents to the R6G) was introduced to the cuvette until reaching 10 molar equivalents to the R6G. After each addition, a fluorescence spectrum was measured. In the same way with the fluorescence titration, absorption titration was conducted in a UV-transparent cuvette using Varian Cary 50 UV-Vis spectrophotometer.

3.2.3. Determination of critical bilayer (micelle) concentration

We used a method mainly stated from a cited reference.[9] 5 µl of a pyrene solution (2 mM) dissolved in methanol, solution A, was placed into a 20 ml vial and the solvent was evaporated by N2 blowing. The lipid solutions at serial dilution, solution B, were added to the evaporated residue and the resulting solution was sonicated in water bath for 10 min. Then, fluorescence spectra of each final solution were measured. The excitation wavelength was 320 nm and the emission wavelength range was between 350 and 450 nm. The fluorescence intensities of the peaks at ~375 nm (I_1) and ~385 nm (I_3) were extracted from the spectra, and the I_1/I_3 values

according to serial diluted lipid concentrations were used for critical bilayer (micelle) concentration determination as an inflection point.

3.2.4. R6G quenching ratio of lipid-R6G complexes against pure R6G solution

We prepared lipid aqueous solution at high concentration, subsequently added 1 molar equivalent of R6G to the lipid molecules. Integral of emission spectrum in the final lipid-R6G complexes solution was measured (integral of emission spectrum, I_f) at serial lipid dilutions. On the other hand, we prepared pure R6G solution and the integral of spectrum was measured emission spectra at above mentioned serial lipid dilutions (integral of emission spectrum, I_i). We collected relative value of I_f/I_i, quenching ratio, at each lipid concentration.

3.2.5. Preparation of turn-on type sensing platform for neomycin detection

PIP_2 (70 μg) and PCDA (20 μg) were dissolved in 0.2 ml of chloroform. In a 50 ml Erlenmeyer flask, the dissolved solution was placed from the bottom and dried using N2 blower. Then, 20 ml of deionized water was added at 80 ^oC water bath and dispersed well by shaking for 10 min to produce the final con-centration of the liposome (5×10^{-5} M). After filtration through a 0.8 μm cellulose acetate syringe filter, the resulting liposome solution was cooled at 5 ^oC at least 2 hours. The liposome was photopolymerized by 254 nm UV lamp for 30 seconds. Eventually, we added R6G solution as much as 2.2 molar equivalents to the PIP2 molecules to make turn-on type sensing platform.

3.3. Results and discussion

We found a very unique phenomenon that Rhodamine 6G (R6G) emission in aqueous solution was suppressed by addition of 1,2-dimyristoyl-sn-glycero-3-phosphate (DMPA). An aqueous solution of R6G (1.25×10^{-6} M) showed bright green fluorescence emission at 556 nm.

Notably, the emission was quenched in the presence of DMPA. As the amount of DMPA increases in solution, the emission intensity of R6G gradually decreases and eventually the emission almost completely quenched (Figure 3.1b). A dramatic change is also observed in the UV-Vis spectrum. The main absorption band at 527 nm progressively decreases and new peaks at around 509 nm and 451 nm appear (Figure 3.1c). These spectral features are ascribed to the H-type aggregates formation of R6G dyes.[10] Thus, we hypothesized that this interesting quenching behavior are attributed to the aggregation-induced emission quenching by means of the formation of H-type aggregates of R6G mediated by DMPA.

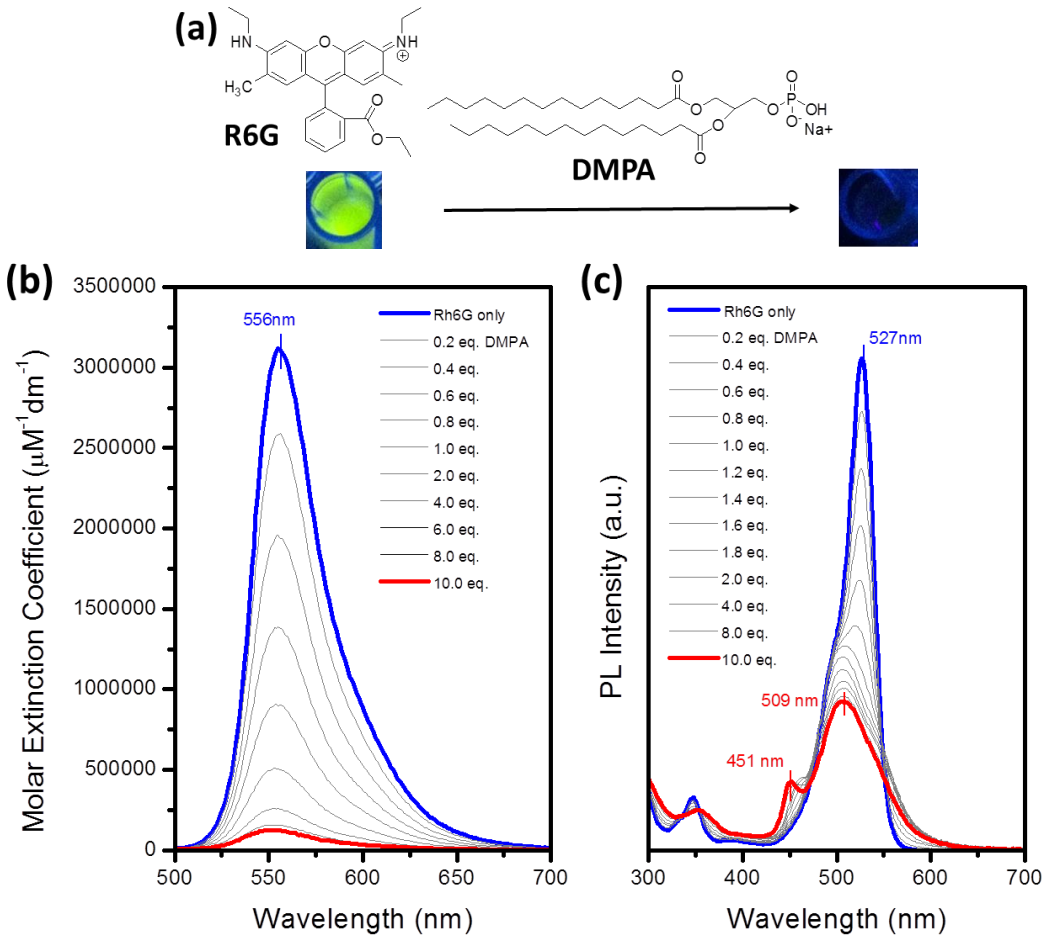

Figure 3.1 (a) R6G quenching phenomena by DMPA. (b) PL spectra and (c) UV-Vis spectra of R6G (1.25 × 10-6 M, blue line) and R6G in the presence of DMPA at various concentrations.

We developed the following understanding about the interesting behavior based on the structural features of DMPA and R6G. DMPA is a phospholipid comprised of a water-soluble anionic head and long hydrophobic alkyl tails. Due to this amphiphilic nature, it can readily form liposome in water above its critical bilayer concentration (CBC). R6G is a water-soluble cationic dye molecule, however, the water solubility is moderate. Therefore, we assumed that negatively charged liposome generated by DMPA would attract cationic R6G dyes on the liposome surface by Coulombic interaction and causes H-type aggregation of R6G (Figure 3.2). Several studies have demonstrated that electrostatic interactions between the cationic dyes and the negatively charged colloids, such as micelles, vesicles, clays, silica, and SAM-treated gold nanoparticles, led to aggregation of dye molecules, supporting our hypothesis.[11]

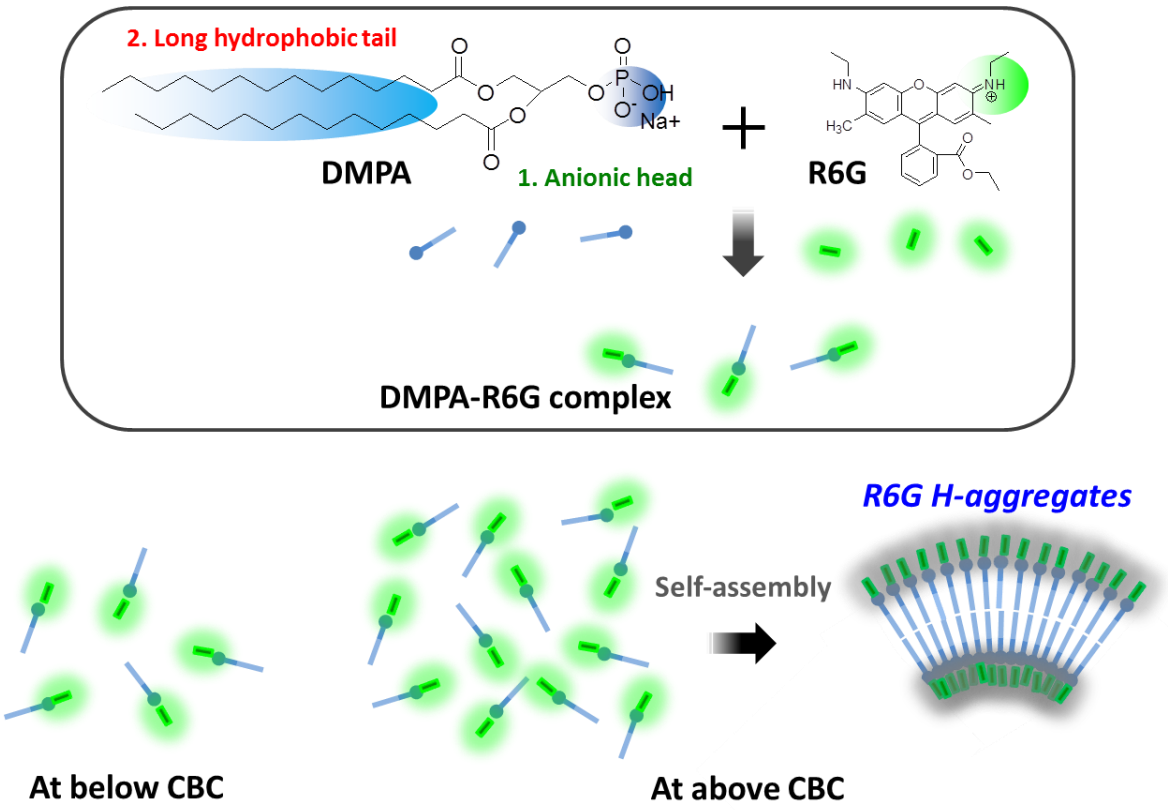

Figure 3.2 Proposed DMPA-R6G complex and self-assembled structures at above CBC.

To confirm clearly our argument, we carefully compared four different amphiphilc molecules with different charge characteristics. Positively charged CTAB, neutral Tween 20 did not show any signature for dye aggregation due to the lack of Coulombic interaction (Figure 3.3). However, negatively charged SDS generated H-type aggregates of R6G dyes consistent with that in DMPA.

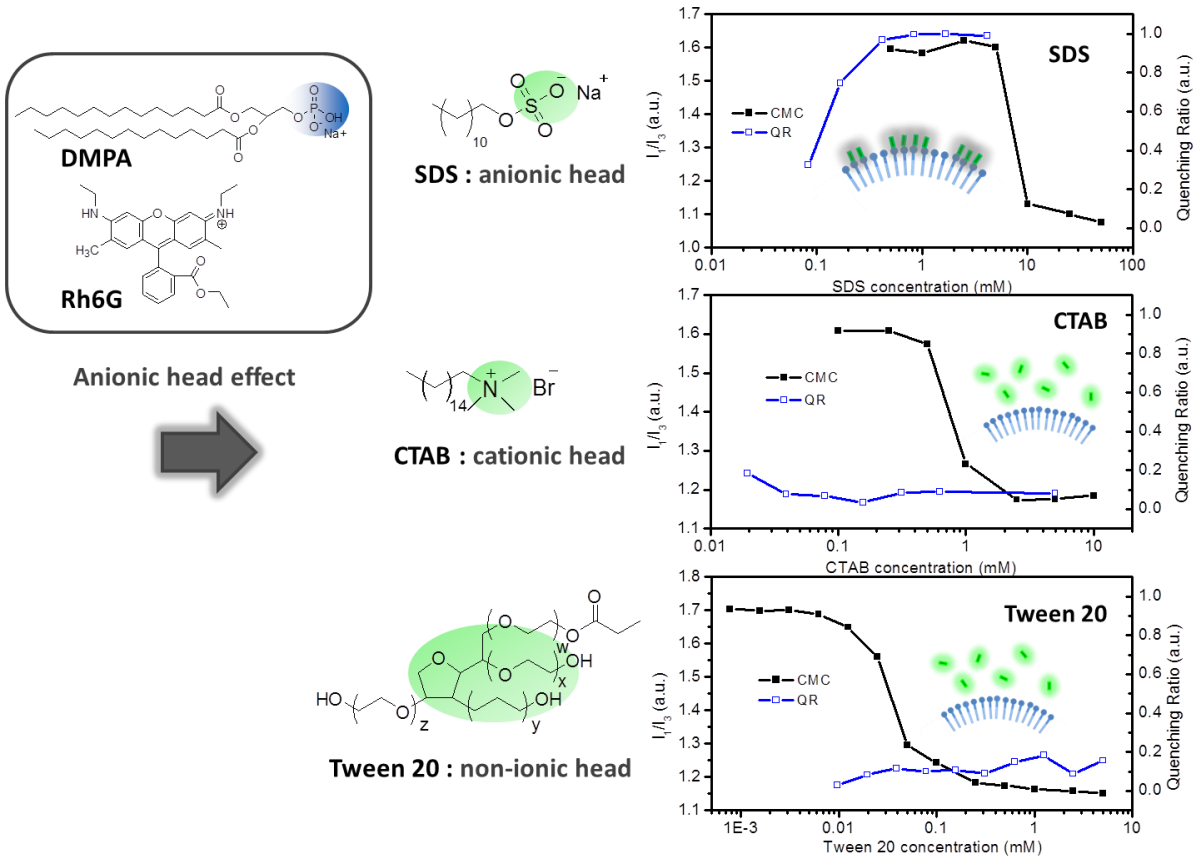

Figure 3.3 I_1/I_3 and quenching ratio are plotted at various DMPA concentration (to see if anionic head effect on R6G quenching).

KH_2PO_4 was also examined to identify the role of long alkyl chain. Micelle and/or liposome cannot be formed by KH_2PO_4 itself because of the absence of hydrophobic chain (Figure 3.4). As expected, KH_2PO_4 did not show emission quenching as well as change in UV-Vis spectrum. These experimental results indicate that the micelle and/or liposome structure generated by long

hydrophobic chain as well as negative charge for Coulombic interaction must be required to generate H-type aggregates of R6G dyes.

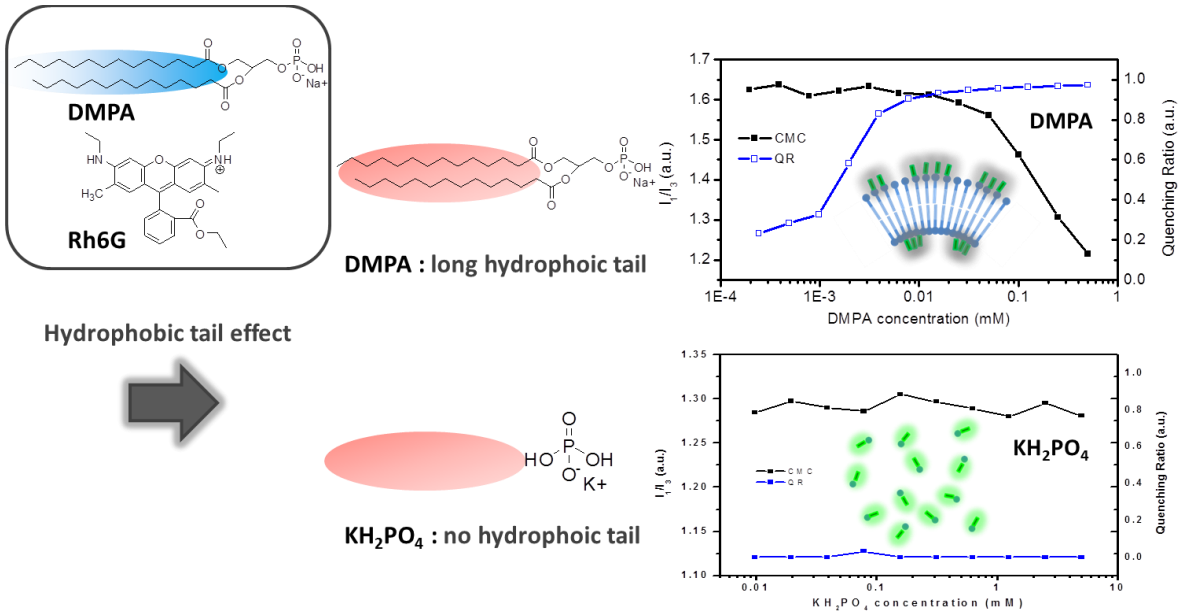

Figure 3.4 I_1/I_3 and quenching ratio are plotted at various DMPA concentration (to see if hydrophobic tail effect on R6G quenching).

We plotted the quenching ratio of R6G dyes versus DMPA concentration in the mixed water solution of R6G and DMPA to understand detailed mechanism of R6G aggregation. We expected that the quenching of R6G might occur at around CBC of DMPA (0.3 mM) because R6G would aggregate on DMPA liposome surface. However, interestingly, the rapid quenching began from 0.001 mM and saturated at around 0.01 mM, which is far lower than the CBC of DMPA (Figure 3.5a).

In order to understand this behavior, we obtained SEM images from the mixed aqueous solution of R6G and DMPA at various concentrations of DMPA, i.e. regions A, B, C, and D in the figure. As shown in (Figure 3.5b), we observed spherical particles having a 100-250 nm diameter in the regions B, C, and D, while no particle was oberved at the region A. The spherical shape and size of the particles indicate liposome formation even at 0.002 mM DMPA. This

significantly smaller CBC is reasonably due to the reduced hydrophobicity of the DMPA head groups by forming the complex with R6G and the R6G aggregation at the liposome surface leads to the concentration quenching of the dye.

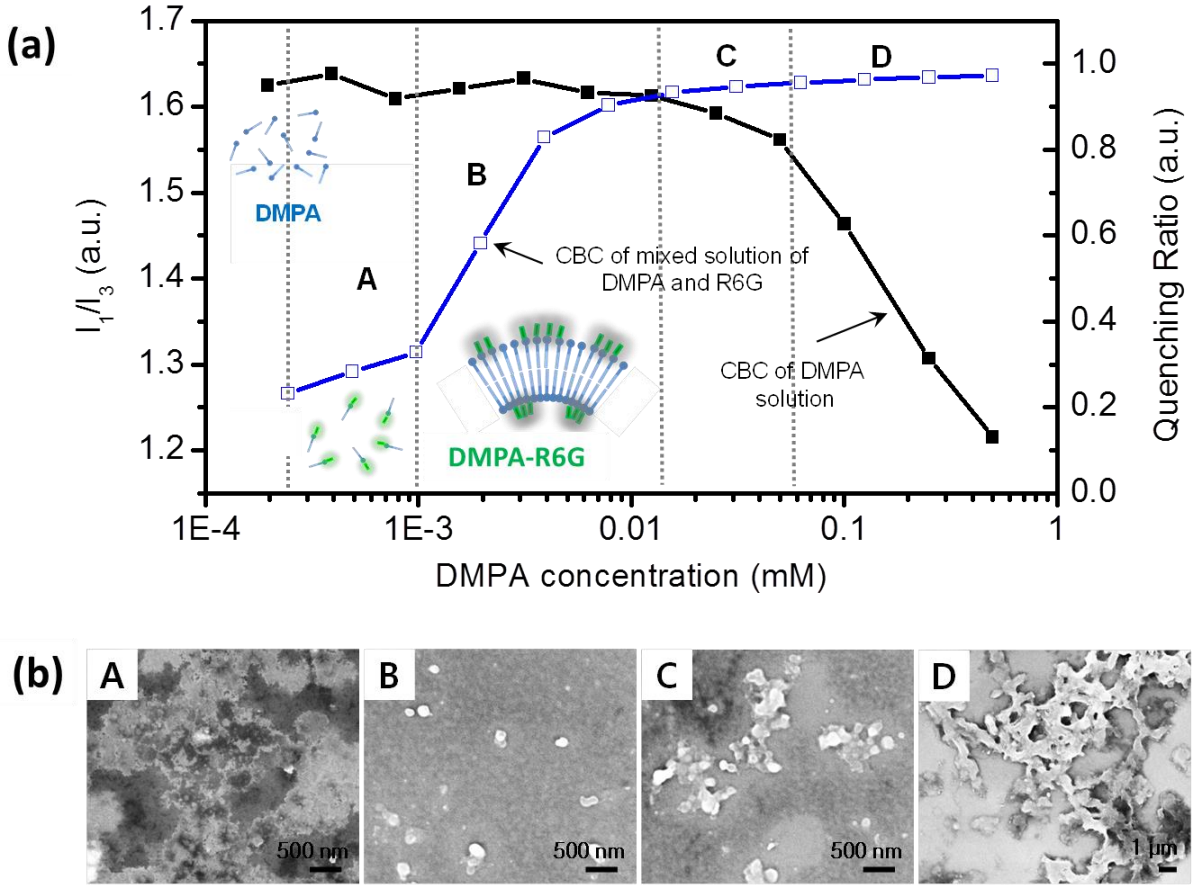

Figure 3.5 (a) I1/I3 and quenching ratio are plotted versus DMPA concentration, (b) SEM images of mixed solution of R6G and DMPA with various concentration of A, B, C, and D, respectively.

Now, the question is why the CBC of DMPA de-creases in the presence of R6G dyes. We hypothesized that Coulombic interaction between DMPA and R6G might induce the formation of hydrophobic DMPA-R6G molecular complexes and they subsequently self-assemble into liposome to minimize their surface energy (Figure 3.5a, inset). Since DMPA-R6G molecular

complexes are more hydrophobic than DMPA, they can form liposome even very low concentration of DMPA.

We have been developing a new sensing platform to detect various bioanalytes based on this new finding of the DMPA liposome-R6G complex formation. However, 100 % phospholipid constructed DMPA liposome is precipitated in a few days at room temperature which is an unsuitable platform for biosensing applications. To stabilize liposome structure for a long term, we used diacetylene monomers that are known to excellent accommodating with phospholipids. Accordingly, we confirmed co-assembled liposome solution stayed without aggregation or precipitation for months (Figure 3.6).

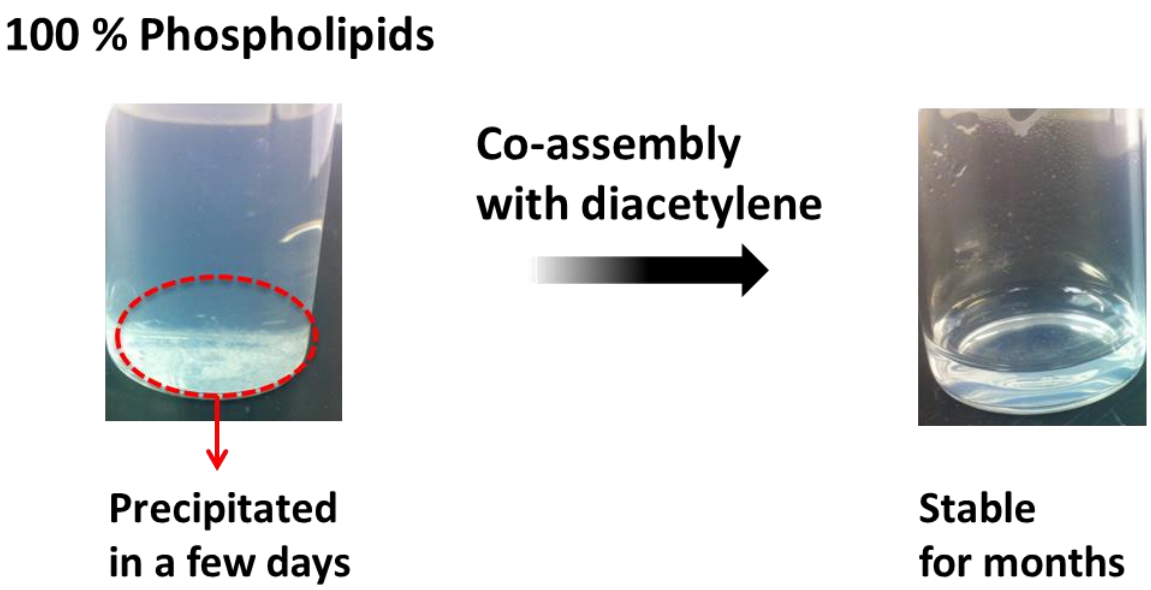

Figure 3.6 Colloidal stability test of liposomes consisted of DMPA phospholipid and DMPA:PCDA (1:1) co-assembly, respectively.

It is well known that phospholipids specifically interact with bioanalytes. We envisioned that specific interaction between a phospholipid and a target analyte would break the non-specific Coulombic interactions between R6G dyes and phospholipids, leading to displacement

of R6G dyes by the target analyte and consequent fluorescence recovery as a sensory signal (Figure 3.7).

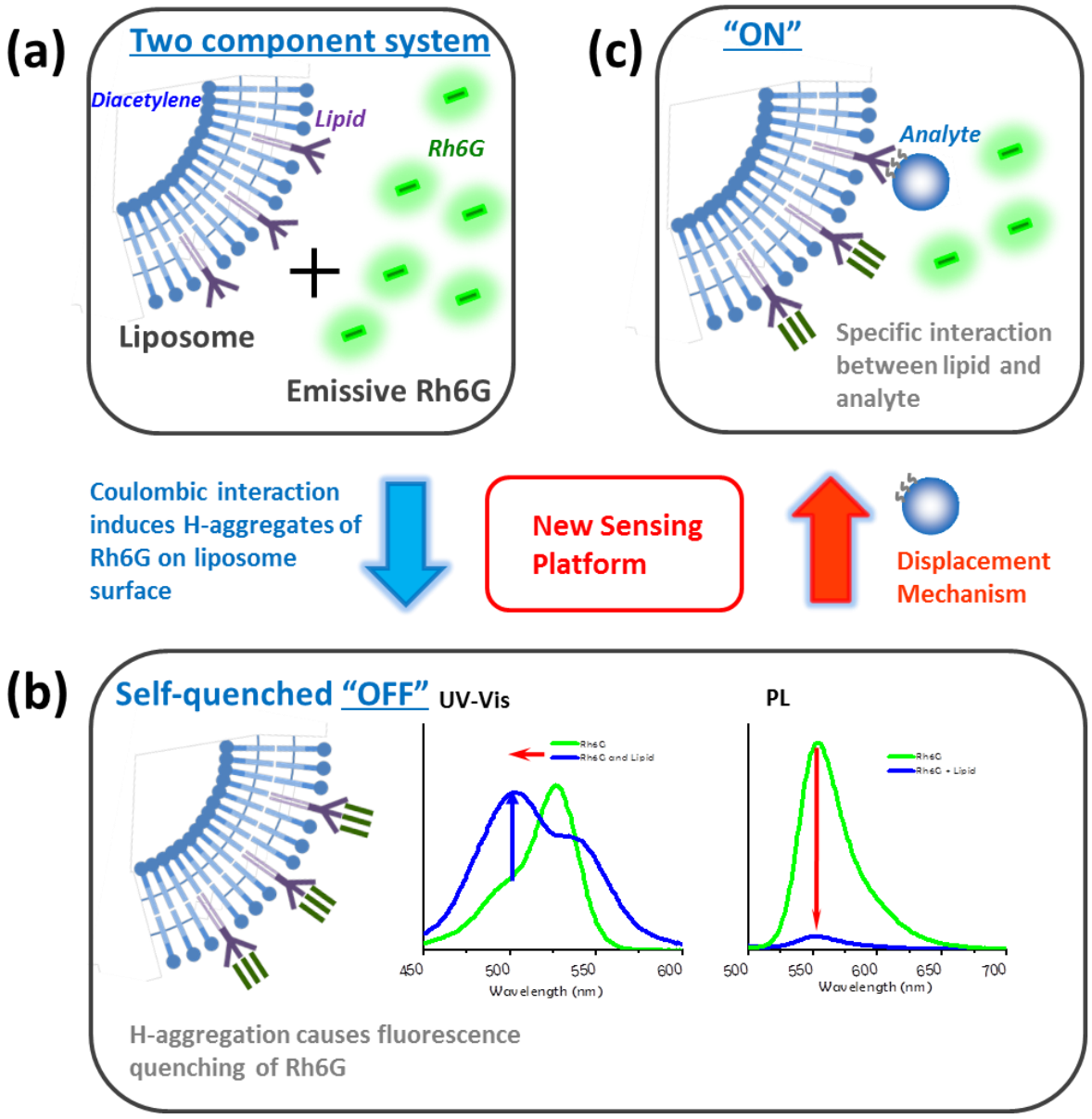

Figure 3.7 (a) Initial two-component system of PCDA:PIP2 liposome and R6G, (b) Self-quenched status by Coulombic interactions between the liposome and R6G, (c) R6G emission recovery "On" by introducing a target analyte, such as neomycin, to displace the surface-bound and aggregated R6G.

We selected neomycin as a target analyte. Neomycin is a representative aminoglycosidic antibiotic prevalently used in hospitals and the livestock industry. Since neomycin is much more nephrotoxic compared to other aminoglycosides, the abuse and misuse of neomycin can cause an allergic response,[12] organ damage (such as ear and kidney), and nerve system malfunction,[13] as well as the emerging super bacteria having a tolerance to antibiotics.[14] Consequently, many agriculture, food, and drug regulatory authorities such as World Health Organization (WHO) and Food and Agriculture Organization of the United Nations (FAO) have set a tolerance limit of neomycin in meat and dairy products including milk and eggs. Neomycin is known to bind to phosphatidylinositol-4,5-bisphosphate (PIP_2) lipids in the cellular membrane.[15] Molecular and cellular biology research revealed that PIP_2 decomposes into diacylglycerol (DAG) and 1,4,5-triphosphate (IP3) by phospholipase C (PLC) through stimulating various hormones and growth factors. Several research groups reported that neomycin binds to PIP2, inhibiting the PIP2 degradation by PLC and thus inhibiting the IP3-related signal cascade, which is a known side effect of neomycin.[15c] We prepared liposome solution comprised of PIP_2 and PCDA (1:1). Two lipid units are compatible to co-assemble to create liposome structures. To stabilize liposome structures, diacetylene monomers are conjugated by photopolymerization (Figure 3.8).

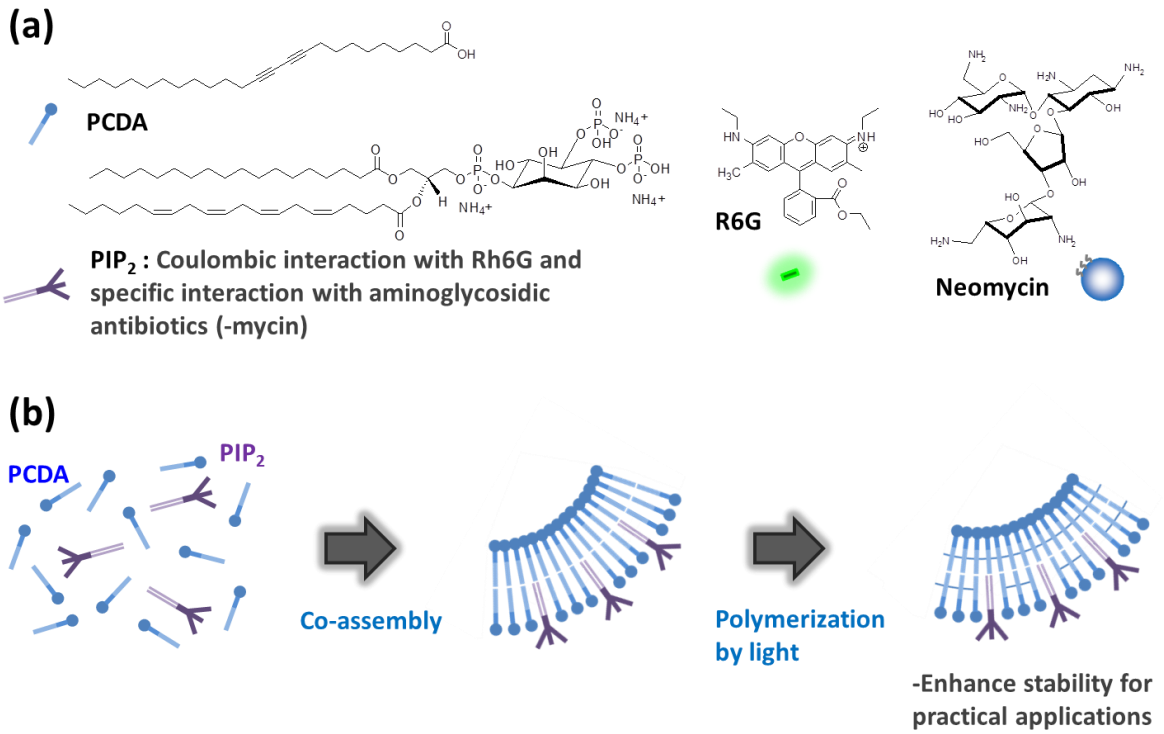

Figure 3.8 (a) Chemical structures of PCDA, PIP2, R6G, and Neomycin, (b) Procedures for stable liposome based sensing platform.

Polymerized PCDA:PIP_2 (1:1) liposome solution showed near 650 nm absorption which is characteristic peak from polymerized blue color of PDA. To the polymerized liposome solution, R6G aqueous solution was introduced until 4 molar equivalents to the PIP_2 in the liposome. Interestingly, R6G, H-type aggregation shoulder peak intensity is maximized relatively to R6G peak intensity at certain equivalent (2.2 eq) of R6G. That means H-aggregates are most cloudy on the PDA liposome and expected most efficient quenching.

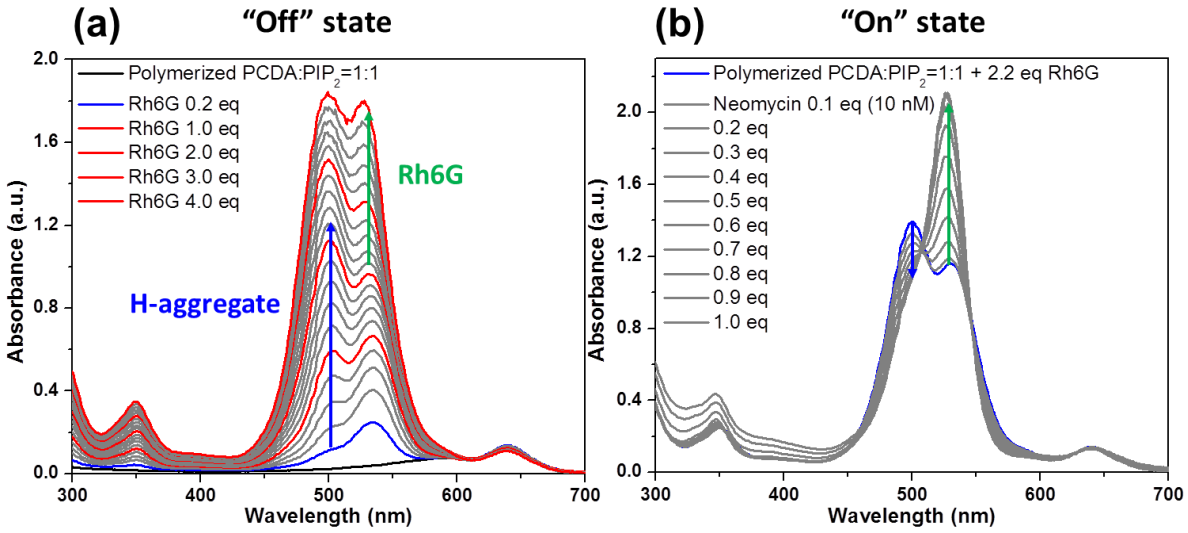

Figure 3.9 UV-Vis spectra presenting (a) Titration study of polymerized PCDA:PIP_2 liposome solution with R6G, (b) Titration study of polymerized PCDA:PIP_2 liposome-2.2 equivalent R6G complex with neomycin.

We conducted selectivity and sensitivity tests with aminoglycosidic antibiotics (Neomycin, Gentamycin, Tobramycin, Streptomycin) and non-aminoglycosidic antibiotic (Oxytetracycline) at various concentrations. Distinguishable R6G emission recovery is observed with 10 nM neomycin, which is at least 10 times better than the established 0.1 μM of detection limit of neomycin in our published literature (Figure 3.10). Also, the liposome scaffolds demonstrates excellent selectivity of the developed novel "turn-on" sensory system toward aminoglycosidic antibiotics particularly Neomycin (Figure 3.11). This novel sensory platform has several merits; it can provide high sensitivity, readily applicable to other sensor designs, and can conveniently use conventional 96-well plates and ELISA apparatus.

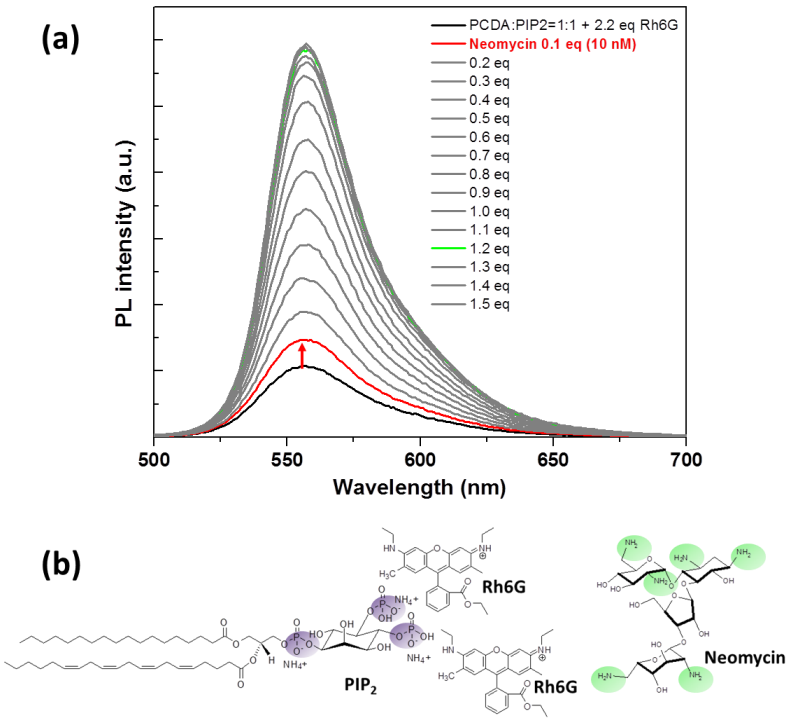

Figure 3.10 (a) Sensitivity test by incubating the PCDA:PIP_2 liposome/R6G complex solution with neomycin at various concentrations, (b) Potential Coulombic binding sites are colored coded in PIP_2 and neomycin.

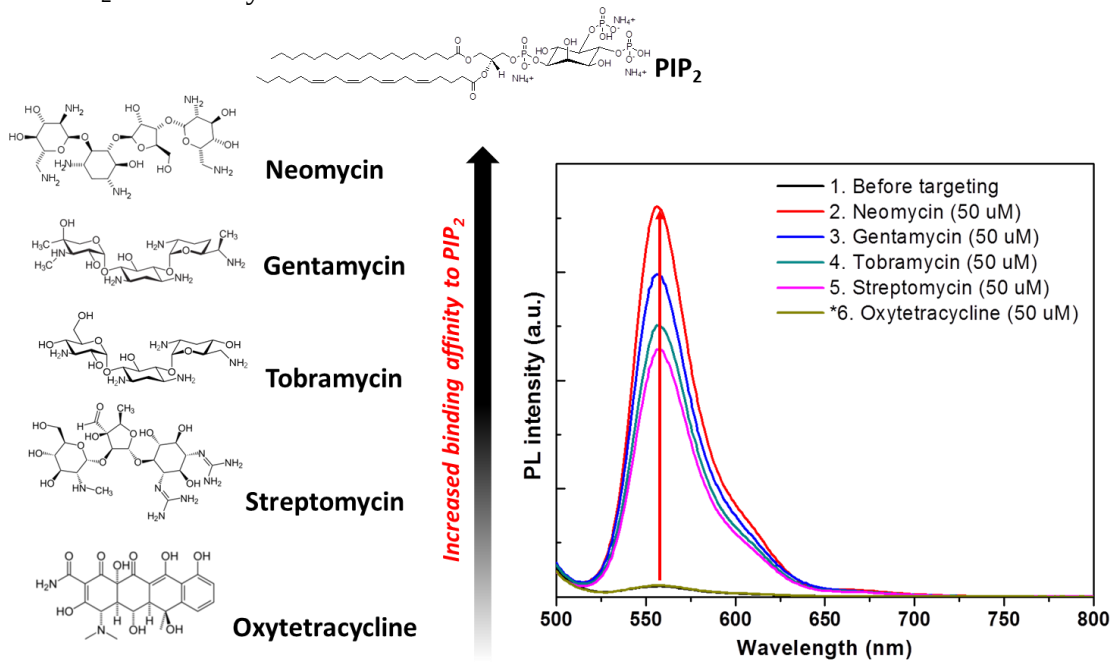

Figure 3.11 Selectivity test with aminoglycosidic antibiotics (Neomycin, Gentamycin, Tobramycin, Streptomycin) and non-aminoglycosidic antibiotic (Oxytetracycline).

3.4. Conclusions

We developed liposome structure based new sensing platform. The designed liposome sensors intrinsically have several benefits as following; high quantum yield from Rhodamine 6G (R6G) fluorophore, replacement detection mechanism by bioanalyte which is selectively bound to lipids, maintaining higher binding numbers, ability to hold R6G fluorophores. R6G emission in aqueous solution was suppressed by 1,2-dimyristoyl-sn-glycero-3-phosphate (DMPA) aqueous solution. From absorption spectra of different ratio of R6G/DMPA mixtures, we apprehended that the R6G quenching was originated from π-π stacked H-type aggregation of R6G fluorophores. To describe how DMPA lipid molecules play roles to generate the specific aggregation with R6Gs, we proposed following scenarios; 1) ionic interactions between aninic head group of DMPA and cationic R6G, formulating individual DMPA-R6G complexes, 2) the complexes are likely to self-assembled to form liposome structure at above critical bilayer concentration (CBC). Dense R6G stacking should be located on liposome surface at higher concentration, consequentially results in H-type R6G aggregation. Firstly, to figure out whether ionic interaction is key function for R6G quenching as we suggested, we conducted quenching efficiency of R6G in cases of various combination mixture such as anionic, cationic, non-ionic surfactants. Anionic sodium dodecyl sulfate (SDS) micelle suppressed R6G emission as anionic DMPA did, while cationic, non-ionic surfactants did not affect R6G quenching. Moreover, we confirmed the DMPA (or SDS) lipids induced shifted to critical bilayer (or micelle) concentration lowered, forming spherical structure at low lipid concentration. Second, to observe hydrophobic tail effect drivable to formulate spherical self-assembly structures, we measured quenching efficiency of R6G with monopotassium phosphate (KH_2PO_4) having no long hydrophobic tail moiety. As we expected, R6G quenching did not happen regardless of lipid

concentrations.

To design liposome sensing platform based on established R6G quenching mechanism, we considered turn-on type sensory system. Initially, R6G quenching on liposome surface is constructed as “off” status. When bioanalyte is introduced, R6G dye is displaced with bioanalyte attached to paired lipid molecules on liposome surface.

3.5. Author contributions

Sungbaek Seo discovered Rhodamine quenching phenomenon with phospholipid solution. Minsang Kwon found the references for possible mechanisms of Rhodamine quenching. Sungbaek Seo and Min Sang Kwon analyzed the quenching mechanism using UV-Vis absorption and PL measurements. They measured CMC and CBC values on series of phospholipid incorporated samples. Sungbaek Seo took SEM images and measured colloidal size using dynamic light scatter. Sungbaek Seo prepared series of liposome solutions and performed selectivity and sensitivity tests with aminoglycosidic antibiotics.

3.6. References

1. Kang, D. H.; Jung, H.-S.; Lee, J.; Seo, S.; Kim, J.; Kim, K.; Suh, K.-Y., Design of Polydiacetylene-Phospholipid Supramolecules for Enhanced Stability and Sensitivity. *Langmuir* **2012,** *28* (19), 7551-7556.
2. Seo, S.; Lee, J.; Choi, E.-J.; Kim, E.-J.; Song, J.-Y.; Kim, J., Polydiacetylene Liposome Microarray Toward Influenza A Virus Detection: Effect of Target Size on Turn-On Signaling. *Macromolecular Rapid Communications* **2013,** *34* (9), 743-748.
3. Kang, D. H.; Jung, H.-S.; Ahn, N.; Lee, J.; Seo, S.; Suh, K.-Y.; Kim, J.; Kim, K.,

Biomimetic detection of aminoglycosidic antibiotics using polydiacetylene-phospholipids supramolecules. *Chemical Communications* **2012,** *48* (43), 5313-5315.

4. Conner, S. D.; Schmid, S. L., Regulated portals of entry into the cell. *Nature* **2003,** *422* (6927), 37-44.
5. (a) Lee, J.; Jeong Jeong, E.; Kim, J., Selective and sensitive detection of melamine by intra/inter liposomal interaction of polydiacetylene liposomes. *Chemical Communications* **2011,** *47* (1), 358-360; (b) Lee, J.; Seo, S.; Kim, J., Colorimetric Detection of Warfare Gases by Polydiacetylenes Toward Equipment-Free Detection. *Advanced Functional Materials* **2012,** *22* (8), 1632-1638.
6. (a) Jundt, C.; Klein, G.; Le Moigne, J., Yields of triplet exciton pairs in polydiacetylene films. *Chemical Physics Letters* **1993,** *203* (1), 37-40; (b) Olmsted, J.; Strand, M., Fluorescence of polymerized diacetylene bilayer films. *The Journal of Physical Chemistry* **1983,** *87* (24), 4790-4792.
7. Yue, X.; Guo, C.; Jing, Y.; Ma, F., Free-standing liposomal nanohybrid cerasomes as ideal materials for sensing of cupric ions. *Analyst* **2012,** *137* (9), 2027-2031.
8. Ma, G.; Müller, A. M.; Bardeen, C. J.; Cheng, Q., Self-Assembly Combined with Photopolymerization for the Fabrication of Fluorescence "Turn-On" Vesicle Sensors with Reversible "On–Off" Switching Properties. *Advanced Materials* **2006,** *18* (1), 55-60.
9. Kalyanasundaram, K.; Thomas, J. K., Environmental effects on vibronic band intensities in pyrene monomer fluorescence and their application in studies of micellar systems. *Journal of the American Chemical Society* **1977,** *99* (7), 2039-2044.
10. (a) Ogawa, M.; Kosaka, N.; Choyke, P. L.; Kobayashi, H., H-Type Dimer Formation of Fluorophores: A Mechanism for Activatable, in Vivo Optical Molecular Imaging. *ACS*

Chemical Biology **2009,** *4* (7), 535-546; (b) Lofaj, M.; Valent, I.; Bujdák, J., Mechanism of rhodamine 6G molecular aggregation in montmorillonite colloid. *cent.eur.j.chem.* **2013,** *11* (10), 1606-1619; (c) Fischer, M.; Georges, J., Use of thermal lens spectrometry for the investigation of dimerization equilibria of rhodamine 6G in water and aqueous micellar solutions. *Spectrochimica Acta Part A: Molecular and Biomolecular Spectroscopy* **1997,** *53* (9), 1419-1430; (d) Halterman, R.; Moore, J.; Yip, W., Cucurbit[7]uril Disrupts Aggregate Formation Between Rhodamine B Dyes Covalently Attached to Glass Substrates. *J Fluoresc* **2011,** *21* (4), 1467-1478.

11. Peyratout, C.; Donath, E.; Daehne, L., Electrostatic interactions of cationic dyes with negatively charged polyelectrolytes in aqueous solution. *Journal of Photochemistry and Photobiology A: Chemistry* **2001,** *142* (1), 51-57.
12. Baldo, B.; Zhao, Z.; Pham, N., Antibiotic allergy: Immunochemical and clinical considerations. *Curr Allergy Asthma Rep* **2008,** *8* (1), 49-55.
13. (a) Guthrie, O. n. W., Aminoglycoside induced ototoxicity. *Toxicology* **2008,** *249* (2–3), 91-96; (b) Durante-Mangoni, E.; Grammatikos, A.; Utili, R.; Falagas, M. E., Do we still need the aminoglycosides? *International Journal of Antimicrobial Agents* **2009,** *33* (3), 201-205.
14. Magnet, S.; Blanchard, J. S., Molecular Insights into Aminoglycoside Action and Resistance. *Chemical Reviews* **2004,** *105* (2), 477-498.
15. (a) Gabev, E.; Kasianowicz, J.; Abbott, T.; McLaughlin, S., Binding of neomycin to phosphatidylinositol 4,5-biphosphate (PIP2). *Biochimica et Biophysica Acta (BBA) - Biomembranes* **1989,** *979* (1), 105-112; (b) Rooijen, L. A.; Agranoff, B., Inhibition of polyphosphoinositide phosphodiesterase by aminoglycoside antibiotics. *Neurochemical Research* **1985,** *10* (8), 1019-1024; (c) Au, S.; Weiner, N. D.; Schacht, J., Aminoglycoside

antibiotics preferentially increase permeability in phosphoinositide-containing membranes: a study with carboxyfluorescein in liposomes. *Biochimica et Biophysica Acta (BBA) - Biomembranes* **1987,** *902* (1), 80-86.

CHAPTER 4

Approaches for Enhanced PDA Sensitivity: Matrix Polymer Assisted Polydiacetylene Chromism

Manuscript in preparation

4.1. Introduction

Polymer hydrogel is an attractive scaffold in biomedical applications: tissue engineering,[1] drug delivery,[2] wound healing,[3] and biosensors.[4] In general, polymer hydrogel materials are stable in aqueous media and also they can maintain their softness in the gel phase.[5] These unique properties provide that the hydrogels are compatible with biological systems. Moreover, polymer hydrogels show reversible swelling-shrinking behavior in response to various external stimuli such as temperature,[6] pH,[7] ionic strength,[8] light,[9] electric field,[10] and bio-analytes.[11] Basically, polymer hydrogels have an open structure with large internal volume, allowing capture of large amount of molecules for detecting chemical or biological analytes. For these reasons, polymer hydrogel is a suitable platform for biosensor applications.

Sensory nanomaterials can be incorporated into polymer hydrogels, creating advanced composite materials to satisfy the demands of various biosensor systems such as flexible electronics[12] and implantable medical devices.[13] For example, Zhai *et al.* developed an amperometric glucose sensor using polyaniline based hydrogel, which has dual properties of

flexibility and conductivity to be biosensor electrodes.[14] Grigoryev *et al.* fabricated electroconductive carbon nanotube embedded alginate hydrogel fibers for humidity and pH sensing, which enables conversion of the swelling-shrinking behavior of the hydrogel into an electrical sensory signal,[15] because the fiber conductivity changes depending on swelling of the hydrogel fiber. Under the humid and basic condition, the fiber hydrogel expands and lowers the number of contact points between the embedded carbon nanotubes. Accordingly, the fiber conductivity decreases as the hydrogel get swell. While electroconductive hydrogel based sensors are extensively investigated, optical biosensors devised from polymer hydrogel are few. Since there are great potential of direct, real-time and label-free detection of chemical and biological analytes, optical detection is one of indispensable biosensor categories.

Polydiacetylene (PDA) is a self-signalizing polymer exhibiting color changes from blue to red upon exposure to external stimuli including temperature,[16] pH,[17] mechanical stress,[18] and chemical/biological analytes.[19] The signal transduction mechanism of PDA is believed to be based on the distortion of the self-assembled and polymerized conjugated yne-ene backbone of PDA by external stimuli. In particular, as for the chemical and biological analytes, steric repulsion at the surface of PDA sensors induced by the specific receptor-target complex formation triggers signal generation as illustrated in Figure 4.1a. In this regard, as for the signal generation, adjacent receptors must be occupied by target molecules so that efficient repulsion between the receptor-target complexes can be induced. This condition can be satisfied only when decent amount of analytes are available to capture, lowering the detection of the PDA sensory system. We investigated an alternative approach by combining stimuli-responsive polymer hydrogel as a matrix and PDA sensory materials as a signal-generating component. In this system, swelling or shrinking response of the polymer matrix to external stimuli imposes stress

on the PDA sensory materials to produce sensory signals. How the polymer hydrogel composite affects chromism of PDA is worthwhile study to build fundamental background for hydrogel based biosensor applications.

4.2. Experimental section

4.2.1. Materials and methods

All solvents were purchased from Sigma-Aldrich. 10,12-pentacosadiynoic acid (PCDA) was purchased from GFS Chemicals. Oxalyl chloride and sodium alginate were obtained from Acros Organics. 5-aminoisophthalic acid, lithium hydroxide, sodium hydroxide, potassium hydroxide and calcium chloride were purchased from Sigma-Aldrich.

The synthesis of PCDA derivatives was described in the literature.[20] The PDA monomers were characterized with 1H NMR spectra (500 MHz) using a Varian Inova 500 instrument. The morphology of the PDA assembly structure was observed with scanning electron microscopy images using an FEI Nova NanoLab instrument. The size and surface charge of the PDA liposome solution were measured by Malvern Zetasizer Nano-ZS. Photographs were taken using Sony NEX-F3 camera. Powder XRD patterns were measured by a Rigaku rotating anode X-Ray diffractometer. UV-Vis absorption spectra were obtained by Varian Cary 50 UV-Vis spectrophotometer.

4.2.2. Preparation of PDA liposome solution

PDA liposome solution was prepared by the injection method. PCDA and PCDA-IPA were each dissolved in 0.3 ml of tetrahydrofuran. The homogeneous solution was injected into a 20 ml of deionized water and subsequently dispersed in a probe sonicator for 10 min to produce the final concentration of 0.5 mM liposome. After filtration through a 0.8 μm cellulose acetate

syringe filter, the resulting PDA liposome solution was stored at 5 ℃ at least 2 hours.

4.2.3. Preparation of PCDA nanowire and PCDA-IPA nanofibers

PCDA nanowires were fabricated according to the literature.[21] To a 10 ml of 4 mM NaOH aqueous solution, 1.52 mg of purified colorless PCDA was added. The mixture solution was heated up to 90 ℃ with stirring to reach a clear homogenous solution. The clear solution was cooled down at 5 ℃ for 2 hours, then sodium 5,7-eicosadiynoic acid (PCDA-Na^+) nanowires began to precipitate from the solution.

Likewise, to a 15 ml of 1 mM of alkali hydroxides (KOH or LiOH) solution, the purified colorless PCDA-IPA was added. The mixture solution was heated to 90 ℃ with stirring to produce a transparent solution. The solution was cooled down at 5 ℃ overnight, then viscous potassium PCDA-IPA (PCDA-IPA-K^+) and lithium PCDA-IPA (PCDA-IPA-Li^+) nanofibers appeared from the solutions, respectively.

4.2.4. Preparation of PDA assembly embedded alginate hydrogel

4.6 ml of 0.5 mM PDA assemblies (liposomes or nanowires or nanofibers) were homogeneously stirred with 4.6 ml of 4 wt % alginate solution in a 20 ml vial. To the mixture solution, 0.6 ml of 2 wt % calcium chloride solution is added to generate crosslinked gel with 30 min stirring. The gel was rinsed with deionized water 3 times to remove unreacted calcium chloride and subsequently dried at 40 ℃.

4.2.5. Characterization of swelling in alginate hydrogel

The dried hydrogels were weighed as dried state (W_d). The dried hydrogels were immersed in 1 ml of deionized water for 1 hour. The hydrogels were removed and were blotted with a paper towel to remove excess water on surface. Then, swollen hydrogels were weighed as swollen state (W_s). The swelling ratio (Q_s) of test samples was calculated from the following equation.[22]

$Q_s = (W_s-W_d)/W_d$,

The condition (concentration of alginate solution and calcium chloride solution), which had the best swelling characteristics was selected for hydrogel swelling driven PDA chromism.

4.3. Results and discussion

We systematically investigated matrix polymer assisted PDA chromism in order to devise a sensitive hydrogel-based hybrid sensory system. We self-assembled PDA into 0-dimensional liposome and 1-dimensional nanowire and nanofiber structures, respectively. As the polymer matrix we used alginate hydrogel that is an anionic linear polymer and highly hygroscopic enough to absorb 200-300 times of its own weight in water. Due to the anionic character alginate can be ionically crosslinked with divalent cations.[22] In order to convey external stimuli directly to the sensory PDA materials, we crosslinked the sensory PDA assembly with alginate matrix using cationic crosslinkers to form hydrogel composite (Figure 4.1b-c). We observed that the nanoscaled thickness of the PDA assembly was critical to produce turn-on chromism through interaction with the swelling of the hydrogel. We investigated the effect of swelling ratio of the matrix polymer on the colorimetric transition of the embedded PDA assemblies.

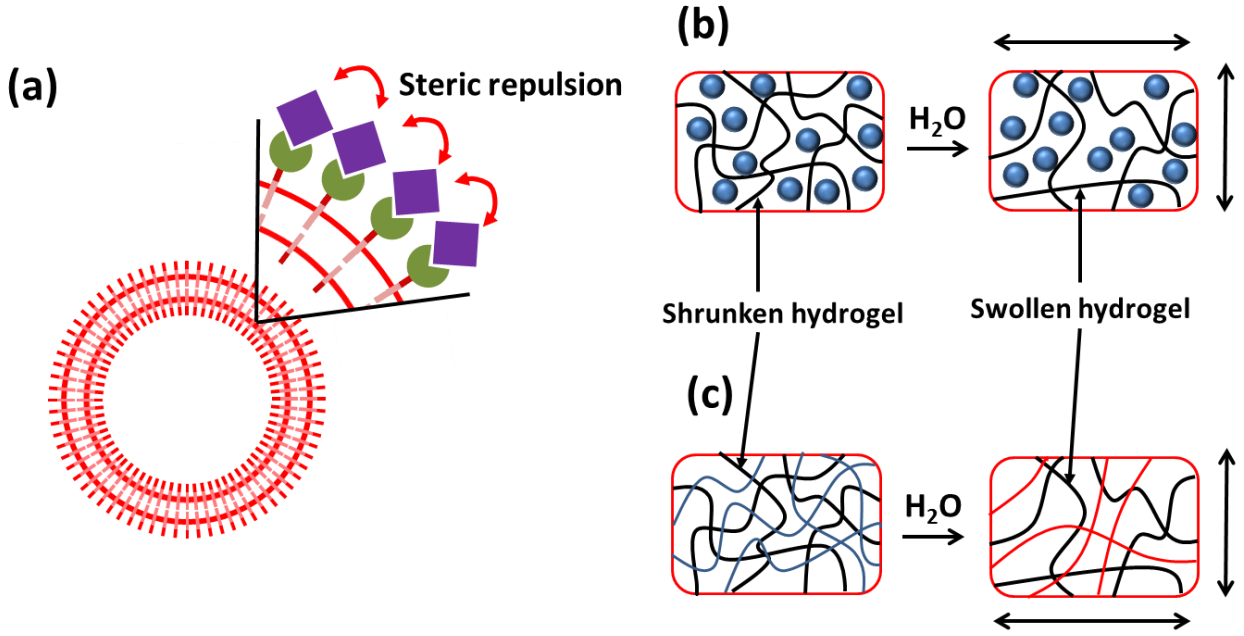

Figure 4.1 Signal transduction mechanism of PDA sensor. (a) Steric repulsion induced by the receptor-target complex formation triggers signal generation. Scheme of PDA-hydrogel composite shrunken and swollen state by immersing water; (b) 0-dimensional PDA liposome embedded alginate hydrogel. 1-dimensional PDA assembly incorporated alginate hydrogel.

10,12-pentacosadiynoic acid (PCDA) and PCDA-IPA are diacetylene monomers self-assembled to generally a liposome form in aqueous medium due to their amphiphilic property. We developed a self-assembly protocol to make 1-dimensional PDA nanowires and nanofibers rather than conventional 0-dimensional liposome by adapting a literature method using alkali metal ions.[21] Therefore, we could formulate 1-dimensional microcrystals, nanofibers, as well as liposome of PCDA and PCDA-IPA, respectively.

We prepared PDA liposomes suspended in deionized water (inset of Figure 4.2a, b). Dynamic light scattering measurement showed that PCDA, PCDA-IPA liposomes have 150 nm (PDI 0.26) and 244 nm (PDI 0.38) in mean diameter, respectively. SEM images showed the spherical shape of liposomes and the diameters are consistent to the values from the light scattering measurement (Figure 4.2a, b). The surface charge of PCDA, PCDA-IPA liposomes are

-34.6 ± 10.6 mV and -56.4 ± 8.57 mV, respectively, due to the carboxylic acid groups at the terminal of the DAs. The anionic surface of the assembled DAs further enables ionic crosslinking of the liposomes with multivalent cations such as Ca^{2+}.

First, we optimized the concentration condition of alginate and $CaCl_2$ solution to achieve large swelling of the alginate hydrogel. To an alginate solution at various concentrations a $CaCl_2$ solution at various concentrations was added. Within 30 seconds, an amorphous gel was formed. After 30 minutes of crosslinking reaction in the gel, any unbound calcium ions were washed off by deionized water several times. After drying the gel, in order to estimate how much swelling the gel can make we measured the volumetric change of the hydrogel before and after immersing into water. Dried alginate gel began to swell within 10 min and saturated by 1 hour in water (inset of Figure 4.3). Through an optimization study, the achievable best swelling ratio was about 60 from the gel prepared with a 2 wt% alginate solution and an 1 wt% $CaCl_2$ solution (Figure 4.3). The swelling ratio was calculated by equation described in the experimental section. As the $CaCl_2$ amount increased, the crosslink between alginate and $CaCl_2$ became denser, resulting in a smaller swelling ratio.

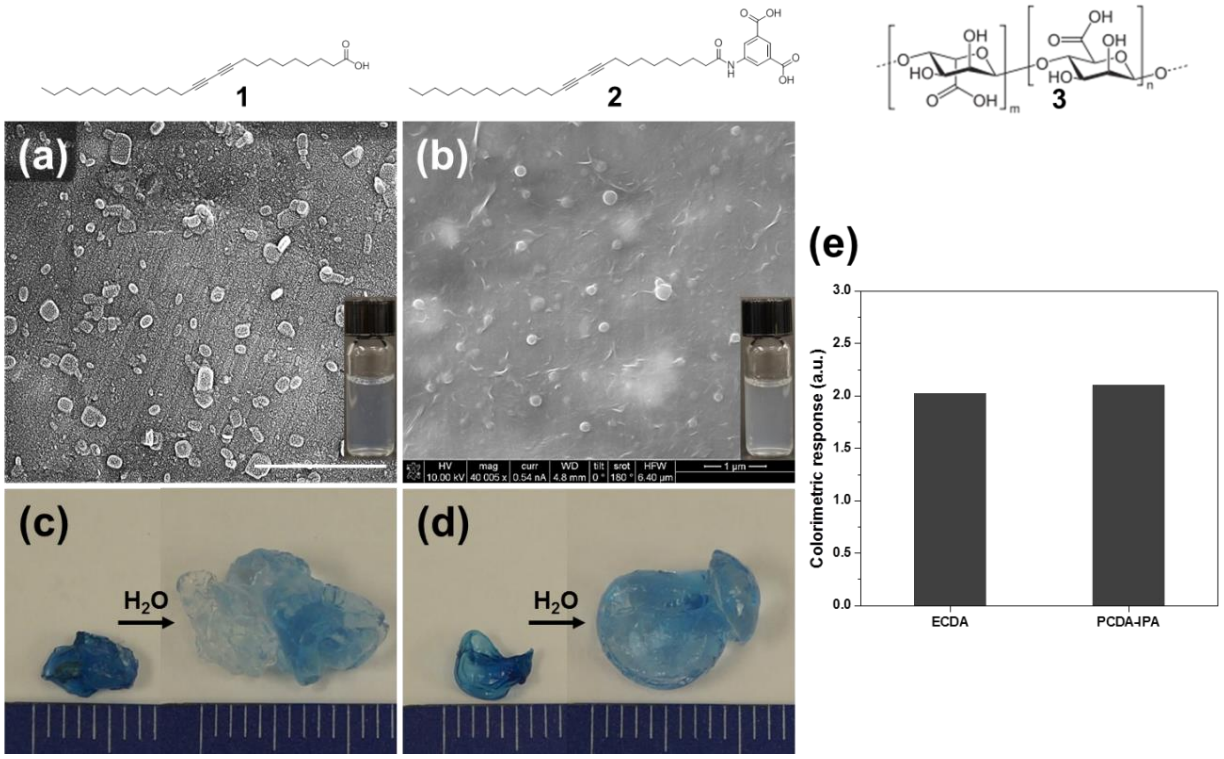

Figure 4.2 Chemical structure of (1) PCDA and (2) PCDA-IPA (3) alginic acid. SEM images of (a) PCDA liposome and (b) PCDA-IPA liposome. Scale bar is 1 μm. Photograph of photopolymerized alginate hydrogel embedded with (c) PCDA liposome, (d) PCDA-IPA liposome. (e) Colorimetric response values (red/blue) calculated from UV-Vis absorption intensities.

After establishing the gel formula, we incorporated PCDA liposomes and PCDA-IPA liposomes into the alginate hydrogel by crosslinking the liposome and alginate with Ca^{2+} to investigate the effect of the hydrogel swelling on the PDA mechanochromism. We could photopolymerize the embedded PDA liposomes to make blue hydrogel, confirming PDA liposomes are stable inside the hydrogel. Afterwards 1 ml of deionized water was added to a dried PDA-alginate hydrogel and the gel was kept at room temperature for 1 hour. The swelling ratio of the two hydrogels having PCDA liposomes and PCDA-IPA liposomes was 34 and 33, respectively (Figure 4.2c, d). The hydrogels were expanded from 5-6 mm to 10 mm in length. However, we could not observe any noticeable chromism from the swollen gels as the

colorimetric response (CR) from UV-Vis absorption was only around 2 (Figure 4.2e). The CRs of the hydrogel composite before and after water uptake were calculated by the well-known equation.[23] Here, the blue percentage (PB) is defined as PB = $A_{blue}/(A_{blue} + A_{red}) \times 100$ % where A_{blue} is the absorbance at the peak around 675 nm and A_{red} is the absorbance at the peak around 550 nm. Then, the CR is defined as CR = (initial PB − final PB)/initial PB × 100%. As illustrated in Scheme 1, we hypothesized that 0-dimensional liposomes can not make enough many crosslinking points with multiple alginate fibers in the gel so that swelling of the gel cannot cause enough deformation of the embedded PDA liposomes to produce mechanochromism.

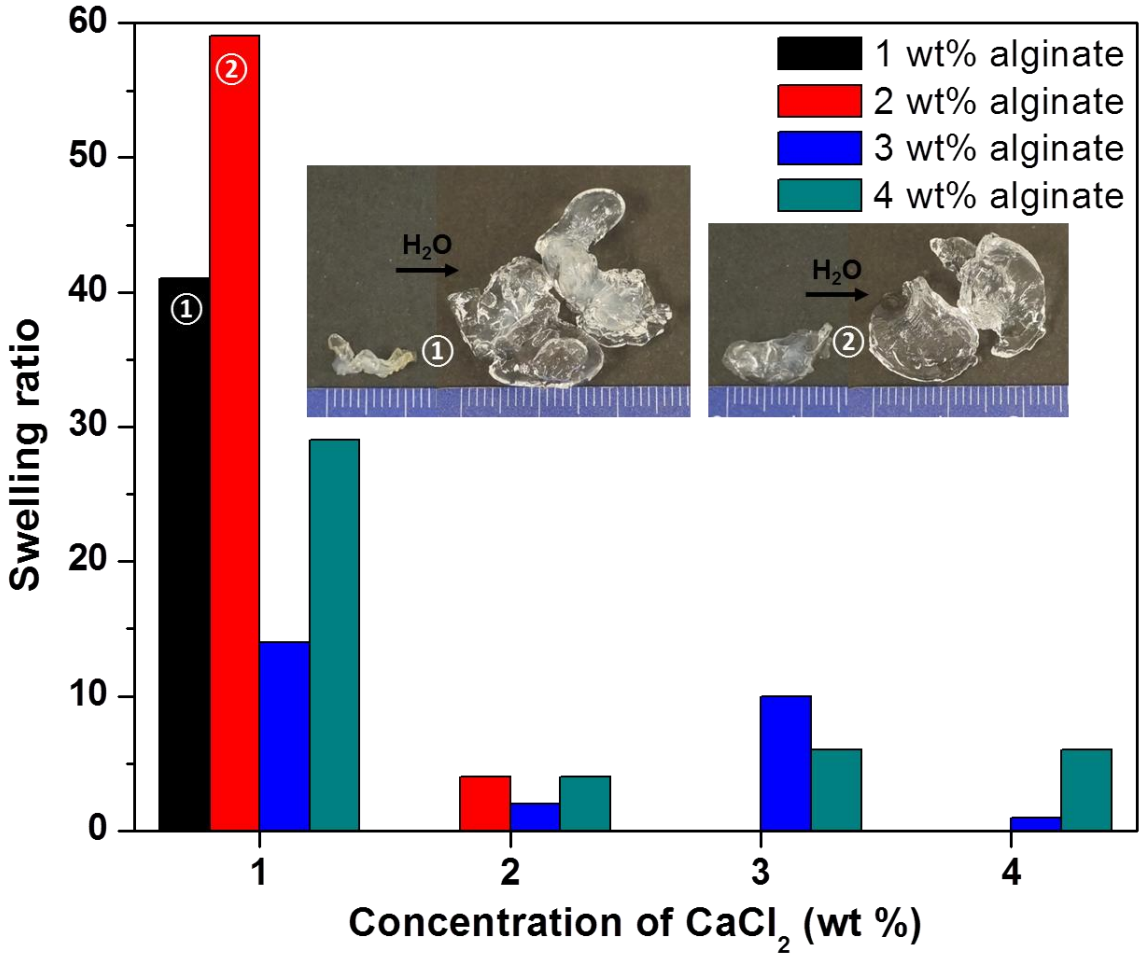

Figure 4.3 Optimization of the alginate and the $CaCl_2$ solution concentration for the best swelling ratio.

In order to examine our hypothesis that 1-dimensional PDA assembly such as nanofiber or nanowire makes more efficient linking with multiple matrix alginate fibers than 0-dimensional PDA liposome does, we prepared 1-dimensional PDA nanowires and nanofibers. Photopolymerization of the prepared PCDA-Na^+ nanowires by a 254 nm UV lamp produced blue color. As shown in Figure 4.4a-c inset, we prepared such 1-dimensional nano-assembly by using alkali metals; PCDA-Na^+ bulky microcrystals, PCDA-IPA-K^+ nanofiber having 50 nm thickness, and PCDA-IPA-Li^+ nanofiber with 20 nm thickness. Even though we do not fully understand the role of the alkali metals, Li^+ produced the thinnest PDCA-IPA nanofiber. XRD analysis on these nano-assemblies revealed a highly ordered lamellar structure (Figure 4.4d-f). The interlamellar distance calculated from the Bragg equation for PCDA-Na^+ bulky microcrystals, PCDA-IPA-K^+ nanofiber, and PCDA-IPA-Li^+ nanofiber was 2.68, 3.15, 4.18 nm, respectively.

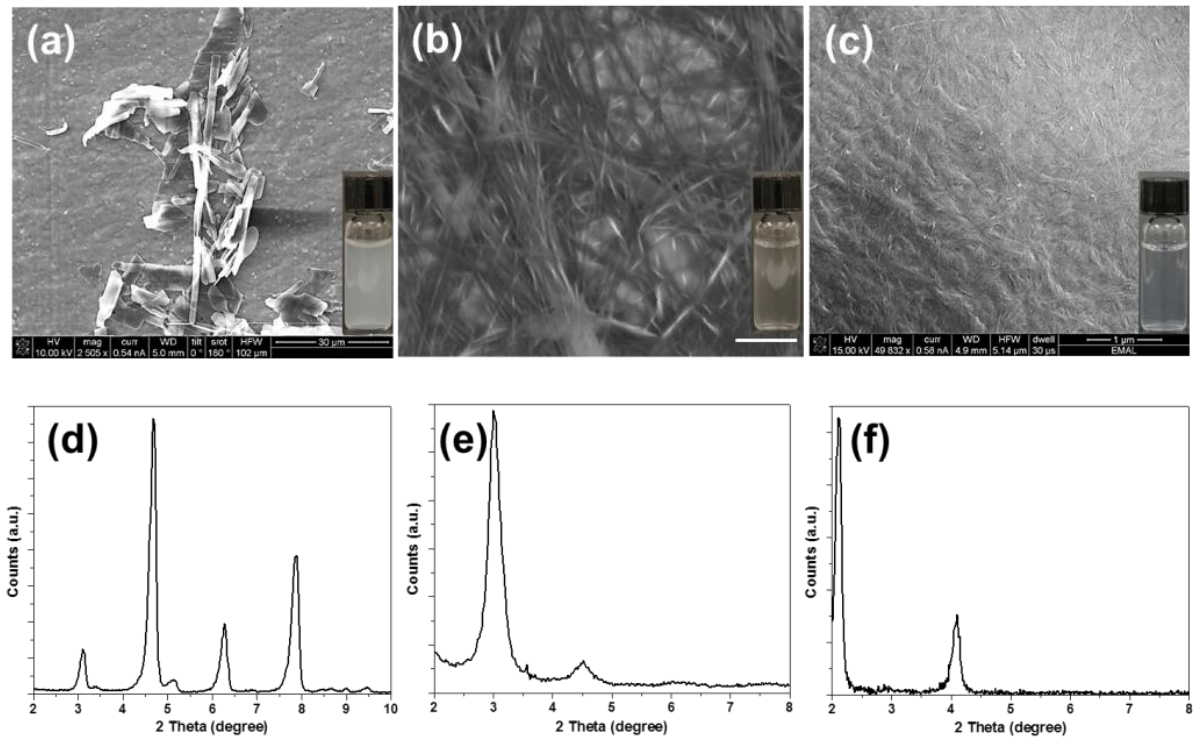

Figure 4.4 SEM images of (a) PCDA-Na^+ microcrystal, (b) PCDA-IPA-K^+ nanofiber, (c) PCDA-IPA-Li^+ nanofiber. Scale bar is 1 µm. XRD patterns of (d) PCDA-Na^+ microcrystal, (e) PCDA-IPA-K^+ nanofiber, (f) PCDA-IPA-Li^+ nanofiber.

This implies that the introduction of alkali metal ions promotes the formation of 1-dimensional structures by means of forming stronger intermolecular interactions, such as electrostatic interactions, π–π stacking and hydrogen bonding between amide groups.[24] Based on the XRD data we proposed the highly ordered molecular packing structure of PCDA-IPA-Li^+ nanofibers in Figure 4.5.

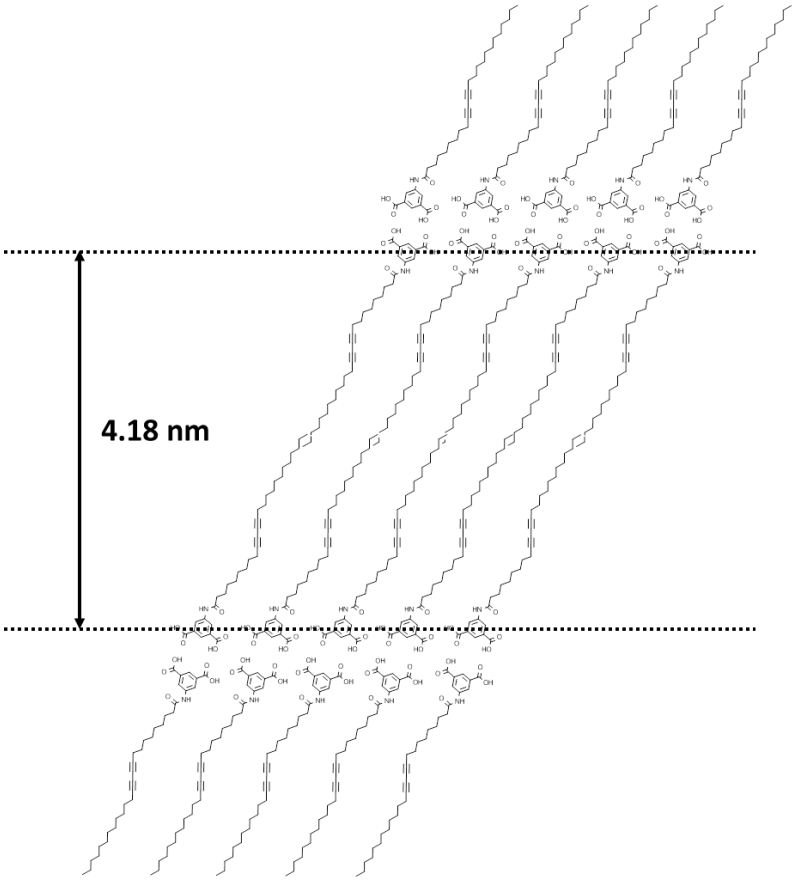

Figure 4.5 A proposed molecular packing structure of PCDA-IPA-Li^+ nanofiber.

Swelling ratio of the hydrogels embedded with the 1-dimensional PDA assemblies (PCDA-Na^+ nanowire, PCDA-IPA-K^+ nanofiber, PCDA-IPA-Li^+ nanofiber) was in the range of 30 - 35 (Figure 4.6a-c). Among the three 1-D nano-assemblies only flexible and thinner PCDA-IPA-Li^+ nanofibers hydrogel composite showed red color in the swollen state, which makes sense

because it is likely that the thinner nanofiber is more sensitive to the same force imposed by swelling of the gel. As one can see the UV-Vis spectra in Figure 4.6d, we could confirm the red phase formation by the swelling. Colorimetric transition of the hydrogel composites in this study plotted in Figure 4.6e clearly shows that PCDA-IPA-Li^+ nanofiber hydrogel is most senstive. 1-dimensional structures provide a lager surface area-to-volume ratio than 0-dimensional liposomes. Accordingly, 1-dimensional nanofibers would form more ionic crosslinking points with multiple alginate fibers to form effective hydrogel network. Flexibility of nanofibers is compatible with the soft hydrogel matrix, and the gel swelling driven stress acts on the nanofibers efficiently, generating red color.

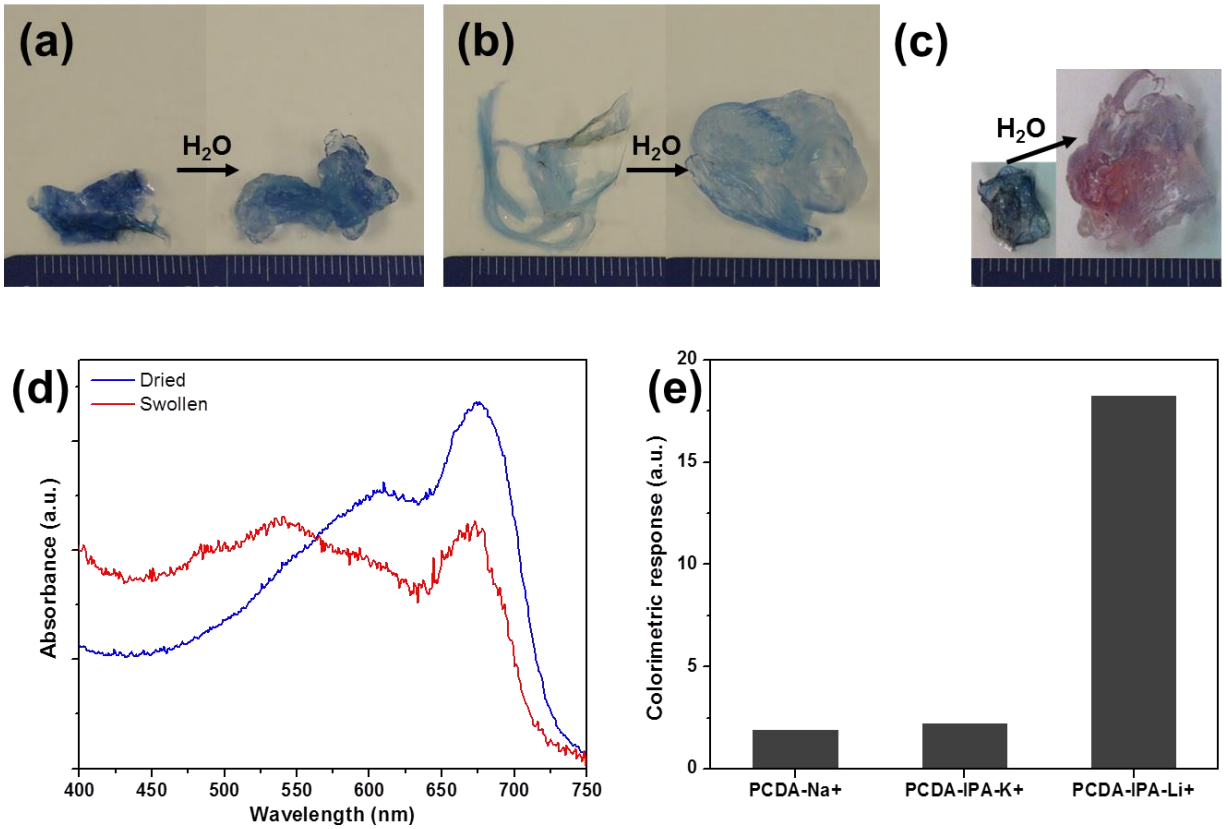

Figure 4.6 Photograph of photopolymerized alginate hydrogel embedded with (a) PCDA-Na+ microcrystal, (b) PCDA-IPA-K^+ nanofiber, (c) PCDA-IPA-Li^+ nanofiber. (d) UV-Vis spectra of PCDA-IPA-Li^+ nanofiber hydrogel in dried and swollen state. (e) Colorimetric response of alginate hydrogel calculated from UV-Vis absorption intensities.

4.4. Conclusions

There is a great need of convenient water detection in dental treatments. We rationally combined PCDA-IPA nanowires as a sensory unit and hygroscopic alginate polymers as a stimuli responsive matrix into a PDA nanowire-alginate network for water and moisture detection. Alginate is a hygroscopic biopolymer having a dramatic volume swelling property up to 200 times when it absorbs water. PDA nanowires were embedded into an alginate solution and the mixture was crosslinked by calcium ions to form a gel. While zero-dimensional PDA liposomes, if used instead, can make only few contact points with alginate polymer chains in the gel, the 1-dimensional PDA nanowires will have many more crosslinking points with multiple alginate polymer chains. Therefore, PDA nanowires are exposed to much stronger tension upon alginate swelling by water, producing a sensitive colorimetric signal.

4.5. Author contributions

Jiseok Lee initially designed the diacetylene monomer (PCDA-IPA). By using the monomer Sungbaek Seo synthesized the polymers and fabricated liposomes and 1-dimensional structures (microcrystals, nanofibers). Sungbaek Seo took SEM images, measured size and zeta potential of liposomes, measured XRD patterns.

4.6. References

1. Lee, K. Y.; Mooney, D. J., Hydrogels for Tissue Engineering. *Chemical Reviews* **2001,** *101* (7), 1869-1880.
2. Shoichet, M. S., Polymer Scaffolds for Biomaterials Applications. *Macromolecules* **2009,** *43*

(2), 581-591.

3. Slaughter, B. V.; Khurshid, S. S.; Fisher, O. Z.; Khademhosseini, A.; Peppas, N. A., Hydrogels in Regenerative Medicine. *Advanced Materials* **2009,** *21* (32-33), 3307-3329.
4. Tokarev, I.; Minko, S., Stimuli-responsive hydrogel thin films. *Soft Matter* **2009,** *5* (3), 511-524.
5. Mateescu, A.; Wang, Y.; Dostalek, J.; Jonas, U., Thin Hydrogel Films for Optical Biosensor Applications. *Membranes* **2012,** *2* (1), 40-69.
6. Hirokawa, Y.; Tanaka, T., Volume phase transition in a nonionic gel. *The Journal of Chemical Physics* **1984,** *81* (12), 6379-6380.
7. Jin, S.; Liu, M.; Zhang, F.; Chen, S.; Niu, A., Synthesis and characterization of pH-sensitivity semi-IPN hydrogel based on hydrogen bond between poly(N-vinylpyrrolidone) and poly(acrylic acid). *Polymer* **2006,** *47* (5), 1526-1532.
8. Elliott, J. E.; Macdonald, M.; Nie, J.; Bowman, C. N., Structure and swelling of poly(acrylic acid) hydrogels: effect of pH, ionic strength, and dilution on the crosslinked polymer structure. *Polymer* **2004,** *45* (5), 1503-1510.
9. Fujigaya, T.; Morimoto, T.; Niidome, Y.; Nakashima, N., NIR Laser-Driven Reversible Volume Phase Transition of Single-Walled Carbon Nanotube/Poly(N-isopropylacrylamide) Composite Gels. *Advanced Materials* **2008,** *20* (19), 3610-3614.
10. TANAKA, T.; NISHIO, I.; SUN, S.-T.; UENO-NISHIO, S., Collapse of Gels in an Electric Field. *Science* **1982,** *218* (4571), 467-469.
11. Maitz, M. F.; Freudenberg, U.; Tsurkan, M. V.; Fischer, M.; Beyrich, T.; Werner, C., Bio-responsive polymer hydrogels homeostatically regulate blood coagulation. *Nat Commun* **2013,** *4*.

12. (a) Pan, L.; Yu, G.; Zhai, D.; Lee, H. R.; Zhao, W.; Liu, N.; Wang, H.; Tee, B. C.-K.; Shi, Y.; Cui, Y.; Bao, Z., Hierarchical nanostructured conducting polymer hydrogel with high electrochemical activity. *Proceedings of the National Academy of Sciences* **2012,** *109* (24), 9287-9292; (b) Xu, Y.; Sheng, K.; Li, C.; Shi, G., Self-Assembled Graphene Hydrogel via a One-Step Hydrothermal Process. *ACS Nano* **2010,** *4* (7), 4324-4330; (c) Sekine, S.; Ido, Y.; Miyake, T.; Nagamine, K.; Nishizawa, M., Conducting Polymer Electrodes Printed on Hydrogel. *Journal of the American Chemical Society* **2010,** *132* (38), 13174-13175.

13. (a) LaVan, D. A.; McGuire, T.; Langer, R., Small-scale systems for in vivo drug delivery. *Nat Biotech* **2003,** *21* (10), 1184-1191; (b) Norton, L. W.; Tegnell, E.; Toporek, S. S.; Reichert, W. M., In vitro characterization of vascular endothelial growth factor and dexamethasone releasing hydrogels for implantable probe coatings. *Biomaterials* **2005,** *26* (16), 3285-3297; (c) Nakabayashi, N.; Williams, D. F., Preparation of non-thrombogenic materials using 2-methacryloyloxyethyl phosphorylcholine. *Biomaterials* **2003,** *24* (13), 2431-2435.

14. Zhai, D.; Liu, B.; Shi, Y.; Pan, L.; Wang, Y.; Li, W.; Zhang, R.; Yu, G., Highly Sensitive Glucose Sensor Based on Pt Nanoparticle/Polyaniline Hydrogel Heterostructures. *ACS Nano* **2013,** *7* (4), 3540-3546.

15. Grigoryev, A.; Sa, V.; Gopishetty, V.; Tokarev, I.; Kornev, K. G.; Minko, S., Wet-Spun Stimuli-Responsive Composite Fibers with Tunable Electrical Conductivity. *Advanced Functional Materials* **2013,** *23* (47), 5903-5909.

16. (a) Carpick, R. W.; Sasaki, D. Y.; Burns, A. R., First Observation of Mechanochromism at the Nanometer Scale. *Langmuir* **2000,** *16* (3), 1270-1278; (b) Ryu, S.; Yoo, I.; Song, S.; Yoon, B.; Kim, J.-M., A Thermoresponsive Fluorogenic Conjugated Polymer for a

Temperature Sensor in Microfluidic Devices. *Journal of the American Chemical Society* **2009,** *131* (11), 3800-3801.

17. (a) Cheng, Q.; Stevens, R. C., Charge-Induced Chromatic Transition of Amino Acid-Derivatized Polydiacetylene Liposomes. *Langmuir* **1998,** *14* (8), 1974-1976; (b) Jonas, U.; Shah, K.; Norvez, S.; Charych, D. H., Reversible Color Switching and Unusual Solution Polymerization of Hydrazide-Modified Diacetylene Lipids. *Journal of the American Chemical Society* **1999,** *121* (19), 4580-4588.
18. (a) Tomioka, Y.; Tanaka, N.; Imazeki, S., Effects of side-group interactions on pressure-induced chromism of polydiacetylene monolayer at a gas-water interface. *Thin Solid Films* **1989,** *179* (1–2), 27-31; (b) Tashiro, K.; Nishimura, H.; Kobayashi, M., First Success in Direct Analysis of Microscopic Deformation Mechanism of Polydiacetylene Single Crystal by the X-ray Imaging-Plate System. *Macromolecules* **1996,** *29* (25), 8188-8196.
19. (a) Lee, J.; Chang, H. T.; An, H.; Ahn, S.; Shim, J.; Kim, J.-M., A protective layer approach to solvatochromic sensors. *Nat Commun* **2013,** *4*; (b) Chen, X.; Kang, S.; Kim, M. J.; Kim, J.; Kim, Y. S.; Kim, H.; Chi, B.; Kim, S.-J.; Lee, J. Y.; Yoon, J., Thin-Film Formation of Imidazolium-Based Conjugated Polydiacetylenes and Their Application for Sensing Anionic Surfactants. *Angewandte Chemie International Edition* **2010,** *49* (8), 1422-1425; (c) Kang, D. H.; Jung, H.-S.; Ahn, N.; Lee, J.; Seo, S.; Suh, K.-Y.; Kim, J.; Kim, K., Biomimetic detection of aminoglycosidic antibiotics using polydiacetylene-phospholipids supramolecules. *Chemical Communications* **2012,** *48* (43), 5313-5315; (d) Seo, S.; Lee, J.; Choi, E.-J.; Kim, E.-J.; Song, J.-Y.; Kim, J., Polydiacetylene Liposome Microarray Toward Influenza A Virus Detection: Effect of Target Size on Turn-On Signaling. *Macromolecular Rapid Communications* **2013,** *34* (9), 743-748.

20. Lee, J.-S.; Lee, S.; Kim, J.-M., Fluorogenic conjugated polymer fibers from amphiphilic diacetylene supramolecules. *Macromol. Res.* **2008,** *16* (1), 73-75.

21. Bai, F.; Sun, Z.; Lu, P.; Fan, H., Smart polydiacetylene nanowire paper with tunable colorimetric response. *Journal of Materials Chemistry* **2012,** *22* (30), 14839-14842.

22. Lin, Y.-H.; Liang, H.-F.; Chung, C.-K.; Chen, M.-C.; Sung, H.-W., Physically crosslinked alginate/N,O-carboxymethyl chitosan hydrogels with calcium for oral delivery of protein drugs. *Biomaterials* **2005,** *26* (14), 2105-2113.

23. Okada, S.; Peng, S.; Spevak, W.; Charych, D., Color and Chromism of Polydiacetylene Vesicles. *Accounts of Chemical Research* **1998,** *31* (5), 229-239.

24. Pang, J.; Yang, L.; McCaughey, B. F.; Peng, H.; Ashbaugh, H. S.; Brinker, C. J.; Lu, Y., Thermochromatism and Structural Evolution of Metastable Polydiacetylenic Crystals. *The Journal of Physical Chemistry B* **2006,** *110* (14), 7221-7225.

CHAPTER 5

Conclusions

5.1. Research summary

The aim of my dissertation work was to develop highly sensitive polydiacetylene (PDA) supramolecule systems for biosensor applications. We recognized the demanding need for rapid and sensitive influenza virus detection and designed a PDA based biosensor for the same (**Chapter 2**). We selected influenza A virus M1 peptide and M1 antibody as a probe-target binding pair. Since PDA liposome solution based detection consumes a lot of high-priced biological moieties such as peptides, antibodies and viruses, we selected microarray sensor format which uses small but suitable amount. Microarray was useful to control tethering efficiency of probe molecules onto PDA liposome surface. To observe target size effect on PDA sensory signal generation, we switched role of probe and target in two different types of sensory system. In the first system, we fully covered PDA liposome onto glass slide and probe molecules were micro-arrayed onto the PDA liposome layer. This post-tethering of probe molecules did not generate noticeable signals regardless of whether the M1 peptide was used as a probe or target. Our calculation implied that the number of probe molecules actually tethered at the PDA liposome surface, 3.3 % at best, was too few to form good enough complex formation for efficient steric perturbation of the PDA conjugated backbone. To enhance the number of tethered probe molecules at the PDA surface, PDA liposomes were spotted by a manual microarrayer.

Then, the PDA microarray was covered with M1 peptide or M1 antibody solution. As increased number of probing molecules, larger number of probe–target complex was expected to form, and indeed we observed strong red emission from the microarray upon incubating with M1 antibody. When M1 antibody was used as a probe for the detection of M1 peptide by means of the same second strategy, on the contrary, we could not observe noticeable sensory signal generation.

From this result described in Chapter 2, we concluded that the intensity of the PDA sensory signal is primarily related to the steric repulsion between probe–target complexes and not the strength of the binding force between the probe and its target. Based on this finding, we anticipated that influenza A virus can be directly detected by PDA liposome having M1 antibody probes because the whole virus is larger than M1 antibody. Indeed, red dots appeared on the PDA liposome microarray after incubation with H1N2 viruses, which confirms the target size effect on the PDA turn-on signal generation. To further improve the sensitivity of the PDA liposome microarray, we incorporated a phospholipid (1,2-dimyristoylsn-glycero-3-phosphate, DMPA) into the PDA liposome to provide more mobility and ensuing easier perturbation of PDA backbone by probe–target complex formation and repulsion. We finally reached the detection limit of 2^{-2} HAU from the PDA liposome microarray, which is comparable to the detection limit of the conventional influenza A virus kit.

We were interested in the approach that inserting phospholipid intentionally weakens the intermolecular strength in PDA liposome thereby resulting in more sensitive PDA signal generation. Moreover, we considered a phospholipid with its own capturing moiety for the target molecule that could be incorporated in the PDA liposome and provide easy disturbance of PDA intermolecular packing by recognition event and generate PDA sensory signal. Through PDA-phospholipid supramolecules studies, we found that Rhodamine 6G (R6G) emission is

suppressed by DMPA aqueous solution. As the amount of DMPA increases in solution, the emission intensity of R6G steadily decreases and ultimately the emission is almost completely quenched. From the spectral features of the appearing new peaks in UV-Vis measurement, this interesting quenching behavior are attributed to the aggregation-induced emission quenching by means of the formation of H-type aggregates of R6G mediated by DMPA. Accordingly, we systematically investigated how DMPA phospholipid functions to create R6G H-type aggregation. We postulated that Coulombic interaction between cationic R6G and anionic DMPA subsequently formulates ionic complexes. As increase concentration of ionic complexes, the lipid complexes start to form spherical structures and simultaneously possess R6G aggregates on the liposome surface. To confirm our expected scheme, we plotted the quenching ratio of R6G dyes versus DMPA concentration in the mixed water solution of R6G and DMPA to understand the detailed mechanism of R6G aggregation. Interestingly, the rapid quenching happened at around 0.01 mM which is far lower concentration than the critical micelle concentration of DMPA. This result implied that DMPA-R6G molecular complexes are more hydrophobic than DMPA, they can form liposome even at very low concentration of DMPA. Moreover, to confirm that Coulombic interaction and hydrophobic tail effect on R6G quenching act in the same way, monopotassium phosphate, positively charged CTAB, neutral Tween 20, zwitterionic CHAPS were tested. But, these did not show any signature for dye aggregation due to the lack of Coulombic interaction and lack of driving force to self-assembled structure.

Chapter 3 described our newly developed sensing platform to detect various bioanalytes based on this new finding of the DMPA liposome-R6G complex formation. It is well known that phospholipids specifically interact with bioanalytes. We envisioned that specific interaction between a phospholipid and a target analyte would break the non-specific Coulombic

interactions between R6G dyes and phospholipids leading to displacement of R6G dyes by the target analyte and consequent fluorescence recovery as a sensory signal. We selected neomycin as a target analyte, phosphatidylinositol-4,5-bisphosphate (PIP_2) as probe phospholipid that can capture neomycin and designed a new turn-on type sensory system. We conducted selectivity and sensitivity tests with aminoglycosidic antibiotics (Neomycin, Gentamycin, Tobramycin, Streptomycin) and non-aminoglycosidic antibiotic (Oxytetracycline) at various concentrations. Distinguishable R6G emission recovery is observed with 10 nM neomycine, which is at least 10 times better than the established 0.1 μM of detection limit of neomycin in the published literature.[1] Moreover, excellent selectivity of the developed novel "turn-on" sensory system toward aminoglycosidic antibiotics particularly Neomycin was demonstrated. This novel sensory platform has several merits; it can provide high sensitivity, readily applicable to other sensor designs, and can conveniently use conventional 96-well plates and ELISA apparatus.

We rationally combined PDA nanofibers as a sensory unit and hygroscopic alginate polymers as a stimuli responsive matrix into a network hydrogel for water and moisture detection (**Chapter 4**). We discovered a promising dimensionality effect on PDA sensitivity from the developed very thin PDA nanofibers. We observed fast colorimetric transition of 1-dimensional PDA nanofiberes embedded in alginate when the gel was swelled by water, while zero dimensional PDA liposome in the same gel did not show any color change. We believe that 1-dimentional nanofibers create more ionic crosslinking with alginate hydrogel network. Therefore, PDA nanofibers can experience much more deformation-induced stress and produce more noticeable color change upon swelling of alginate.

In summary, overall design principles for highly sensitive PDA supramolecules biosensors are discussed and described in detail in this dissertation (Figure 5.1). We verified target size

effect and developed understanding of protein-protein interactions as most of the binding pairs in biosensor development. To enhance the sensitivity of the PDA sensory system, we suggested ways of inserting phospholipid into PDA liposome to weaken PDA intermolecular packing or utilizing phospholipids with functional probe moiety. Moreover, we devised a novel fluorescence turn-on sensory platform by regulating R6G H-aggregates on the liposome surface. We also developed matrix polymer-assisted sensitive PDA sensory system and 1-dimensional PDA nanofibers were considered to enhance the colorimetric sensitivity of PDA systems.

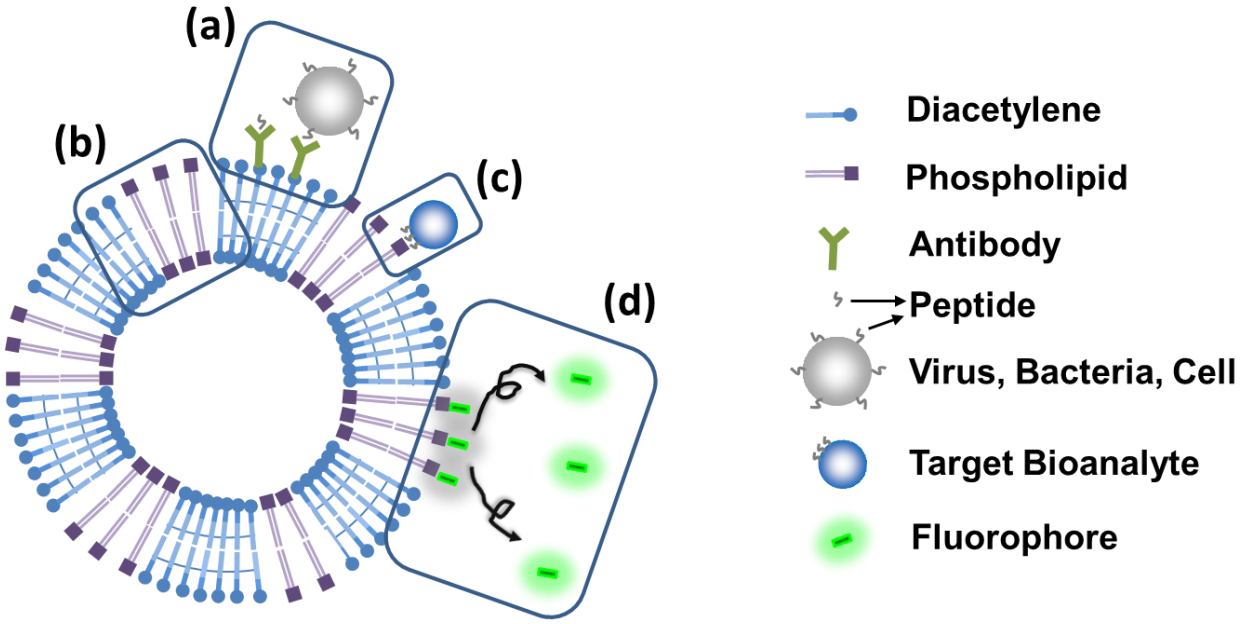

Figure 5.1 Schematic illustration presenting design principles for PDA supramolecules biosensor. (a) Target size and number of probes tethered on PDA surface influence on PDA signal generation, (b) Co-assembly of phospholipid which enables form liposome structures with diacetylenes properly weakens PDA intermolecular packing, providing sensitive signal generation. But, to maintain long term colloidal stability, the co-assembly should be polymerized, (c) Phospholipid can be utilized as target molecule seizing moiety, ensuing PDA sensory signal, (d) Coulombic interaction between fluorophore and phospholipid can be exploited for regulating aggregation and dissociation of fluorophores for "On-Off" sensors.

5.2. Future considerations

In our established sensing platform, fluorescent rhodamine 6G (R6G) (or conjugated

polyelectrolyte) that attached to liposome surface are displaced by target molecules binding to lipids of liposome surface. The turn-on type sensor system worked within known pairs such as PIP_2-aminoglycosidic antibiotics, sulfatide-myelin basic protein. However, whenever we have meaningful target analytes to detect, identifying appropriate probing moiety to target analytes is extremely time consuming. Therefore, we suggest to employ molecular imprinting technique to fabricate binding cavities regardless of analytes which we are interested (Figure 5.2). Molecular imprinting technique (MIP) is very powerful approach for sensor applications, because molecular imprinting makes cavity which is exactly same template structure, so that can bind selectively to the analyte.[2] Therefore, MIP based sensors reduce the number of false positive sensory signal.

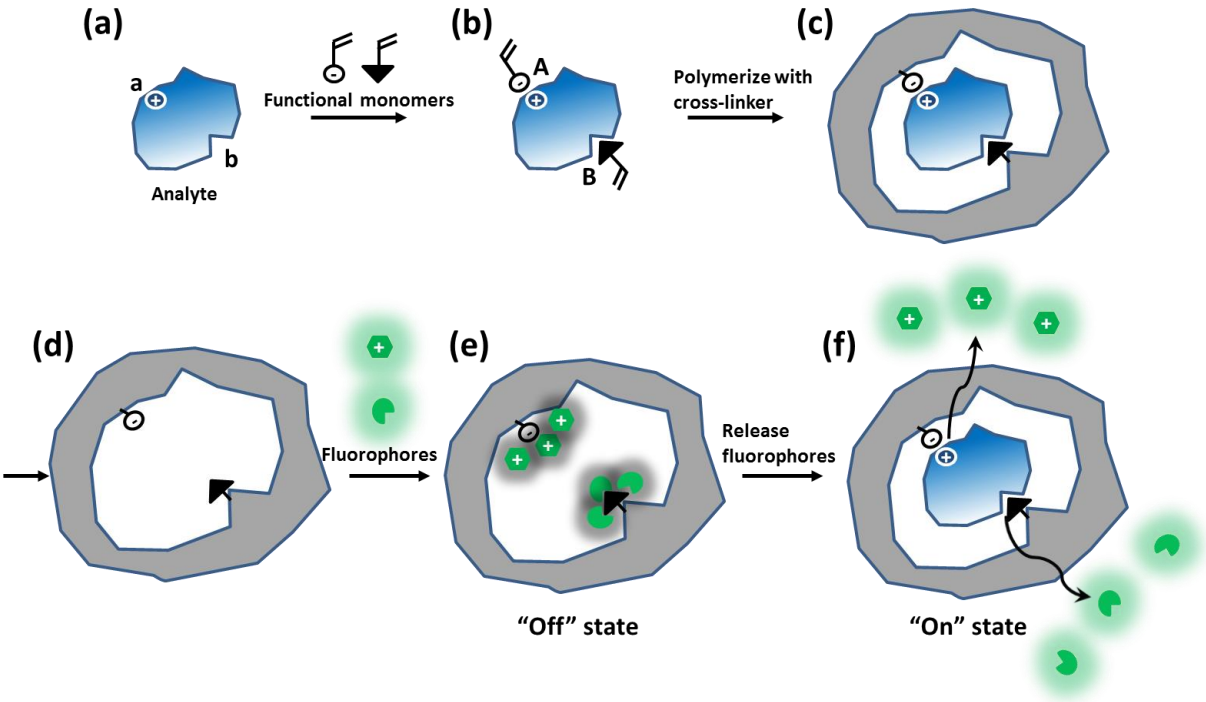

Figure 5.2 Scheme of turn-on type sensors using molecular imprinted polymer. (a) Functional moieties in analyte surface involve following reversible interactions, (b) A: electrostatic interactions, B: non-covalent interactions (hydrogen bonding, hydrophobic or Van der Waals interactions), (c) A subsequent polymerization with cross-linkers generate polymer matrix. (d) Then, the analyte is removed from the matrix. (e) Fluorescent R6G or conjugated polyelectrolytes are attached to analyte surface due to binding interactions. And the fluorophores are quenched by H-type aggregates ("Off" state) (f) The analyte is selectively rebound to the cavity within polymer matrix, releasing fluorophores ("On" state).

We have potential development of novel turn-off biosensors such as viruses, bacteria, cells detection. We recognized that proteins (BSA, Myelin basic protein and Concanavalin A) compete with R6G for the DMPA liposome surface and can partly occupy the surface. Based on these results, we devised a new sensory platform, in which DMPA liposome surfaces are partly covered with a specific antibody, for selective virus/bacteria/cell detection. We examined the feasibility of this sensing strategy by applying the platform to influenza A virus detection. We used DMPA liposomes as a scaffold and attached M1 antibodies at the surface of the liposomes. M1 antibodies have selective binding affinity to H3N2 influenza A virus, but not to H1N1 virus (Figure 5.3). The Coulombic interaction between M1 antibody and DMPA is somehow stronger than the interactions between R6G and DMPA liposomes. Therefore, initially both M1 antibodies and R6Gs occupy the DMPA liposome surface and unbound R6Gs in the aqueous medium are fluorescently emissive. This is the initial "On" status. After the target H3N2 viruses are introduced, the viruses interact with the surface-bound M1 antibodies and break the Coulombic interactions between M1 antibodies and DMPA. This specific recognition make more available DMPA liposome surface for the R6Gs in the aqueous medium to attach, which consequently induces H-type R6G aggregation at the DMPA liposome surface ("Off" status). The system reached equilibrium within 30 minutes and the consequential fluorescence quenching was 48 %. We anticipate a novel fluorescence-based bio detection system based on these promising preliminary results. The system optimizations, such as the mole ratio control of DMPA, R6Gs, and M1 antibodies, have to be investigated to maximize the sensitivity and selectivity.

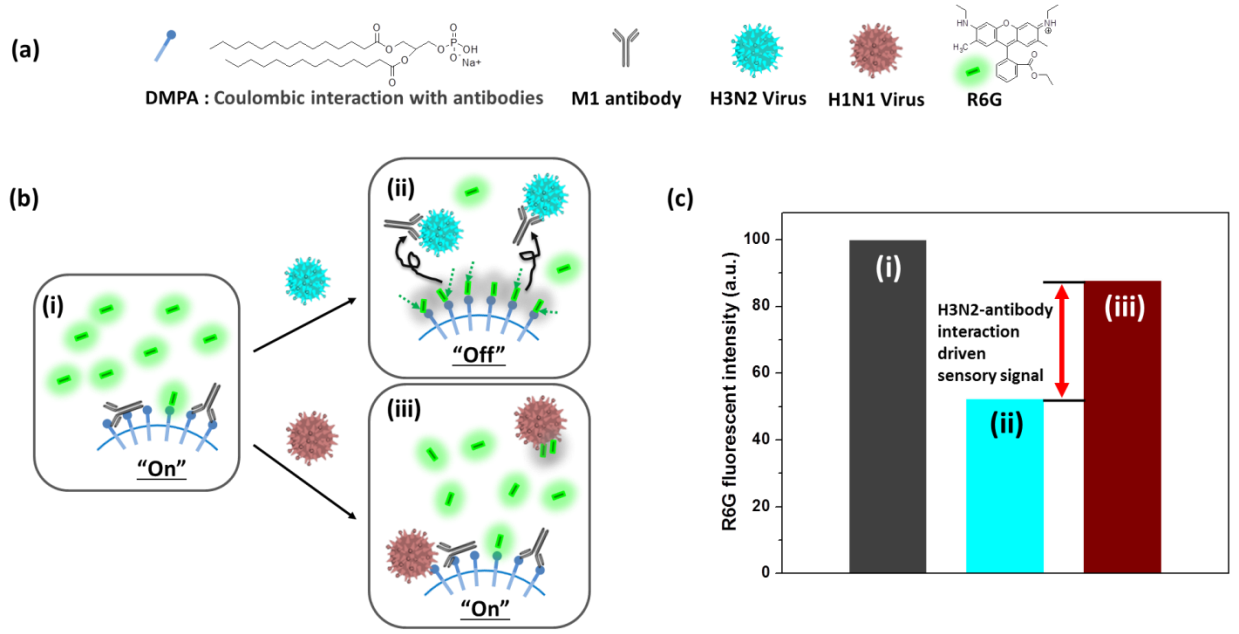

Figure 5.3 (a) Chemical structures of DMPA, M1 antibody, H3N2, H1N1 influenza A viruses and R6G, (b) Schematic illustration of influenza A viruses detection. (i) M1 antibodies and R6Gs initially occupy the DMPA liposome surface and unbound R6Gs in the aqueous medium are fluorescence emissive. (ii) After the target H3N2 viruses are introduced, the viruses interact with the surface-bound M1 antibodies and break the Coulombic interactions between M1 antibodies and DMPA. This specific recognition make more available DMPA liposome surface for the R6Gs in the aqueous medium to attach, which consequently induces H-type R6G aggregation at the DMPA liposome surface ("Off" status). (iii) If H1N1 viruses are introduced, the viruses do not bound to M1 antibody due to the lack of specific binding affinity. Instead, its non-specific binding with DMPA releases some of the surface-bound R6Gs from the DMPA liposome surface, resulting in fluorescence recovery of R6Gs. On the other hand, some H1N2 viruses stay in the aqueous medium and attract R6Gs by means of non-specific interactions, which cause certain level of fluorescence quenching of R6Gs. These two non-specific interactions of H1N2 virus with DMPA and R6Gs act in opposite directions in terms of fluorescence intensity of R6G and the overall net effect on the emission intensity is minimal, (c) R6G emission intensity in cases of (i), (ii), (iii) at 2^{-2} HAU virus concentration.

5.3. References

1. Kang, D. H.; Jung, H.-S.; Ahn, N.; Lee, J.; Seo, S.; Suh, K.-Y.; Kim, J.; Kim, K., Biomimetic detection of aminoglycosidic antibiotics using polydiacetylene-phospholipids supramolecules. *Chemical Communications* **2012,** *48* (43), 5313-5315.

2. (a) Niu, Q.; Gao, K.; Lin, Z.; Wu, W., Surface molecular-imprinting engineering of novel

cellulose nanofibril/conjugated polymer film sensors towards highly selective recognition and responsiveness of nitroaromatic vapors. *Chemical Communications* **2013,** *49* (80), 9137-9139; (b) Lin, H.-Y.; Hsu, C.-Y.; Thomas, J. L.; Wang, S.-E.; Chen, H.-C.; Chou, T.-C., The microcontact imprinting of proteins: The effect of cross-linking monomers for lysozyme, ribonuclease A and myoglobin. *Biosensors and Bioelectronics* **2006,** *22* (4), 534-543; (c) Jenkins, A. L.; Ellzy, M. W.; Buettner, L. C., Molecularly imprinted polymer sensors for detection in the gas, liquid, and vapor phase. *Journal of Molecular Recognition* **2012,** *25* (6), 330-335; (d) Haupt, K.; Mosbach, K., Molecularly Imprinted Polymers and Their Use in Biomimetic Sensors. *Chemical Reviews* **2000,** *100* (7), 2495-2504.